POLYSACHARIDE BASED HYBRID ‘GREEN’ COMPOSITES

A Thesis

Presented to the Faculty of the Graduate School

of Cornell University

In Partial Fulfillment of the Requirements for the Degree of

Master of Science

by

Namrata Vinay Patil

February, 2016

ABSTRACT

In this thesis, completely green ‘sustainable’ fiber reinforced composites were fabricated using biomass. A biobased thermoset resin was developed from a non-edible waste starch source obtained from mango processing industry and further reinforced with microfibrillated cellulose and sisal fibers to form a hybrid composite.

Starch was obtained from the defatted mango seed kernel (DMSK) cake using simple filtration process. The mango seed kernel (MSK) starch was crosslinked using a benign crosslinker 1,2,3,4-butane tetracarboxylic acid (BTCA) using two different catalysts, sodium propionate (NaP), a novel green catalyst, and the currently used sodium hypophosphite (SHP). Properties and characteristics of the crosslinked resin prepared using the two catalysts were studied and compared. To improve the resin strength, it was crosslinked and reinforced with a commercially available microfibrillated cellulose (MFC). MFC was completely homogenized with water and starch in order to achieve good dispersion of MFC in the starch. It was observed that with the increase in the MFC content, the tensile properties of the resin improved. Further, sisal fibers were modified using a combination of alkali treatment and drying under tension to enhance their tensile properties. Alkali treatment removed hemicellulose and lignin keeping pure cellulose that results in better adhesion with the starch. Hybrid unidirectional composites were fabricated using the strength-enhanced sisal fibers, MFC and the crosslinked MSK starch. The final hybrid composites fabricated showed Young’s modulus of about 8.5 GPa and tensile strength of around 165 GPa. While these composites are inexpensive, they can replace wood and wood based products such as particle boards, wafer boards, medium density fiber boards. The MSK resin can be used in place of petroleum based resins such as epoxy, polypropylene, etc., as well as edible starch and protein based resins.

BIOGRAPHICAL SKETCH

Namrata Vinay Patil was born in Aurangabad, Maharashtra, India on 2nd October, 1991. She received a Bachelor of Technology (B. Tech) degree in Fiber and Textile Processing Technology from Institute of Chemical Technology (formerly known as UDCT), Mumbai, India in 2013. In August 2013, she was admitted in the Fiber Science program at Cornell University and worked with Dr. Anil N. Netravali in his 'Green Materials' group to earn a Master of Science (M.S.) degree in Fiber Science. She will continue working towards her Doctor of Philosophy (Ph.D.) in the same research group under the guidance of Dr. Anil N. Netravali.

Dedicated to my Family and Friends

ACKNOWLEDGMENTS

My deepest gratitude is to my advisor, Prof. Anil N. Netravali for his constant support and encouragement. I have been fortunate to receive his guidance as well as the freedom to explore on my own. Also, I would like to thank my minor advisor, Prof. Lara A. Estroff for the valuable suggestions and the lectures on related topics which helped me improve my knowledge in the area and apply in my research.

I would like to acknowledge the Cornell Center for Materials Research (CCMR) and the Department of Fiber Science and Apparel Design for the use of instruments.

I am also indebted to all my colleagues at the Department of Fiber Science, friends and family for all the support.

TABLE OF CONTENTS

LIST OF FIGURES

LIST OF TABLES

CHAPTER 1: INTRODUCTION

1.1 Fiber Reinforced Composites

Composites are naturally occurring or engineered materials which consist of two or more constituents with significantly different physical or chemical properties than the constituents. In the simplest form, they consist of the reinforcements (discontinuous phase) that usually provides strength and stiffness and the more ductile matrix or resin (continuous phase) which bonds the reinforcements and holds them in place and provides toughness to the composites.[1] It is the macroscopic combination between the matrix and the reinforcement materials with recognizable interface between them.[2] Composites exist everywhere from naturally occurring human body to sophisticated engineered spaceships. A very common example of the naturally occurring composite is the human bone in which the collagen fibers are the reinforcement materials arranged within the gel like matrix of calcium phosphate or hydroxyapatite mineral.[3] Other examples of naturally occurring composites are the biological materials such as nacre, dentin, wood, bamboo, etc. The engineered composites can be divided into two different classifications. The first classification is based on their continuous phase and include metal-matrix composites, ceramic-matrix composites or polymeric-matrix composites (also called as organic-matrix composites).[4] The second classification of composites is based on the form of the reinforcement used. Several different kinds of reinforcement forms are used and include particulate or flake reinforcements, whisker reinforcements (chopped or discontinuous fibers), continuous fibers and fabrics (woven, knitted or nonwovens).[2] Thus, a composite consists of a continuous phase or constituent (matrix/resin) which binds together and provides form to an array of stronger and

stiffer discontinuous phase.[2] The combination of matrix and reinforcement synergistically results in improved properties that are superior to either of the constituents individually. Fiber reinforced composites form the most important composite category because of the highest specific mechanical properties they can achieve. This improvement in the properties is mainly due to the transfer of load from broken fibers onto the intact fibers through the shear in the resin. Since the actual load is transferred at the interface fiber/resin interfacial adhesion is important. Composites have various applications due to their structural/mechanical properties. Along with their structural applications, they are also used in various applications because of their electrical, thermal and tribological properties.[2] Modern composites are optimized to achieve the required properties for given range of applications.[2]

Fiber reinforced polymeric composites have many advantages over conventional metal or ceramic based composites because they have lower density and, as a result, have excellent specific mechanical properties. Thus they are widely used in aerospace,[5] automotive, sports, medical (e.g. bone plates for fracture fixation, implants, and prosthetics)[6,7] and many other applications. The polymeric composites can be thermoplastic or thermoset depending on the resin used. Many synthetic fibers such as glass fiber, Kevlar®, carbon fibers, etc., have been used as reinforcing materials for preparing high strength and light-weight composites for structural, aerospace, marine, automobile and many other applications. These fibers are embedded in a relatively compatible polymeric resin, such as epoxy, unsaturated polyester, polypropylene and many others.[8] However, the reinforcements are not restricted to be in the form of continuous fibers. They can be in the form of particles, flakes, whiskers, nanomaterials, short fibers or sheets.[9] In general, however, most commercial composites used today have fibrous form because most materials are stronger and stiffer in the fibrous form as compared to any other form. Many

efforts have also been spent in the past by modifying the polymeric resin with nanofillers such as graphene, carbon nanotubes (CNTs) or nanoclay to improve their mechanical properties.[8,10-13] Most of the currently available composites are light in weight and have good mechanical properties. Also, most of them have been designed keeping in mind their applications but little consideration for their ultimate disposability or the effect on the resources (feed stocks) used to make them. Their properties such as high molecular weight with excellent chemical stability makes it difficult to be degraded by microbes in normal environment. As a result, they persist in nature for long time after their disposal. Since composites, made up of two materials, cannot be reused or recycled easily, majority of them end up in landfills. Unfortunately, the number of landfills worldwide, including the US, are decreasing with the growth in population and increase in living habitat.[14] Another major problem associated with these synthetic polymers is that the monomers used to obtain them is essentially the petroleum which is a non-renewable resource. The worries about the petroleum supplies, environmental pollution and increasing problems associated with the waste disposal of composite materials based on epoxies, polyolefin, polyurethane and other petroleum based products calls for the development of 'green' materials to substitute these non-biodegradable petroleum based plastics.[15]

1.2 Green Composites

Plastics and composites industry has relied on fossil fuels as a source of materials for many decades. About 5-6% of petroleum is used for making polymers, chemicals, etc. With growing environmental awareness, material scientists have been constantly trying to replace the petroleum based plastics or products with greener and environmentally friendly alternatives. It involves substituting carbon from the petroleum-based sources by the plant-extracted carbon in the polymer. 'Green' composites are biobased composites where both resin and reinforcement

are derived from renewable resources, mostly based on yearly renewable plants. For example, vegetable oils or plant oils have been used to make bio renewable epoxy resin.[16,17] Poly(lactic acid) (PLA) has been extensively explored and utilized as biodegradable and renewable thermoplastic polyester as a potential replacement for some conventional petrochemical-based polymers.[18,19] Poly(3-hydroxybutyrate)-based composites have received significant attention in the past as they are biodegradable and are produced by various organisms.[20,21] The most common and extensively studied source of making green resins for composites in the last few decades is the soy protein. Soy protein has been modified or crosslinked to form the matrix material which can be reinforced with various natural fibers to form completely green biodegradable composites.[22-27] Because soy protein is a good source of food and using it for composites has raised 'food vs material' related ethical questions, other proteins such as neem (*Azadirachta indica*)[28], karanja (*Pongamia pinnata*)[29], which are non-edible, are now being explored. Various kinds of starches have also been used as good candidates to replace the petroleum based polymeric resins as they are available in plentiful in nature and can easily biodegrade. Corn starch, wheat starch, tapioca starch, potato starch, etc., have been used to make resins for biodegradable composites.[30-32] These edible starches also pose the same 'food vs. material' dilemma.

Natural plant-based fibers are excellent candidates for reinforcing the biobased resins to obtain completely green composites that can easily degrade in normal environments as well as can be composted at the end of their life. Most of the available natural fibers are not as strong as synthetic ones such as carbon/graphite, Kevlar® or ultra-high molecular weight polyethylene fibers. But, they are yearly renewable as they are obtained from annually grown plants. They have low density, high toughness and acceptable modulus and strength for majority of the

composite applications. Significant research has been done in this area and completely 'Green' fiber reinforced composites have been fabricated using natural polymeric materials mentioned above as the resin along with the natural fibers which act as the reinforcing agent. These composites conserve natural resources, decrease carbon emissions, being biodegradable can be composted and also come from yearly renewable sources.[15,33]

1.3 Can We Get "GREENER"?

Plant based materials including soy protein, corn starch, potato starch have been studied extensively to form biobased resins. The limitation of using these starches for making biobased composites is that they are edible sources and, as mentioned earlier, have raised an ethical dilemma of 'food vs. material'. Starch is a principal source of dietary calories to the world's human population. It is one of the major ingredients in the food industries due to its versatile applications in food and beverages. Pharmaceutical, paper and textile industries also use starch for various purposes. The world population is predicted to reach 9 billion by 2050. Increase in population directly translates to increase in food demand. This also means a significant increase in the food processing by-products or wastes that tend to be non-edible. These non-edible by-products or wastes are mostly limited to low-value applications or simply thrown as trash. The green materials and chemistry researchers have been constantly trying to utilize the non-edible sources from plant based products to convert it into useful and value-added fibers, materials, chemicals, food, animal feed and fuels.[34] Natural fibers and bioprocessing wastes have become interesting sources to be used as reinforcement and resin, respectively, to develop green composites.[35] Though natural fibers have moderate strength, they can be modified by chemical or mechanical treatments to improve their performance and then used as reinforcement in

composites.[36-38] Robust research and development over the coming years is expected to provide entirely new market for green composites and clean technologies.[2]

In the present research polysaccharide based completely 'green' hybrid fiber reinforced composites were fabricated and characterized for their tensile properties. Starch was extracted from agricultural/fruit processing industrial waste of defatted mango seed kernels. It was then analyzed for its proximate chemical analysis to confirm the exact starch content. The viscosity profile of this starch and the ATR-FTIR spectra showed behavior similar to any other starches such as potato and corn. Further, it was crosslinked using a benign crosslinker and a novel green catalyst to form the resin material and characterized for its mechanical and thermal properties. Crosslinking was confirmed using ATR-FTIR spectroscopy. Schematic 1 shows the starch extraction from mango seeds and crosslinking to form a thermoset resin.

Schematic 1. Starch extraction from mango seeds and crosslinking to form a thermoset resin

It was then reinforced with nano- and micro-fibrillated cellulose (NFC/MFC) to improve the mechanical properties and obtain green biocomposites. Schematic 2 shows the crosslinking of MSS and MFC using BTCA as crosslinker and NaP as catalyst. Characterization of tensile properties of this green biocomposites revealed a significant increase in the tensile properties and comparable to edible starch based resins.

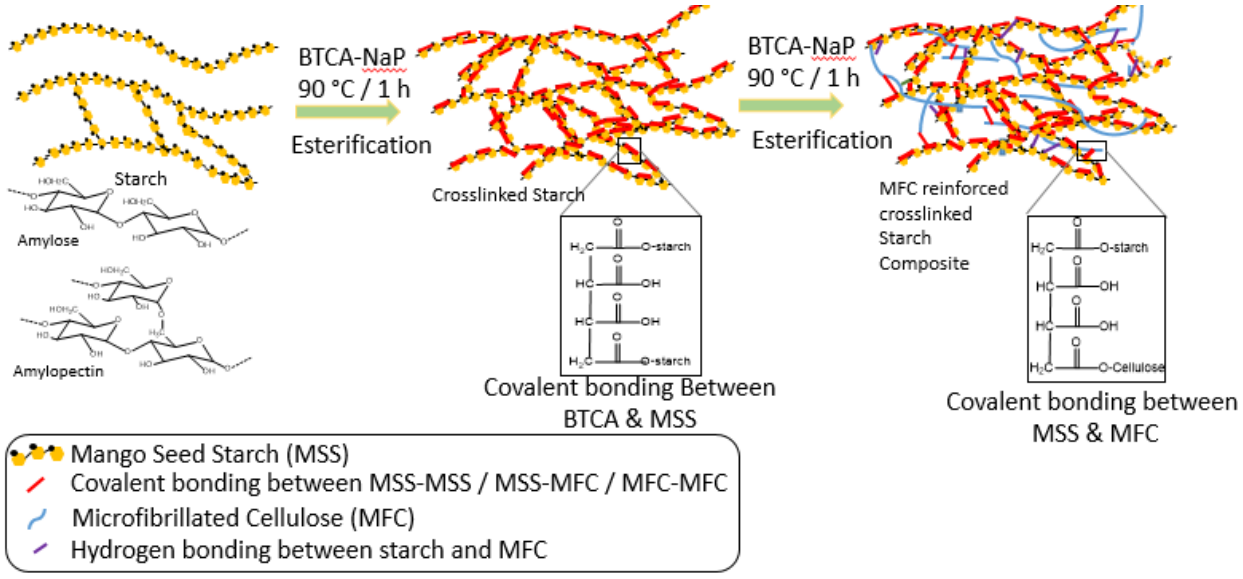

Schematic 2. Crosslinking of MSS and MFC using BTCA as crosslinker and NaP as catalyst

Further, unidirectional composites were made using mercerized and heat treated sisal fibers and characterized for their mechanical properties and fracture surfaces. Properties suggest that such fully 'green composites' can replace the current synthetic composites which are not biodegradable. Schematic 3 shows the alkali and heat treatment of sisal fibers and the fabrication of unidirectional hybrid MSS composites with MFC and sisal fibers.

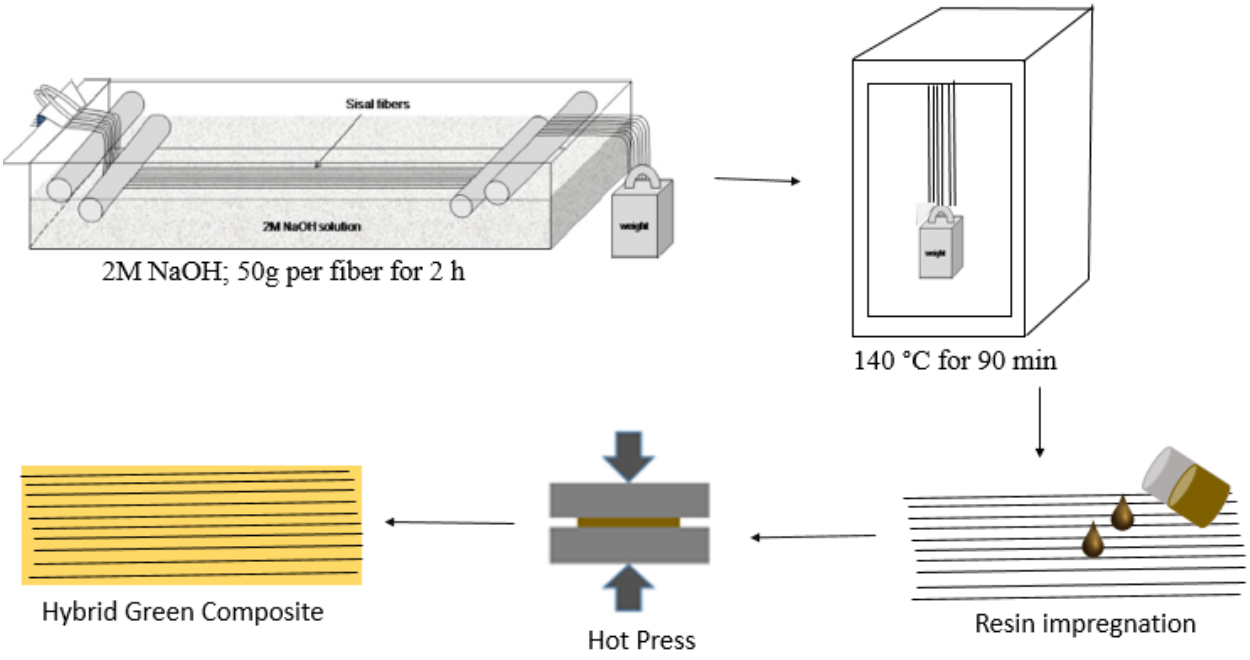

Schematic 3. Alkali and heat treatment of sisal fibers and the fabrication of unidirectional hybrid MSS composites with MFC and sisal fibers

CHAPTER 2: LITERATURE REVIEW

2.1 Starch: From Plants to Plastics/Resins

Over the past several decades there have been severe concerns about the harmful effects of synthetic plastics discarded in the environment. This has led to the growth in the research and development of biodegradable polymers. Biobased biodegradable plastic is a polymer which has been derived completely or partially from the renewable resources (polysaccharides or proteins). It has been referred to as biobased plastic or simply bioplastic.[39,40] Starch is one such renewable raw material used in bioplastics. There has been an increasing trend in the development of materials from biomass such as starch for non-food applications as it is the second most renewable biomaterial available in nature, after cellulose. This is also because of the growing societal demands and government regulations that dictate the use of more eco-friendly materials. Durable and long-lasting plastics are not always appropriate for short-term packaging, agricultural, catering and other such applications. Thus, starch has attracted the attention of many researchers working on developing environmentally friendly materials because it is inexpensive, abundant in nature, yearly renewable and biodegradable.[30] Significant efforts put in this research has led to the development and commercialization of starch-based bioplastics in the recent past.[40]

2.1.1 Source, Structure and Functionality

Starch is the major polysaccharide reserve in the photosynthetic tissues in many kinds of plant storage organs like roots, tubers, seeds or fruits.[30] The structure of starch has been studied extensively. Figure 1 shows the chemical structure of starch (a) amylose (b) amylopectin. It is a carbohydrate consisting of many glucose units connected by 1-4 glycosidic linkages and 1-6 glycosidic linkages. The 1-4 glycosidic linkages leads to a linear polymer structure within the starch known as amylose (Figure 1a). Glucose units connected by 1-4 and 1-6 glycosidic

linkages form the branched chain molecules called as amylopectin (Figure 1b). The molecular weight of amylose is found to be in the range of 10^5 to 10^6 g/mol while that of amylopectin is 10^7 to 10^9 g/mol.[30] Starch has a semi crystalline structure and the amylopectin molecules of the starch account for most of the crystallinity of starch.[30] Different starches have different inherent material functions like viscosity, gelatanization temperature and crystallinity because they have different crystalline arrangements. The carbohydrate monomer D-glucopyranose has three hydroxyl groups. The hydroxyl groups from the starch molecules are the reactive sites. But their reactivity depends on their position in the ring. The two secondary hydroxyl groups are less reactive than the free primary hydroxyl groups due to stearic hindrance.[41] The presence of these groups allows modifying the starch to convert them to more useful and beneficial chemical structure.

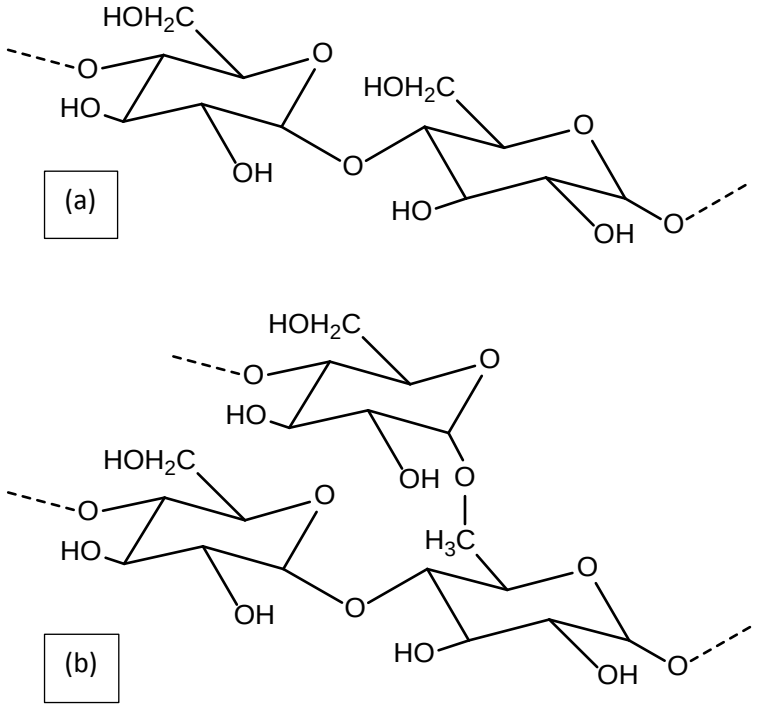

Fig.1 Chemical structure of starch (a) amylose (b) amylopectin

2.1.2 Physical and Chemical Modifications of Starch

A couple of major challenges associated with using starch as resin is its high hydrophilicity and weak mechanical properties, a tensile strength of around 5 MPa.[42] Various attempts have been made to overcome these problems. The commercial starch based bioplastics consists of thermoplastic starch (TPS) or starch blends. The commercial technologies for making starch based bioplastic products involve film blowing, thermoforming, extrusion, injection molding, foaming, etc.[40] Early patents mention complete disruption of the molecular order within the starch granules by mechanical or thermal energy and adding suitable plasticizers such as water, glycerol, etc., to form TPS.[40] Later, researchers have used starches in blends or grafted a polymer onto it to overcome the problems faced due to hydrophilicity and low thermal and mechanical properties. Since the mid-1970s, polymer-starch blends with acceptable physical properties have been developed.[43] These types of physical or chemical modifications are used to synthesize starch based materials which have various applications like in plastic industry, paper-making, drug-delivery, hydrogels or making materials for adsorption of heavy metals.[30,39] Various kinds of starches including potato, maize/corn, cassava, wheat, rice and many others have been explored for their industrial applications. While chemical modification of starch is possible in variety of ways, the most common and easiest reaction with starch involves esterification or crosslinking.[41] Crosslinking of starch has been carried out in many different ways.[44] Potato starch has been crosslinked using epichlorohydrin using homogeneous and heterogeneous conditions and the extent of crosslinking was studied based on the degree of swelling. The side reaction occurring leading to the formation of monoglycerol ether starch derivative has also been studied.[45] Starch has also been crosslinked with epichlorohydrin in the presence of ammonium hydroxide, sodium hydroxide and water.[46] Cassava starch has been

crosslinked using epichlorohydrin in different media such as water or DMF to study the crosslinking effect.[47] Sodium trimetaphosphate (STMP) and sodium tripolyphosphate (STPP) are other commonly used crosslinkers to enhance the mechanical properties of starch. These crosslinkers also reduce the moisture absorption and swelling behavior of the starch when exposed to moisture or water because they convert the hydrophilic hydroxyl groups on the starch to ester or ether groups which are much less hydrophilic. Phosphoryl chloride ($POCl_3$) has also been effectively used to crosslink various types of starches[48,49] Carboxymethylation of starch is another way of modifying starch by introducing bulky carboxymethyl groups on starch which aid crosslinking. But, all these crosslinkers are either complex, expensive or toxic. Various bi or polycarboxylic acids which are nontoxic have known to crosslink starch and used on industrial scale in textile sizing, wet-rub resistant starch paper coating or water resistant adhesives.[30] Crosslinking interconnects starch molecules by covalent bonding and forms a tight molecular organization in starch by reducing the mobility of the amorphous chains in the starch granules. This leads to the increase in the molecular weight as well as the tensile properties of the starch films. It also decreases dissolution of starch in water and the hydrophilicity. Reddy and Yang[50] crosslinked commercially available corn starch using citric acid and concluded that about 10% citric acid (by wt. of starch) leads to better mechanical properties as the tensile stress of 24 MPa was observed. Ghosh Dastidar and Netravali[41] used 37.5% malonic acid to crosslink corn and potato starches and found that the potato starch has better reactivity and higher mechanical properties as compared to corn starch. They reported a tensile stress as 23 MPa and the modulus of 2701 MPa for crosslinked potato starch. Waxy maize starch was also crosslinked using 1,2,3,4-butane tetracarboxylic acid (BTCA) by Ghosh Dastidar and Netravali.[51] They reported a tensile strength of 18 MPa of the crosslinked waxy maize starch using BTCA and Young's

modulus of 1354 MPa. These properties were further improved by reinforcing the crosslinked starch using microfibrillated cellulose (MFC).[51] Using nanoparticles has become another common way to increase the mechanical properties of the starch based composites because these particles have very high surface area and can be processed in water. For example, starch has been reinforced with various nanoparticles such as chitin nanoparticles.[52] Wilhelm et al.[53] used mineral clay to reinforce the starch film while Huang et al.[54] used montmorillonite to reinforce starch. Starch has also been reinforced with micro and nano sized fibers or chopped fibers of various kinds. Lu et al.[55] studied the thermal and mechanical properties of the ramie-crystallites reinforced plasticized starch biocomposites. Such nano-biocomposites are emerging as a new generation composites in the world of material science. In the past few decades starch has been modified and used as a resin for fabricating fiber reinforced composites. This modified starch can be used to replace petroleum based resins or plastics such as epoxy, polymethylmethacrylate (PMMA), polypropylene (PP) and may others which are very difficult to dispose at the end of their lives because they do not biodegrade. Replacing such synthetic resins with biobased renewable materials will help to reduce the consumption of non-replenishable fossil fuels from nature and also eliminate the problems caused due to petroleum based products disposed of at the end of their life.

It is clear from the foregoing discussion that starch has a great potential for industrial applications. It is yearly renewable and produced in all parts of the world. In fact, it is the second most naturally available biopolymer after cellulose. It is abundantly available at low cost. The only drawbacks it suffers from are the low mechanical properties and high hydrophilicity. But these can be easily tackled by suitable physical or chemical modifications. Modifications of starch have been carried out to increase its processability and fabrication of starch based

materials. It exists in granular form and can be plasticized or crosslinked easily to get tunable properties to form films which can replace many synthetic plastics. Several kinds of starches are available and have been studied for its film formation abilities and application in fiber reinforced composites.[30] Green, environment friendly modifications of starch such as crosslinking or reinforcing it with nanoparticles is key to obtain high performance materials. These modifications not only increase the strength of the starch based films but also makes them less sensitive to water by converting the hydroxyl groups to ester groups through covalent bonding. The key for replacing the petroleum based resins/plastics, perhaps, is developing new biobased materials with desired functionality and stability during storage and use. These biobased materials are stable in indoor environments and susceptible to microbial or environmental degradation only when disposed outdoors in moist environments such as compost and thus do not cause any harmful environmental impact.[38]

2.2 Defatted Mango Seeds: Non-edible, Non-Conventional Starch Source

The concept of sustainability has attracted a great deal of interest in utilization of the plentiful available biomass. Conversion of biomass into useful chemicals, fuels, fibers, materials and other useful products is a part of this recent sustainable development trend. This has a great environmental and economic importance, especially in the present times of global warming and diminishing petroleum reserves. As discussed above in section 2.1, various kinds of starches are being recently studied and industrially processed to obtain biobased materials. These starches are plant based and thus renewable and biodegradable and utilizing this as raw material source can be beneficial for the environment. However, the biggest issue of utilizing these starches for non-edible purpose brings the ‘food vs non-food’ issue, particularly because of the tremendous growth in population and proportional increase in demand for the nutritional food supply.[34] This

has encouraged the researchers to study and utilize the biowaste and convert it into useful and value-added products. Agricultural or food processing industrial wastes are now being explored for its applications as feedstock for conversion into fuels or resins.[34] Some of these agricultural residues can have a large amount of starch or protein which can be extracted and modified as required using current technologies.[29] The materials developed from such sources will not only be biodegradable but also help in channelizing the agricultural and food processing residues for better applications.

The use of starch as resin in composites is relatively recent as compared to its applications in textile sizing, adhesives, hydrogels or in paper industry. But what's even more attractive is the use of waste starch for composite applications. Agricultural residues are abundant in nature and available for free. They can be rich sources of starches or proteins. For example mango (*Mangifera indica*) is an important fruit crop cultivated in tropical regions including South Asian countries, Mexico, Brazil and many others and distributed worldwide.[56] It is native to eastern India and Burma and exists in several varieties but only few of them are commercialized. More than 90 countries in the world grow mango and not counting banana, mango is the most consumed tropical fruit in the world. Global production of mangoes was around 35 million metric tonnes in 2009. About 77% of the global production comes from Asia while America and Africa produces 13% and 10% respectively. Mango and mango products are popular all over the world. Mango fruit processing industry has a huge market as the mangoes are processed to make ice creams, juices, jams, flavors, fragrances, colors and many other food products. Recently different varieties of mangoes have been used to produce and characterize wine from the fruit.[57-60] After processing of mangoes on an industrial scale, the seeds are discarded as waste. Mango seeds are bigger as compared to most fruits and account for 9% to

23% of the fruit weight. They are flat, oblong and fibrous on the surface. The seed consists of a tenacious coat enclosing the kernel. The seed kernel makes up 45.7% to 72.8% of the seed weight. Oil has been extracted from the mango seeds and used in various applications as the interest in newer sources of edible oil has grown due to oil shortage.[61] Mango seed kernel (MSK) oil has low acidity as it is found to be almost free from hydrolytic rancidity brought by lipases and, as a result, it can be directly used in the industry without any further neutralization.[61] It has also been mixed with cocoa butter and studied as an inexpensive substitute for cocoa butter.[62] Since the fatty acid and the triglyceride profile is similar to that of cocoa butter, the mango seed kernel fat can also be used as cocoa butter equivalent.[63] The MSK oil also has some phenolic compounds which are useful in cosmetics or pharmaceutical industries for skin care products. The residue left after oil extraction is called as defatted mango seed kernels (DMSK) and in the process of extracting oil from the seeds, large amount of DMSK (by-product or waste product) is generated.[64] Roughly 40% to 60% waste is generated after processing mangoes of which 15% to 20% are kernels.[65] While the constituents of the waste kernel vary according to the variety of mangoes, about 77% of it is carbohydrate (mostly starch). Protein and fats account for 6% and 11%, respectively.[61]

The DMSK waste is a rich source of carbohydrates, mainly starch that can be extracted and used for non-edible applications such as packaging, adhesives and resins for composites. While MSK is used for various applications mentioned above, the residue generated from oil extraction process (DMSK) is mostly discarded as waste. Few papers discuss the extraction of starch from the mango seed kernels. In this research starch was extracted from DMSK and chemically/physically modified to obtain desirable properties. Thus, it can be a promising source of starch for non-edible applications such as green composites.

2.3 Microfibrillated Cellulose: Reinforcement for Composites

A new class of biobased nanomaterials promises to deliver environmentally friendly, high performance bio-fiber materials which can replace some of the synthetic materials.[66] Wood fiber, which is the primary source of this biobased nanomaterial is the most abundant biomass resource on earth.[66] Cellulose is the most common organic polymer, representing about 1.5×10^{12} tons of the total annual biomass production.[66] Cellulose is synthesized not only in plants but also in algae, tunicate sea animals, and some bacteria.[67] Wood fibers consist of ubiquitous cellulosic material which is the structural component of the cell walls of the plants. Plant cell wall consists of nanofibers (nanofibrils) which are made up of cellulose embedded in a matrix of hemicellulose and lignin.[68] Many of the nanofibrils combine to form microfibrils and microfibrils combine to form fibers. Such hierarchical structures are seen in every plant. Cellulose and hemicellulose form a biological nanocomposite which gives plant cells their rigidity, strength as well as flexibility. This has inspired many material scientists to build strong biobased composites using such micro and nano sized cellulose fibrils.[66,69,70] Researchers believe that cellulose nanofibers have a high potential to be used as transparent and extremely strong films in many different areas like packaging, flexible electronics, composites, etc. Because of their nano size the composites made with transparent resin can remain transparent. This research effort could lead to environmentally compatible and high-performance components for various products.[66] As a result, these cellulosic materials in nano/micro forms are rapidly emerging as one of the most promising future materials with outstanding physical, chemical, mechanical and thermal properties for multifunctional applications in different fields, especially in composites.

2.3.1 Source, Structure and Production

Microfibrillated cellulose (MFC) is obtained by mechanical disintegration of cellulose followed by several passes of pulp fiber slurry through high pressure homogenizer.[71] This process was developed by Turbak et al. in 1983 which leads to the production of an interconnected network of submicron cellulose fibrils with diameters up to 1 μm and after further shearing the diameters are in the nano range from 10 to 100 nm and aspect ratios from 500-100.[71,72] The morphology and orientation of cellulose in cell walls of straw have been studied extensively and it was reported that the vascular bundles consist of highly orientated cellulose in the framework.[66] In the thicker parts of the vessels, cellulose exists in the form of crystalline lamellae and not as microfibrils. Cellulose is a linear homopolymer consisting D-glucopyranose units linked by β-1,4-glycosidic bonds [$C_{6n}H_{10n}$ + $2O_{5n+1}$ (n = degree of polymerization of glucose)]. The chemical structure of cellulose is shown in Figure 2. Three hydroxyl groups, placed at the positions C2 and C3 (secondary hydroxyl groups) and C6 (primary hydroxyl groups) can form intra- and inter-molecular hydrogen bonds. These hydrogen bonds allow the creation of highly ordered, three-dimensional crystal structures. As the main component of cell wall, cellulose is predominantly located in the secondary wall of the plant cell wall. In the primary cell wall, cellulose consists of roughly 6000 glucose units. Significant scientific literature has been available in the last 2 decades on cellulose nanofibers as reinforcement and is still continuing to be an interesting research subject.[66] There are two main types of plant based nanocellulose. One is the cellulose nanocrystals and the other is the cellulose microfibrils.[73] Cellulose nanocrystals or whiskers are the elongated crystalline rod-like nanoparticles whereas nanofibrils or microfibrils are the long flexible cellulose nanofibrils with alternating crystalline and amorphous regions.[66] Microfibrils or the nano-order-unit fibrils consist of monocrystalline

cellulose domains with cellulose chains parallel to the microfibril axis. Figure 3 shows the cellulose source to cellulosic fibers, microfibrils and molecules. As the cellulose molecules are devoid of chain folding and contain only a small number of defects, MFC fibrils have a modulus close to that of the perfect crystal of native cellulose which was reported to be 138 GPa.[74] The Young's modulus and fracture stress of commercial MFC (Daicel Chemical Industries, Japan) films is reported to be 10 GPa, and 150 MPa respectively.[75] Because of such high properties as well as their high specific surface area their use is gaining attraction to enhance the properties of resin in composites.[73] The other advantage of using MFC is that it can be produced from agricultural by-products such as wheat straw, soy hull, potato pulp, sugar beet pulp, bagasse or practically any plant stem or stalk.[75] Many sources, new mechanical processes and post treatments are currently being developed to reduce the high energy consumption of repeated shearing using large homogenizers and to produce new types of MFC materials on industrial scale.[73] MFC is a commercial product available from various companies like Diacel, Japan; Tettenmaier, Germany; Innventia, Sweden.

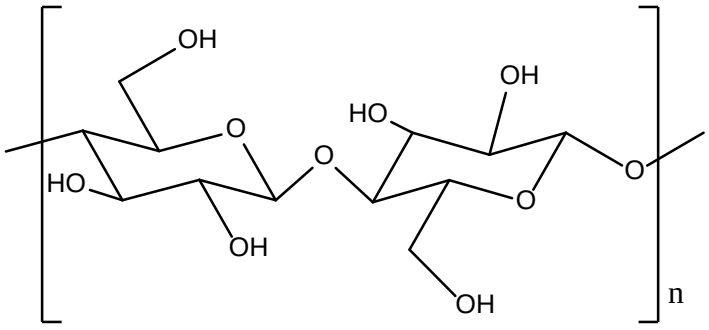

Fig. 2 Chemical structure of cellulose

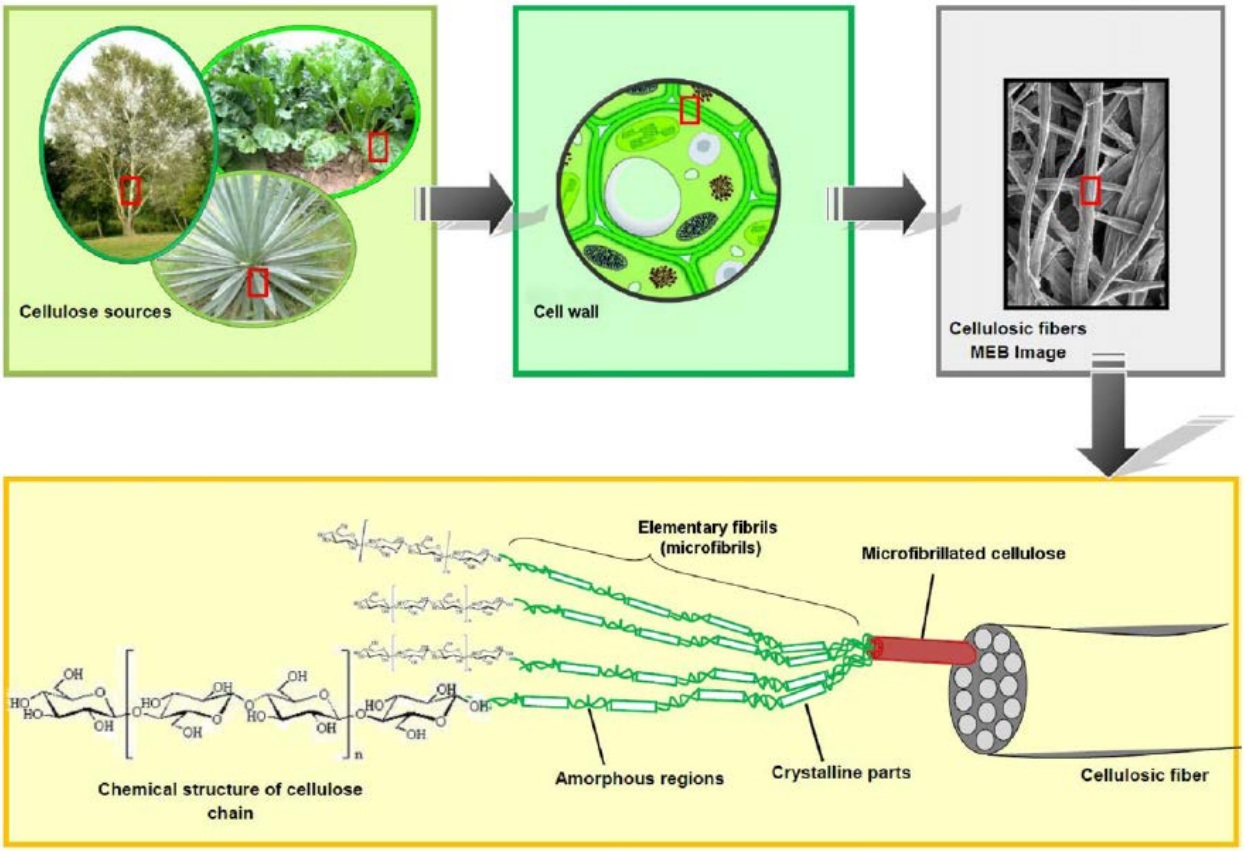

Fig. 3 From cellulose source to cellulosic fibers, microfibrils and molecules [73]

2.3.2 Microfibrillated Cellulose based Nanocomposites

Nanocomposites are at least two phase materials in which at least one of the phases has at least one dimension in the nanometer 1 nm - 100 nm range. Nanocomposites are superior as compared to the conventional composites because they show better thermal, chemical, mechanical or barrier properties at very low reinforcement loading levels.[66]

MFC has been studied as an excellent reinforcing agent to various polymers to make high strength sustainable materials. For example, MFC sheet-molded phenolic resin composites with 80–90 wt% fiber content have been reported to exhibit strength equivalent to that of mild steel or magnesium alloy.[70] Lu et al.[75] modified MFC using three different coupling agents: 3-

aminopropyltriethoxysilane, 3-glycidoxypropyltrimethoxysilane, and a titanate coupling agent and dispersed it into the epoxy resin using acetone as solvent and observed that with this treatment the fibers change from hydrophilic to somewhat hydrophobic which also lead to better fiber/epoxy adhesion leading to a higher strength of the composites.[76] The effect on thermal and mechanical properties by adding MFC to thermoplastic polyurethanes (PU) was also studied.[67] The results showed that both microfibers and nanofibrils reinforced the polyurethane and provided better heat stability. The addition of 16.5 wt% of cellulose nanofibrils to PU increased the strength nearly 500% form 5 MPa for neat PU to 28 MPa and the modulus by 3000% from 25 MPa to 725 MPa.[77] Composites have also been made using MFC and poly(vinyl alcohol) (PVA).[77,78] Authors reported improvement in mechanical properties on addition of MFC and also mentioned the composites being chemical resistant but biodegradable.[78,79] Though MFC is bio-based and hence biodegradable, epoxy based resins, PU and several other polymers are derived from petroleum sources and hence composites based on these are not completely biodegradable. However, PVA and polyethylene oxide (PEO), although petroleum based, are biodegradable. On the other hand, the monomers for polylactic acid (PLA) are derived from plants and thus composites based on PLA and MFC are completely biobased and sustainable. Suryanegara et al.[79] added MFC up to 20% to PLA on weight basis to increase its storage modulus at high temperature. MFC and PLA were mixed in an organic solvent with various fiber contents and dried, kneaded and hot pressed into sheets with good MFC dispersion.[80] Drzal and Wang[81] also successfully dispersed cellulose nanofibers in PLA by solvent evaporation technique and reported an increase in Young's modulus and tensile strength of the composites by 58% from 3.8 to 6.0 GPa and 210% from 25 to 78 MPa, respectively. The simplest of the family of polyhydroxyalkanoate (PHA) biopolymers is poly-R-3-hydroxybutyrate or PHB. PHAs have

received much attention as it can be derived from renewable resources and its physical properties resemble those of the conventional plastics, particularly PP. Composites have been made by dispersing cellulose nanocrystals by acid hydrolysis of cellulose microfibrils in cellulose acetate butyrate resin by solution casting of the dispersions.[66] Such composites are good alternatives to petroleum based composites as the raw materials required to obtain these polymers are plant based and thus yearly renewable and inexpensive. They are termed as nano-biocomposites. The major challenge associated with using MFC as a reinforcing agent with such polymeric materials to form biocomposites is the problem of 'hornification', a term used to describe the irreversible agglomeration of MFC in nonpolar solvents matrices.[72,82] This situation can be avoided by using starch as the resin because it is water soluble at high temperature and can also form strong hydrogen bond with MFC and can be covalently bonded using suitable crosslinkers. Protein based resins can also be reinforced with MFC to form completely green composites. Huang and Netravali[83] fabricated biocomposites based on bamboo microfibrils and modified soy protein resin while Ghosh Dastidar and Netravali[51] fabricated waxy maize starch and MFC based composites. The properties of such modified protein and starch reinforced with MFC composites reveal that they can be used to replace the synthetic composites derived from petroleum products. Their barrier properties can be utilized to make composite films for food packaging application. There has also been an increasing interest of using MFC in battery applications as it possesses piezoelectric properties and is light in weight.[84,85]

2.4 Sisal Fibers: Reinforcement for biobased composites

Natural fibers are considered to be prime candidates to replace synthetic fibers for fiber reinforced composites. Although they are not as strong as some of the synthetic fibers, they have

acceptable strength.[86] Recent advances in natural fiber development and genetic engineering offers significant opportunities for improving the performance of natural fibers.[86] Many of the plant based fibers are yearly renewable. This also decreases the dependence on petroleum products which act as raw materials for most of the synthetic fiber manufacturing process. It also helps in reduction of carbon emission as they biodegrade and thus contribute towards a sustainable environment. Natural fibers can be divided based on their origin as plant/vegetable, animal or mineral based fibers. The plant/vegetable based fibers are further identified as (1) leaf: sisal, pineapple, henequen; (2) bast: flax, ramie, kenaf, hemp, jute; (3) seed: cotton; (4) fruit: coir, etc.[87]

2.4.1 Production and Characteristics of Sisal Fibers

Sisal fiber is one of the most widely used natural fibers as it is very easily cultivated. It is a hard fiber extracted from the leaves of sisal plant (*Agave sisalana*).[85] It has short renewal times and grows wild in the hedges of fields and railway tracks. Nearly 4.5 million tons of sisal fiber is produced annually throughout the world.[85] Sisal plant is a native to tropical and sub-tropical North and South America. It is also cultivated in tropical countries of Africa, the West Indies and the Far East. Tanzania and Brazil are the two main producing countries.[86] Figure 4 shows a sketch of the sisal plant (a), cross-section of a sisal leaf (b) and cross-section of ribbon fiber bundle (c).[86] A sisal plant produces about 200-250 leaves and each leaf contains 1000-1200 fiber bundles. These bundles are composed of 4% fiber, 0.75% cuticle, 8% dry matter and 87.25% water.[87] The leaf consists of three kinds of fibers: mechanical, ribbon and xylem. As seen the sketch in the Figure 4 (b), the mechanical fibers are mostly present on the periphery of the leaf, which have a roughly thickened horseshoe shape. They are the most commercially useful sisal

fibers. The second kind of sisal fiber is also shown in Figure 4 (b) called as the ribbon fiber. They occur in association with the conducting tissues in the median line of the leaf which gives them considerable mechanical strength. They are the longest fibers and compared with mechanical fibers, they can be easily split longitudinally during processing. Xylem fibers have an irregular shape and occur opposite the ribbon fibers through the connection of vascular bundles as shown in Figure 4 (c). These fibers are composed of thin walled cells and are therefore easily broken and lost during the extraction process. The process of extracting the fibers has been described by Chand et al.[88] and Mukherjee and Satyanarayana.[89] In general, two processes for extracting fibers are used. First one is the retting process followed by the scrapping. This method gives a large yield but the quality of fibers is poor. Another method is the mechanical method with decorticators which gives a yield of about 2-4% fibers (15 kg in 8 h) of good quality with luster.[85] Sisal fibers consist of 78% cellulose, 10% hemicellulose, 8% lignin, 2% waxes and 1% ash by weight. Therefore, chemically, sisal fibers can be considered to be consisting of cellulose chains and hemicellulose intimately associated with lignin. These fibers have both crystalline as well as non-crystalline components which can undergo deformation under tension. Compared to other fibers, the price of sisal fiber is very low (0.36 US$/Kg) while glass fiber is about (50 US$/Kg).[86]

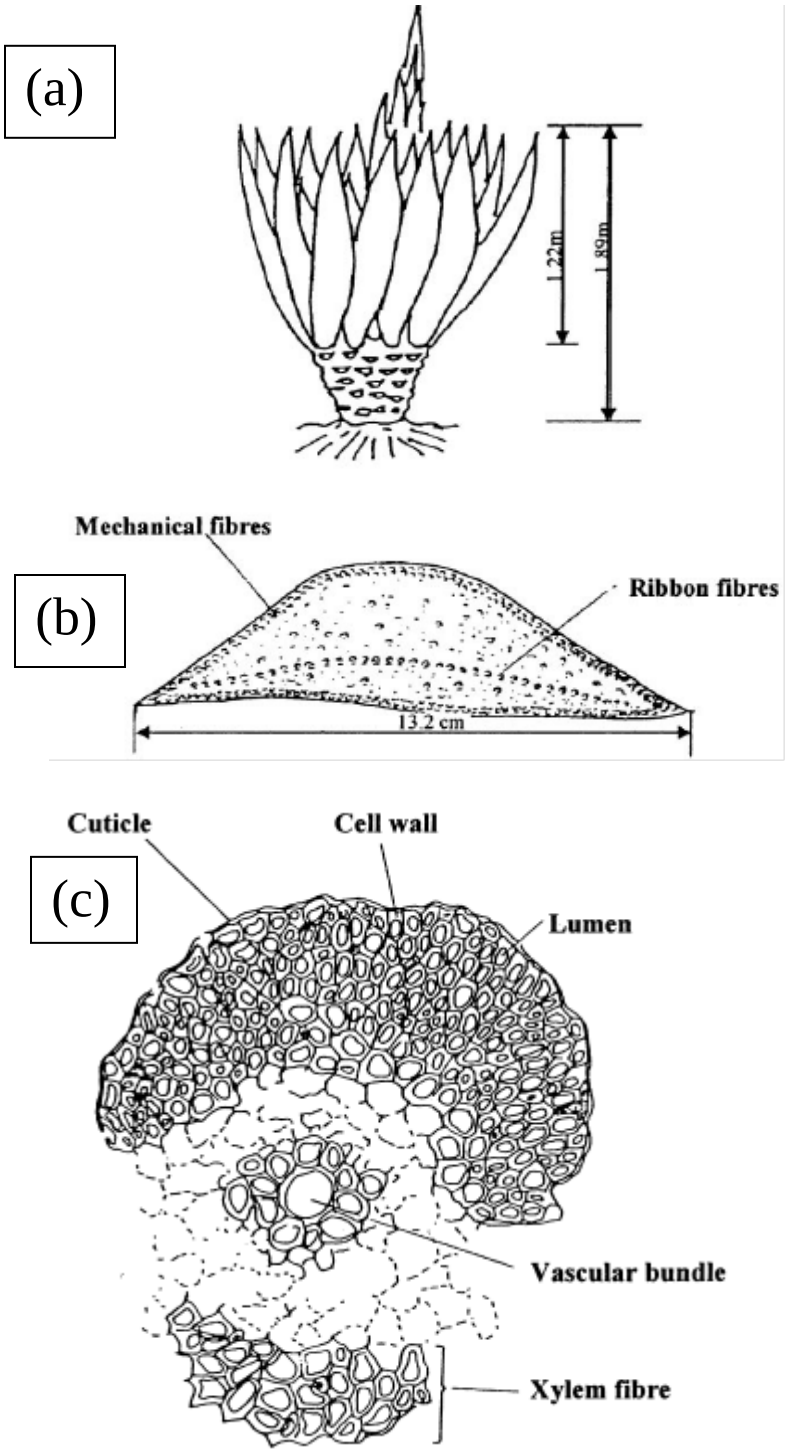

Fig. 4 Sketch of (a) sisal plant (b) cross-section of sisal leaf and (c) cross-section of ribbon fiber bundle[86]

2.4.2 Sisal Fiber based Advanced Composites

Various chemical modifications of sisal fibers have been proven beneficial in terms of increasing the strength of the fibers as well as the moisture absorption and the interfacial bonding with the resins in the composites. Singh et al.[90] studied the effects of several chemical treatments like organotitanate, zirconate, silane and N-substituted methacrylamide on the properties of the sisal fibers and used them as a reinforcement in unsaturated polyester resin. They found an improvement in the properties of the composites with the modified sisal fibers. The composites formed with N-substituted methacrylamide exhibited improved properties under dry as well as wet conditions. Kumar et al.[91] incorporated sisal fibers in epoxy resins and compared its properties to glass-fiber-epoxy composites of the same composition. They reported the tensile strength and modulus to be nearly half for sisal-epoxy composites as compared to that of glass-epoxy composites. As the density of sisal fibers is low (1.45 g/cc) compared to glass (2.5 g/cc), the specific strength (strength/density) was better for sisal-epoxy composites. They mentioned extensive applications of these composites in consumer goods, low cost housing and other structures as they are easy and inexpensive to process. Rong et al.[92] also studied sisal-epoxy composites with sisal fiber modifications such as alkalization, acetylation, and cyanoethylation. Various researchers have also studied sisal fiber reinforced thermoplastic composites based on polymers such as low density polyethylene (LDPE), polypropylene (PP), poly (vinyl chloride) (PVC) and polystyrene. Some researchers reinforced two or more fibers into a single resin to develop hybrid composites. Sisal/glass fiber-reinforced LDPE composite is a good example of a hybrid composite. The properties of the composites depend on the fiber orientation, fiber modification and the surface of the fiber as well as the composition of each component fibers and their bonding with the resin. Since the glass fiber is stronger as compared to sisal fiber, the

properties increase on addition of glass fibers. The properties are stated as 'negative' or 'positive' hybrid effect based on the properties theoretically calculated on the basis of the rule of mixture.[86] Yang et al.[93] studied the properties of sisal-glass fiber reinforced PVC hybrid composite while Mishra et al.[94] studied the properties of sisal-glass fiber reinforced polyester hybrid composites.

From the above discussion we see that the sisal fiber can be modified and used as a reinforcing fibers for various kinds of polymers, both thermoplastic as well as thermoset. It can also be embedded into rubber or cement matrices. As mentioned above various kinds of hybrid composites have been made combining sisal with other fibers to get better properties. The mechanical properties of such fiber reinforced composites mainly depend upon the fiber strength and the fiber/resin adhesion. Various treatments on sisal fibers have been shown to help improve their mechanical properties and the moisture resistance of the composites made using them. Overall, sisal fibers possess enormous potential for use in composites because of its high specific strength and modulus, low density, low cost, no health risk and easy availability.

2.5 Green Composites

The word 'green' affiliated with composites refers to materials which are biodegradable, renewable and thus attributes to twin issues of 'sustainability' and 'environmental impact'. Green composites are becoming more popular recently due to persistent problems such as fossil fuel depletion, increase in oil prices and need for clean environment.[95] Using resources that are yearly renewable is a simple solution to all the problems mentioned above. Green composites are particular class of composites which uses biodegradable polymeric material as the resin reinforced with natural fibers.[95] Polymer composites with plant fibers are manufactured using compounding and mixing and also by applying polymer processing techniques such as extrusion,

injection or compression molding. The most commonly used plant and microbe-derived resin materials include polylactic acid (PLA), poly(butylene succinate) (PBSu) and Poly(hydroxyl alkanoate) (PHA).[94] Aliphatic polyesters such as PHAs are fully degradable in normal environment as opposed to aromatic polyesters. However, aliphatic polyesters have poor thermal and mechanical properties.[94] But copolymerization of aromatic and aliphatic diacids with an aliphatic diol leads to the synthesis of copolyesters with balanced mechanical and biodegradable properties.[94] Such polymers are called alipharomatic polyesters. Poly(butylene terephthalate-*co*-butylene adipate) copolyesters or similar copolymers are already commercially available under the trade names as Ecoflex® or others.[94] while numerous other types of such materials have been investigated. These alipharomatic polyesters have higher degradability than aromatic polyesters like poly(ethylene terephthalate), which is the most used polyester, but lower mechanical properties. In order to increase their properties several kinds of fibers can be used.[94] Several other biodegradable, natural polymers exist, such as polysaccharides (starch, chitin, collagen, gelatins, etc.), proteins (casein, albumin, silk, elastin, etc.), polyesters (e.g., PHA, PHB, PLA), lignin, lipids, natural rubber. These are used as matrix for green composites.[96]

Oksman et al.[97] fabricated flax-PLA composites and compared it with flax-PP composites which are used in many automotive panels. They found that the composite strength is about 50% better for flax-PLA (44 MPa) compared to similar flax-PP composites (29 MPa). While a similar modulus value was observed in both. Thus, PLA can be used to replace conventional resins such as PP. Plackett et al.[98] reported the tensile strength value of 100 MPa and modulus of 9.5 GPa jute-PLA composites (using 40% jute on wt. basis). Various nanocomposites have been fabricated using organo-modified montmorillonite clays to improve the thermal stability of the PLA-based composites.[99]

Various plant oils can also be used to obtain bio-based resins or adhesives. Many active sites from the triglycerides like double bond, allylic carbons and ester groups can be used to introduce polymerizable groups. Wool and Sun[99] prepared soybean oil based resins by functionalizing the triglycerides by attaching polymerizable chemical groups such as maleinates and acrylic acid. This made the triglyceride capable of polymerizing via ring opening, free-radical or polycondensation reactions.[100] Composite materials made out of plant oil-based resin and plant fibers using VARTM process showed properties desired for many applications.[101] Research on biodegradable polymer composites containing lignocellulosic fibers is also generating increasing attention due to dwindling petroleum resources, low cost of lignocellulosic reinforcements with a variety of properties and increasing ecological considerations.[102]

Luo and Netravali[21] used Biopol® (poly(hydroxybutyrate-co-hydroxyvalerate) or PHBV resin from Monsanto Company) with pineapple and henequen fibers to make green composites. The tensile and flexural strengths of green composites were reported to be significantly higher than many wood varieties in the grain direction, even at a low fiber content of 28%. With higher fiber content and better processing, the mechanical performance could be improved further for use in applications such as secondary structures in housing and transportation.[21] Lodha and Netravali[102] fabricated green composites using soy protein isolate as resin and reinforced it with ramie fibers.[103] They further modified the soy protein resin with stearic acid to reduce moisture absorption and obtain better tensile properties.[104] Huang and Netravali[104] incorporated nanoparticles such as nanoclay into the soy protein based resins and further reinforced it with flax fibers and characterized the composites.[105] Nanoclay incorporation increased the Young's modulus of the resin as well as that of the composite. Nanoclays also reduce the moisture absorption of the resin. Rout et al.[105] studied the effects of different fiber treatments including

alkali treatment, bleaching and vinyl grafting on coir fibers and the effect of treatment on the composite performance.[106] They showed that all modifications of the fiber surfaces increased the mechanical properties of composite.[105]

The role of automotive industry in the field of green composites is of prime importance. The first carmaker to use polymer (epoxy) filled with natural fibers was Mercedes-Benz in the 1960 by manufacturing door panels containing jute fibers.[107] Another paradigm of greener composites' application appeared commercially in 2000, when Audi launched the A2 midrange car: the door trim panels were made of polyurethane reinforced with a mixed flax/sisal material. Mitsubishi motors also used green/greener composites in the interior components which combine bamboo fibers and a plant-based resin polybutylene succinate (PBS), and floor mats made from PLA and nylon fibers.[108] Toyota has claimed to be the leading brand in adoption of environmentally friendly, 100% bioplastic materials.[38] The natural fiber reinforced green composite was used in the RAUM 2003 model in the spare tire cover. The part was made using PLA resin from sugar cane and sweet potato and was reinforced with kenaf fibers. Toyota added the Matrix and RAV4 models to the list of vehicles using soy-based seat foams in the summer of 2008.[107] Recently, Ford selected wheat straw as reinforcement for a storage bin and inner lid in its 2010 Flex crossover vehicle while BMW, for the 7 Series sedan used prepreg natural fiber mats and a unique thermosetting acrylic copolymer for the lower door panel.[107] The shift to more sustainable construction in automotive industry, particularly in Europe, is not only the company initiative towards a more viable environment and cost efficiency but also a requirement through European regulations. According to the European Guideline 2000/53/EG issued by the European Commission, 85% of the weight of a vehicle had to be recyclable by 2005. This recyclable percentage was expected to be increased to 95% by 2015. Composites made of renewable

materials are now commonly used in interior and exterior body parts. Similar components are used as trim parts in dashboards, door panels, parcel shelves, seat cushions, backrests and cabin linings. In recent years there has been increasing interest in the replacement of fiberglass in reinforced plastic composites by natural plant fibers such as jute, flax, hemp, sisal and ramie. Materials experts from various automakers estimate that an all-advanced-composite auto-body could be 50–67% lighter than the current similarly sized steel auto-body as compared with a 40–55% mass reduction for an aluminum auto-body and a 25–30% mass reduction for an optimized steel auto-body. Specifically for the future electrical vehicle's chassis, the light-weighting materials approach is vital in order to offset the added weight of batteries while at the same time lowering the curb weight and increasing their maximum range. Such an automobile body could be even lighter with the addition of natural fibers in the composite because these are less dense than the synthetic types. The concept of natural fiber incorporation in exterior car parts is not new. Dealing with an exterior part though is a more complex in comparison to the interior parts which are protected from the weather, particularly water. In addition, the exterior components must be able to withstand extreme conditions such as exposure to heat and cold and mechanical impacts resulting in chipping and splintering.[38] The first release of exteriors greener composites appeared in 2000, when the Mercedes-Benz Travego travel coach model, was equipped with a polyester/flax-reinforced engine and transmission enclosures for sound insulation.[107] These are the first examples of natural fibers' use for standard exterior components in a production vehicle and represents a milestone in the application of natural fibers.[38]

CHAPTER 3: EXPERIMENTAL METHODS

3.1 Materials

Defatted Mango seed kernels (DMSK) were obtained from Manorama Industries Pvt. Ltd., Raipur, Chhattisgarh, India. MFC in water (Celish KY-100G) was obtained in the form of a paste from Diacel Corporation, Japan. Sisal fibers were obtained from Yucatan, Mexico. Analytical grade 1,2,3,4-butane tetracarboxylic acid (BTCA), sodium hypophosphite monohydrate (SHP), Sodium propionate (NaP) were purchased from Sigma Aldrich, (Saint Louis, MO).

3.2 Extraction of Starch from Defatted Mango Seed Kernels

DMSK obtained after oil extraction was converted to powder form using a blender and then passed through a 250 μm sieve to obtain fine granules/particles. The fine powder obtained after sieving was washed with water by magnetic stirring overnight and vacuum filtered using a microfiber polyester fabric. The residue obtained after filtration was subjected to washing process again to obtain maximum amount of starch. Double washing of the residue was also carried out to get rid of the water soluble sugars. It was vacuum filtered again after washing. The filter residue thus obtained was dried in an air circulating oven at 60 °C for 24 h. The dried starch lumps were ground in a blender to obtain powder which was then passed through a 250 μm sieve to obtain fine powder with submicron particles. Steps showing MSS extraction process from mango seeds are shown in Figure 5. The MSS obtained was analyzed for the constituents by Dairy One, Ithaca, NY. The entire starch extraction process was green and used only water as the solvent.

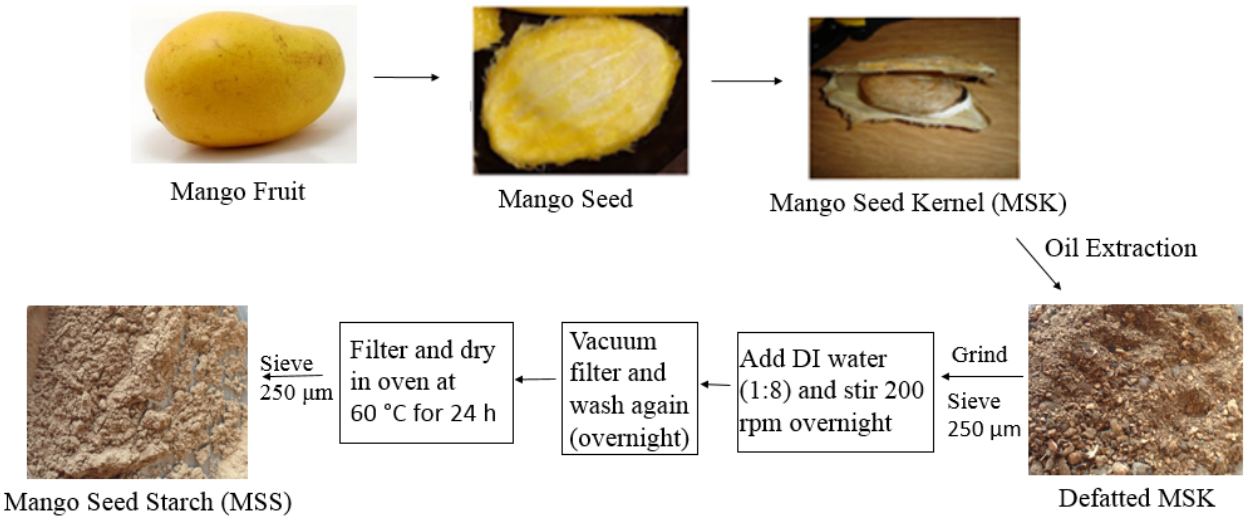

Fig.5 Steps showing MSS extraction process from mango seeds

3.3 Preparation of Crosslinked Starch Films:

The method used to prepare resin from starch was a slight modification of the methods used to crosslink other starches studied earlier.[41,51] Figure 6 shows the schematic of gelatinization and crosslinking of MSS to form thermoset MSS resin films. Starch was first gelatinized in water at high temperature and then crosslinked with BTCA. Water (150 ml) was heated to 85 °C in a water bath and 8 g of MSS was added while constantly stirring. To ensure maximum gelatinization, the mixture was maintained at 85 °C in a water bath for 1 h with continuous magnetic stirring at 200 rpm. With increase in time, the viscosity of the mixture increases as the starch gelatinizes. After 1 h, 40% BTCA (on dry wt. basis of starch) and catalyst (50% of wt. of BTCA) were added to the gelatinized starch in the same water bath and stirred continuously for 1 h at 200 rpm. BTCA and catalyst were solubilized in water before adding to the gelatinized starch. Heating and stirring ensured complete and homogeneous mixing of these chemicals with the starch, allowing the carboxylic groups from BTCA to react with the accessible hydroxyl groups from the starch to form the ester groups by covalent bonding. The

mixture was then poured into a Teflon® coated glass plate of 150 mm × 150 mm dimensions and cooled down to room temperature to form films. The films were dried in an air circulating oven for 48 h. The dried, crosslinked starch film was then peeled off the plate and hot pressed to complete the crosslinking (curing) reaction in a hydraulic hot press (Carver, model 3891-4PROA00, Wabash, IN). The hot pressing was carried out at 120 °C for 20 min at 0.38 MPa. The entire process is shown schematically in Figure 6. The film was further washed by soaking it in DI water to remove the unreacted BTCA as well as to wash out the catalyst completely. This washing step is important as it removes the catalyst which is highly hygroscopic and tends to absorb a significant amount of water when exposed to humid conditions. Two different films were made by crosslinking MSS with BTCA using SHP as a catalyst in one (MSS-BTCA-SHP) while using NaP as a catalyst in the other (MSS-BTCA-NaP). Both processes were identical except for the different catalyst used. The results were used to judge the efficacy of NaP as a catalyst as compared to SHP.

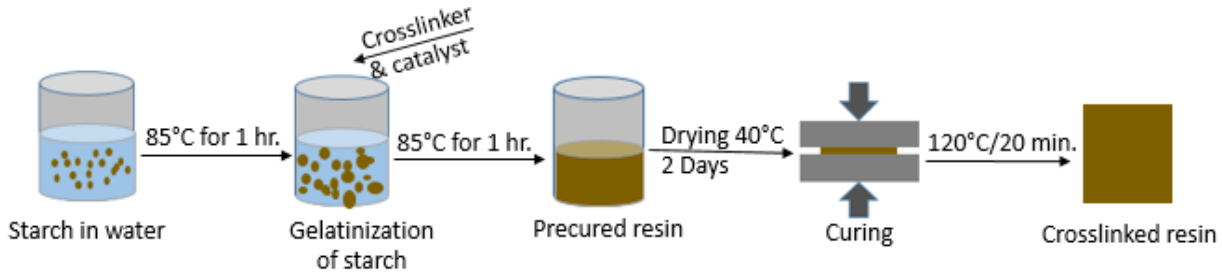

Fig. 6 Schematic of gelatinization and crosslinking of MSS to form thermoset MSS resin film

3.4 Preparation of Biocomposites

Biocomposites were fabricated using MFC and MSS where MFC in nano/micro form was used as the reinforcing fiber in the MSS resin. These are known as biocomposites as much of the reinforcing agent is in the nano form and both reinforcement and resin are biobased. Figure 7 shows the schematic of the MFC-MSS biocomposite fabrication process. Excellent dispersion of MFC and MSS in water is the key to obtaining good MFC-MSS biocomposite films. This was obtained using a homogenizer as shown in Figure 7. Desired amount of MFC:MSS (20:80, 30:70 and 40:60) dispersion in water was obtained using VWR 250 homogenizer. Water was added at a ratio of 200:1 based on weight of MFC and homogenized at 20,000 rpm for 15 min and then stirred overnight at 1000 rpm with magnetic stirrer. Later, this dispersion was heated to 80 °C with continuous high speed stirring at 1000 rpm in order to gelatinize MSS. After 1 h, 40% BTCA on weight basis of MFC:MSS and 50% NaP on weight basis of BTCA was added to the dispersion of gelatinized starch and MFC. BTCA was used as a crosslinker while NaP was used as a non-phosphorous based catalyst for esterification. The stirring and heating was continued for 1 h and then the mixture was poured into a Teflon® coated glass plate of 100 mm × 100 mm dimensions and allowed to dry at room temperature until it could be peeled off from the glass plate. It was then cured in Carver hydraulic hot press (model 3891-4PROA00, Wabash, IN) to ensure complete crosslinking of the film. The curing was carried out at 140 °C for 15 min at 0.38 MPa pressure.

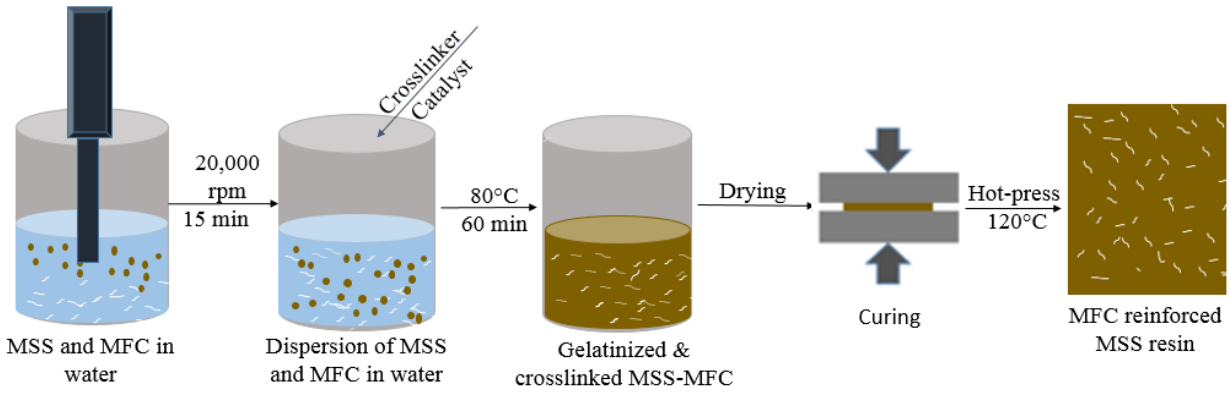

Fig. 7 Schematic of the MFC-MSS biocomposite fabrication process

3.5 Mercerization and Heat Treatment of Sisal Fibers

Mercerization of sisal fibers was carried out in 2 M NaOH solution under tension. Figure 8 shows the photograph of the mercerization bath apparatus used to carry out mercerization of sisal fibers under tension. Fifty gram load was applied per single fiber in the NaOH bath in order mercerize the fibers under stress. The 50 g value was determined as per the procedure mentioned by Kim and Netravali.[36] As seen in the Figure 8, 20 fibers within a narrow range of diameters were chosen and clamped with the clip on one side and 1000 g load was attached to the other end. Two hundred ml of 2 M NaOH solution was then pour into the apparatus shown in the picture and fibers were treated under tension for 2 h at room temperature. It was later washed with DI water and then neutralized using acetic acid and washed again with DI water. Then they were heat treated under the same tension applied during mercerization in an air circulated oven maintained at 140 °C for 90 min to increase fiber crystallinity and obtain orientation within the fiber.

Fig. 8 Photograph of the mercerization bath apparatus used to carry out mercerization of sisal fibers under tension

3.6 Preparation of Hybrid-Green Composites using Mango Seed Starch, Microfibrillated Cellulose and Modified Sisal Fibers

A composite is termed as ‘hybrid composite’ when two or more fibers are used to reinforce a single type of resin. In this case, the MSS resin was reinforced with two different kinds of fibers. The first reinforcement was in the nano/micro form and randomly dispersed in the MSS resin (MFC) while the second reinforcement was unidirectionally aligned sisal fibers in the MSS resin reinforced with MFC. For the preparation of these hybrid-green composites, the dispersion of 30:70 MFC:MSS was prepared and crosslinked as per the procedure mentioned above in section 3.4. Two grams of control (untreated) and mercerized and heat treated sisal fibers (procedure mentioned in section 3.5) were used to prepare composite strips of 150 mm × 20 mm. The fibers were soaked in the precured (partially crosslinked) MSS containing dispersion of MFC and the excess resin was squeezed out using hand. This process of soaking and squeezing out the excess resin was repeated until all the parts of the fibers in the bundle were found to be satisfactorily impregnated with the resin. The fibers were then laid down straight on an aluminum plate in the form of a tape and allowed to dry at the room temperature. These are terms as prepregs. It took about 1 day for the prepregs to dry. It should be noted that the fibers in the prepregs should not

be bone dry. A small amount of moisture in it helps to obtain better adhesion between the resin and fibers and between the prepregs during the curing (hot pressing) process. On the other hand there should not be too much moisture in the fibers that the fibers start to lose their alignment in the resin while hot pressing. After drying, the prepregs were cured in the Carver hydraulic hot press (model 3891-4PROA00, Wabash, IN) for 20 min at 140 °C at 0.56 MPa pressure in order to obtain strong biobased hybrid composites. They were then washed and conditioned at 21 °C and 65% RH for its characterization. This washing step is important as it removes the catalyst which is highly hygroscopic and tends to absorb a lot of water when exposed to humid conditions.

3.7 Characterization of the Extracted Mango Seed Starch (MSS)

3.7.1 Chemical Analysis of the Starch

The 'as received' DMSK and specimens of MSS extracted after washing, grinding, sieving and drying were characterized for their chemical composition and, in particular, to study the increase in the starch content. All specimens were analyzed by Dairy One, Forage testing laboratory, Ithaca, NY. All the analyses were performed in triplicate to ensure the reproducibility and to obtain average values.

3.7.2 Rheological Properties of the Starch

The MSS obtained after extraction was studied for its rheological properties to obtain its gelatinization temperature. Advanced Rheometer-2000 (TA Instruments, New Castle, DE) equipped with a standard steel parallel plate with 60 mm diameter was used for this purpose. The gap between the plates was adjusted to 1000 μm and a shear rate of 20 s^{-1} was adjusted to study

the change in the viscosity of the starch as a function of temperature. The initial temperature was set to 20 °C and the final temperature was set to 95 °C, when gelatinization was expected to be complete. The temperature ramp rate of 20 °C min^{-1} was maintained.

3.8 Characterization of Crosslinked Starch Films Using Different Catalysts

3.8.1 Attenuated Total Reflectance- Fourier Transform Infrared (ATR-FTIR) Analysis

ATR-FTIR spectra were obtained to detect the ester groups formed due to crosslinking of the hydroxyl groups from starch and the carboxyl groups from BTCA, in the presence of the catalysts (both SHP and NaP) separately. The ATR-FTIR spectra were collected using Thermo Nicolet Magna-IR 560 spectrometer (Madison, WI) with a split pea accessory. Each scan was an average of 150 scans from 4000 cm^{-1} to 500 cm^{-1} wavenumbers.

3.8.2 Degree of Substitution

The degree of substitution was calculated for the films crosslinked with BTCA using both catalysts, SHP and NaP, using titration method.[41] Film with 1 cm × 1 cm dimensions was cut and placed in a sealed 100 ml vial containing 50 ml deionized (DI) water. The sealed vial with water and MSS in one and the two films crosslinked using different catalysts in separate vials were agitated in a shaker bath at 200 rpm for 4.5 days. The excess unreacted BTCA that leached out into the water was neutralized with standard sodium hydroxide solution using phenolphthalein as indicator. Excess standard NaOH (1 N, 10 ml) was added and shaken on a shaker bath for 1 h at 200 rpm to achieve homogeneous mixing. The entire set up was stored at 50 °C for 3 days with occasional shaking for complete hydrolysis. At the end of 3 days the excess alkali was back-titrated with standard HCl (0.4 M) solution. A blank (control) was simultaneously titrated with

MSS instead of crosslinked films. Degree of substitution was calculated using the following formula: [41]

% carboxylate = {[ml (blank) - ml (sample)] * normality of acid * 0.234100}/dry wt. of sample

Degree of substitution (DS) = 162 × % carboxylate/ [234 × 1000 − (233 × % carboxylate)]

3.8.3 Degree of Swelling

Degree of swelling of the crosslinked films was found using a slight modification of the method described by Niazi and Broekhuis.[109] Washed and dried MSS-BTCA-SHP, MSS-BTCA-NaP crosslinked films and the non-crosslinked (MSS-BTCA-No catalyst) films were weighed (W_i) and immersed in distilled water at room temperature until they reached an equilibrium after which they did not absorb any water. After 24 h, moisture on the surface was removed using Kimwipes® and the films were weighed (W_f). The specimens were immersed in distilled water again and weighed after 24 h or until they reached a point when the weight did not increase further. Degree of swelling was calculated using the formula,

Degree of swelling = $(W_f - W_i)/W_i$

3.8.4 Tensile Properties

The crosslinked starch resin films with the two catalysts, NaP and SHP, as well as without any catalyst were cut into rectangular pieces of 10 mm × 50 mm dimensions from different parts of the film to be tested for tensile properties using laser cutter. These cut films were conditioned for 2 days at ASTM standard conditions of 21 °C ± 1 °C and 65% ± 1% relative humidity before characterization. The tensile properties were characterized using Instron, model 5566 (Instron

Co., Canton, MA) according to ASTM D882-02 standards and tensile strength, tensile strain and Young's modulus were determined. The film thickness was measured using a vernier caliper at three different locations along the length of each conditioned film specimen and the average was used to calculate the mechanical properties. Roughly, the film thickness was found to be 0.50 mm ± 0.20 mm. The gauge length was adjusted to 30 mm and the strain rate was 0.6 min^{-1}. Specimens were tested from three different films of each type, cast at different times, to ensure reproducibility of the results. These specimens were cut from different parts of the films. At least three specimens from each of the three film were used for the calculation of average and standard deviation.

3.8.5 Differential Scanning Calorimetry

Differential scanning calorimetry (DSC) of the washed and unwashed MSS-BTCA-NaP film was studied, in a nitrogen environment, to characterize their thermal properties. To conduct the tests, DSC-2920 thermal analyzer (TA Instruments, Inc., New Castle, DE) was used and accurately weighed samples were placed, individually, in hermetically sealed aluminum pans. The specimens were scanned from 40 °C to 350 °C at a ramp rate of 10 °C/min, individually. MSS-BTCA-SHP crosslinked films were also characterized using the same procedure.

3.8.6 Thermal Degradation

Thermogravimetric analysis (TGA) of both MSS-BTCA-NaP and MSS-BTCA-SHP crosslinked films as well the MSS (powder) was performed to characterize the thermal degradation behavior of these crosslinked films as compared to MSS. TGA-2050, TA Instruments, Inc., New Castle, DE, was used for this purpose. Specimens weighing 5-10 mg

were scanned from 25 °C to 600 °C using the thermogravimetric analyzer at a heating ramp rate of 10 °C/min in nitrogen atmosphere to characterize their thermal stability and degradation behavior.

3.9 Characterization of Biocomposites

3.9.1 ATR-FTIR Analysis

ATR-FTIR spectra of BTCA, MFC and the crosslinked MSS resin and the composites were obtained to confirm the crosslinking reaction between MSS and MFC using BTCA as a crosslinker and NaP as a catalyst. Pure MSS and MFC were crosslinked separately using BTCA and NaP to check if BTCA can esterify MSS as well as MFC, individually. The ATR-FTIR spectra were collected using Thermo Nicolet Magna-IR 560 spectrometer (Madison, WI) with a split pea accessory. Each scan was an average of 150 scans from 4000 cm^{-1} to 500 cm^{-1} wavenumbers.

3.9.2 Surface Characterization

The fracture surfaces of the MFC-MSS biocomposites fractured during tensile testing were studied using LEO 1550 field emission scanning electron microscope (Germany). The specimens were placed on standard aluminum specimen mounts with double sided electrically conductive carbon tape (SPI supplies, West Chester, PA). In order to avoid charging, it was carbon coated in a Denton vacuum coater (model BTT IV, Denton Vacuum, Moorestown, NJ). The coated specimens were then observed on the SEM using accelerating voltage of 2 kV to study the fracture behavior of the composites and the surface topography of the protruding fibers.

3.9.3 Tensile Properties

The prepared biocomposites were characterized for their tensile properties to study the effect of addition of MFC to MSS. Composite films consisting of 0%, 20%, 30% and 40% MFC in the MSS resin were prepared and specimens of 50 mm × 10 mm were cut from different parts of the films. The specimens were conditioned for 1 day at ASTM standard conditions of 21 °C ± 1 °C and 65% ± 1% relative humidity before characterization. The tensile properties were characterized using Instron, model 5566 (Instron Co., Canton, MA) according to ASTM D882-02 standards and properties such as tensile strength, tensile strain and Young's modulus were determined. The film thickness was measured using a vernier caliper at three different locations along the length of each conditioned film specimen and the average of the three readings was used to calculate the mechanical properties. Roughly, the thickness was found to be 0.20 mm ± 0.10 mm. The gauge length was adjusted to 30 mm and the strain rate was 0.6 min^{-1}. Specimens were tested from three different films of each type, cast at different times, to ensure reproducibility of the results. These specimens were cut from different parts of the films to achieve random sampling. At least three specimens from each of the three films were used for calculating average and standard deviation values.

3.9.4 Thermal Degradation

Thermogravimetric analysis (TGA) of the 30:70 MFC:MSS biocomposite was performed to characterize their thermal stability and degradation characteristics. TGA-2050, TA Instruments, Inc., New Castle, DE, was used for this purpose. Specimens weighing 5-10 mg were scanned from 25 °C to 600 °C using the thermogravimetric analyzer at a heating ramp rate of 10 °C/min in a nitrogen atmosphere.

3.10 Characterization of the Mercerized and Heat Treated Sisal Fibers

3.10.1 Attenuated Total Reflectance - Fourier Transform Infrared (ATR-FTIR) Analysis

Thermo Nicolet Magna-IR 560 spectrometer (Madison, WI) with a split pea accessory was used to analyze the changes in the chemical composition of the sisal fibers after mercerization. Each scan was an average of 150 scans from 4000 cm^{-1} to 500 cm^{-1} wavenumbers. The ATR-FTIR spectra were obtained for both control and treated (mercerized and heat treated) fibers.

3.10.2 Surface Characterization

The surface properties the fibers before and after mercerization and heat treatment were studied using Tescan-Mira3 field emission FESEM, (Czech Republic). The specimens were placed on standard aluminum specimen mounts with double sided electrically conductive carbon tape (SPI supplies, West Chester, PA). Specimen surfaces were sputter coated with a thin layer of gold to prevent charging. These coated specimens were then observed on the SEM using accelerating voltage of 15 kV to study the surface topography of the fibers.

3.10.3 Tensile Properties

Tensile properties of sisal fibers were characterized using Instron, model 5566 (Instron Co., MA) as per ASTM D3822 standards. Control (untreated) and treated fibers were conditioned at 21 °C and 65% RH for 24 h before testing. Paper tabs were prepared as shown by Kim and Netravali[36] and single fibers were individually mounted on the paper tab using cyanoacrylate glue. Fiber diameter was measured at three different places on the fiber specimen within the 30 mm gauge length of the fibers to be tested and the average value was taken for calculations. Gauge length was adjusted to 30 mm and the strain rate as 0.6 min^{-1}. At least 25 fibers of each kind were tested to report the average and standard deviation.

3.11 Characterization of the Hybrid-Green Composites

3.11.1 Tensile Properties of the Hybrid-Green Composites

The mechanical properties of the hybrid composites were determined as per the ASTM D303-00 standard. The composites were first conditioned at 21 °C and 65% RH for 24 h. Then strips of the composites of 50 mm × 10 mm dimensions were cut and tested on Instron model 5566 (Instron Co., MA). The gauge length was set to 30 mm and the strain rate 0.6 min^{-1}. Nine specimens were tested from composite sheets fabricated at different times in order to ensure the reproducibility of the data.

3.11.2 Fracture Surface of Hybrid-Green Composites

The fracture surfaces of the composites made using control sisal fibers as well as mercerized and heat treated sisal fibers were studied using Tescan-Mira3 field emission SEM (FESEM). The fractured hybrid-green composite specimens were placed on standard aluminum specimen mounts with double sided electrically conductive carbon tape (SPI supplies, West Chester, PA). Specimen surfaces were sputter coated with a thin layer of gold to prevent charging. These coated specimens were then observed under the SEM using accelerating voltage of 15 kV to study the fracture behavior of the composites and surface topography of the protruding fibers.

CHAPTER 4: RESULTS AND DISCUSSION

4.1 Characterization of the Extracted Mango Seed Starch

4.1.1 Chemical Analysis of the Starch

Table 1 presents the proximate analysis of the chemical constituents of as received DMSK as well as the MSS extracted as per procedure mentioned in section 3.2. All tests were performed thrice to ensure that the values obtained were reproducible. As can be seen from Table 1, DMSK consists of carbohydrates, proteins, fibers, fats and ash. Since DMSK was obtained after oil extraction from the mango seeds, the fat content of DMSK was very low. Carbohydrates in DMSK exist in the form of simple sugars, water soluble carbohydrates and starch with the starch content of 43%. After repeated washing (removing water soluble carbohydrates and simple sugars) and vacuum filtration process a starch content of 59.5% was achieved in the MSS. This is an increase of about 40% compared to as received DMSK.

Table 1. Proximate chemical analysis of as received defatted mango seed kernels (DMSK) and extracted mango seed starch (MSS)

Constituents	**DMSK (%)**	**MSS (%)**
Moisture	11.4	3.2
Dry Matter	88.6	96.8
Starch	43.1	59.5
WSC (Water Soluble Carbs.)	12.9	6.3
ESC (Simple Sugars)	5.2	0.4
Crude Protein	6.3	6.8
Adjusted Crude Protein	6.3	6.8
Crude Fiber	3.3	3.1
Crude Fat	1.9	1.2
Ash	3.7	4.2

4.1.2 Rheological Properties of MSS

Figure 9 shows the viscosity plot for MSS as a function of temperature from 20 °C to 95 °C. As can be seen in Figure 9, the viscosity of MSS suddenly increased when the temperature reached 80 °C. Different starches have different inherent material characteristics including viscosity, gelatanization temperature and crystallinity because they have different crystalline arrangements.[30] Starch which exists in the form of granules is insoluble in water at room temperature but soluble at higher temperatures. High temperature of water disrupts the crystallinity of the starch structure as it breaks down the intermolecular forces present in the starch causing water to penetrate.[110] Water is first absorbed in the amorphous regions of the starch and the higher temperature breaks the crystalline region into separate amorphous regions causing diffusion of water into the crystalline regions as well. Starch granules swell as they absorb water and finally rupture. The increase in viscosity seen in Figure 9 is due to the rupture of the starch granules releasing the starch molecules in the solution. The process of rupturing of granules and releasing of starch molecules is known as gelatinization. The gelatinization temperature of MSS was found to be 80 °C. Above this temperature, with molecules opened up, the hydroxyl groups present on the glucose ring are easily available for any reaction. The gelatinization temprerature was higher than the commercial corn starch[111] of 71 ^{o}C and potato starch[112] of 65 ^{o}C. Higher gelatinizing temperature may be a characteristic of the MSS or a result of the impurities it contained, compared to the corn and potato starches mentioned above.

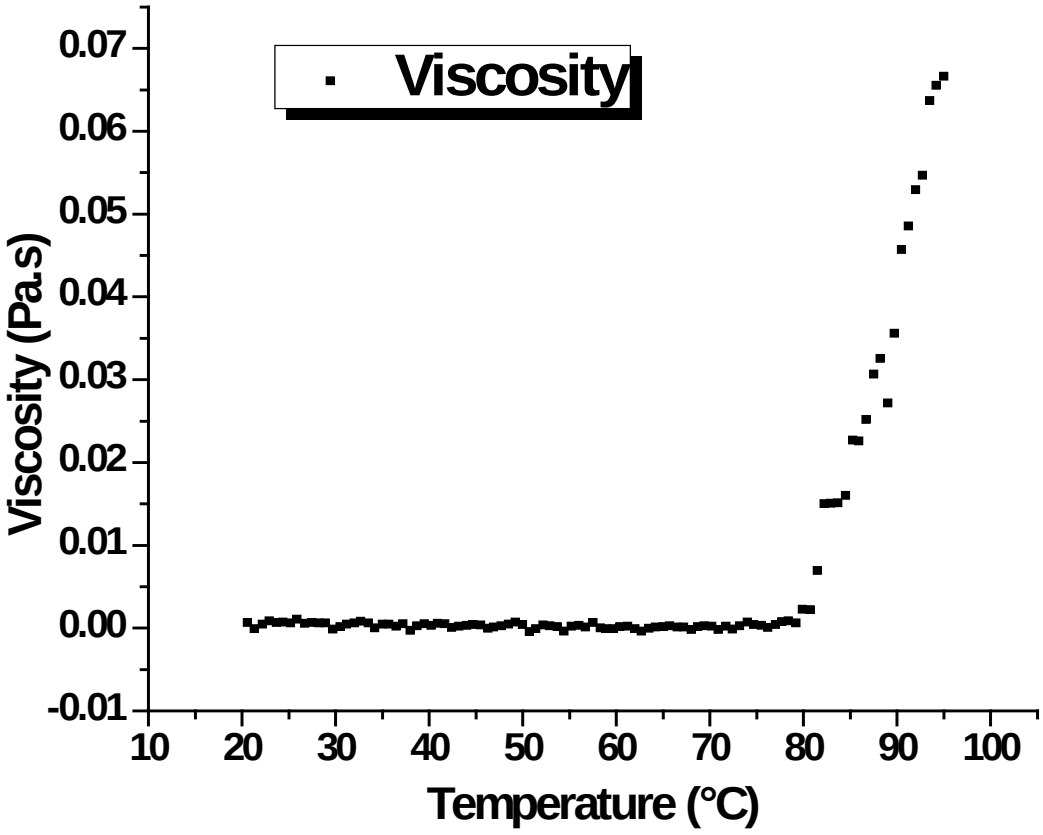

Fig. 9 Viscosity of MSS as a function of temperature from 20 °C to 95 °C

4.2 Characterization of Crosslinked Mango Seed Starch Resin using different Catalysts

4.2.1 Attenuated Total Reflectance - Fourier Transform Infrared (ATR-FTIR) Analysis

ATR-FTIR spectra of the crosslinked films using both the catalysts were studied to confirm the esterification reaction between the hydroxyl groups of the starch and the carboxyl groups of BTCA. The ATR-FTIR spectra of MSS, BTCA, MSS-BTCA-SHP and MSS, BTCA, MSS-BTCA-NaP films are presented in the Figures 10(a) and 10(b), respectively. The carboxyl carbonyl group of BTCA gives a sharp absorption peak at 1689 cm^{-1} while no such peak is possible, hence not seen, in MSS. The ATR-FTIR spectrum of MSS was similar to other

common starches such as waxy maize, corn and potato starch. These starches have been reported to have three C-O stretching peaks between 923 cm^{-1} and 1162 cm^{-1}.[30,41,51] The MSS-BTCA-SHP and MSS-BTCA-NaP crosslinked films showed peaks around 1715 cm^{-1} and 1716 cm^{-1}, respectively, which were neither observed in BTCA nor in MSS (Figures 10(a) and 10(b), respectively). This peak corresponds to carbonyl of the ester crosslink, thus, confirms the crosslinking. Ghosh Dastidar and Netravali[41] observed an ester carbonyl peak at 1725 cm^{-1} formed after crosslinking pure corn and potato starches with malonic acid whereas Reddy and Yang[50] observed the peak at 1724 cm^{-1} for corn starch crosslinked with citric acid. Both of them used SHP as a catalyst. BTCA has four reactive carboxyl groups and offers higher possibility for crosslinking. Starch has one primary hydroxyl group that is readily available for reaction with carboxylic group while two secondary hydroxyl groups are difficult to reach due to stearic hindrance. The esterification reaction between the carboxylic groups of acid and hydroxyl groups of starch proceeds faster in the presence of a catalyst. Welch[113] who earlier reported on the esterification of cellulose using BTCA stated that sodium salts catalyze the reaction and thereby reduce the reaction time and temperature.[113] BTCA was found to form a cyclic intermediate at temperature close to its melting point (190 °C) which can further react with the hydroxyl group from starch.[98] Sodium carboxylate acts as a catalyst for the esterification reaction as it helps the formation of cyclic anhydride at lower temperatures by weakening the hydrogen bond between the carboxylic groups of BTCA.[114] According to Harifi and Montazer[99] this reaction takes place in two steps. It first forms a cyclic anhydride by dehydration of two adjacent carboxylic groups. This anhydride intermediate then reacts with the hydroxyl group from the starch (shown in Scheme 1). Crosslinking occurs when there are more than one anhydride groups created on the acid. As BTCA has four carboxylic groups, it is possible to form more than one anhydride

intermediates. Thus BTCA is more efficient than citric acid which has only three carboxylic groups.[114,115] Both SHP and NaP catalyze the esterification reaction as the carbonyl peak from ester was observed at 1715 cm^{-1} using SHP and 1716 cm^{-1} using NaP. NaP is a sodium salt of weaker acid, propionic acid, as compared to SHP, which is a sodium salt of hypophosphorous acid. Propionic acid has a pKa of 4.8 while hypophosphorous acid has a pKa of 1.2. Being a stronger base compared to SHP, NaP dehydrates BTCA faster as compared to SHP to form cyclic anhydrides and, thus, provides higher crosslinking efficiency. This was also confirmed by the higher degree of substitution (DS) as well as by reduced swelling behavior in water obtained for the crosslinked starch when NaP was used as the catalyst. The pH of the reaction using NaP as a catalyst was found to be 3.75 ± 0.2, which was higher compared to that obtained when SHP was used as a catalyst which was found to be 2.3 ± 0.1. From these observations it can be concluded that NaP is able to produce carboxylate esters faster as compared to SHP. This carboxylate ester peak was detected at 1560 cm^{-1}. Three types of carbonyl groups can be seen when esterification reaction occurs: a) the carbonyl peak from the ester formed due to reaction between BTCA and starch, b) the carbonyl peak from unreacted BTCA and c) the carbonyl peak form carboxylate anions. The former two peaks, ester and carboxylic group, are overlapped in the peak at 1716 cm^{-1} while the carboxylate peak appears at 1560 cm^{-1}. Figure 11 shows ATR-FTIR spectrum of the MSS-BTCA-NaP crosslinked film after treating with 0.1 M NaOH. The peak at 1560 cm^{-1} grows sharper when treated with 0.1M NaOH because it converts the anhydride groups into sodium carboxylate.[116] Thus separating and confirming the ester carbonyl peak observed at 1716 cm^{-1}. The ester group (peak observed at 1716 cm^{-1}) is hydrolyzed in the presence of an alkali. Thus the peak at 1716 cm^{-1} reduces when treated with NaOH while the peak at 1560 cm^{-1} grows sharper due to the formation of sodium carboxylates.

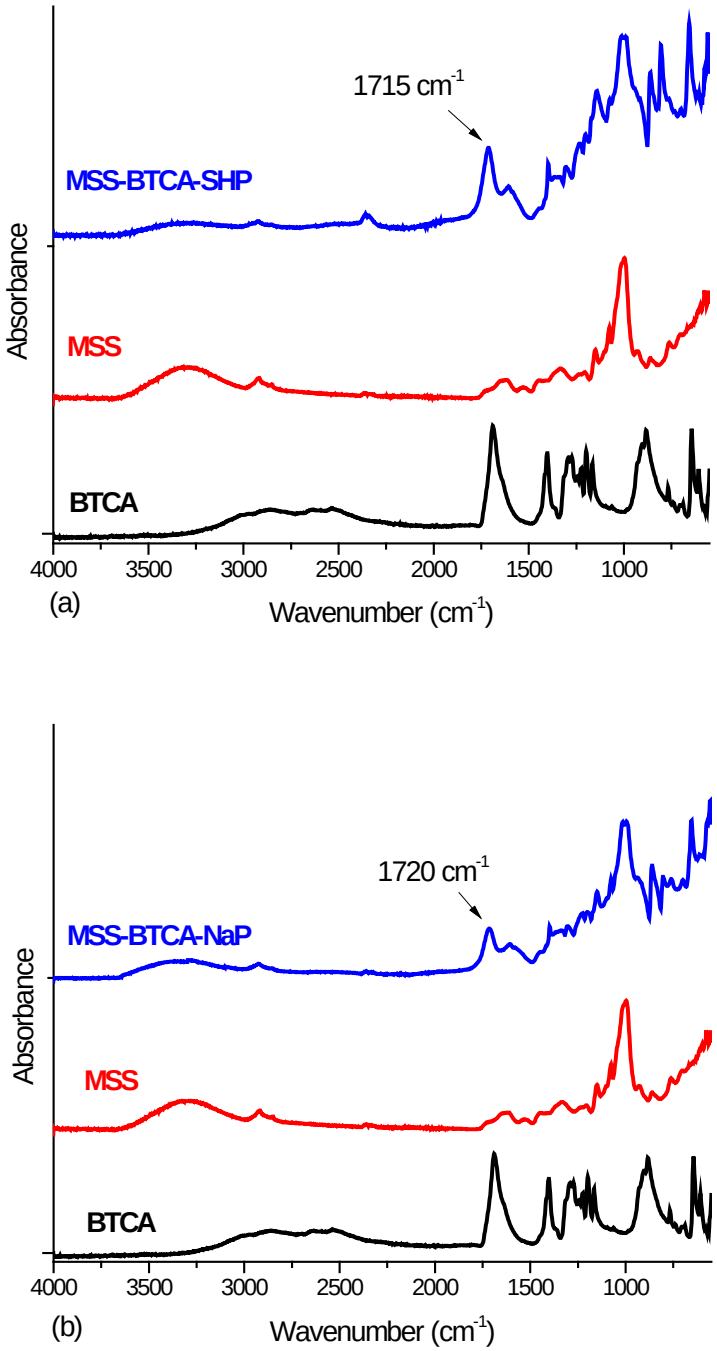

Fig. 10 ATR-FTIR spectra of (a) BTCA, MSS, MS-BTCA-SHP crosslinked film and (b) BTCA, MSS, MSS-BTCA-NaP crosslinked film

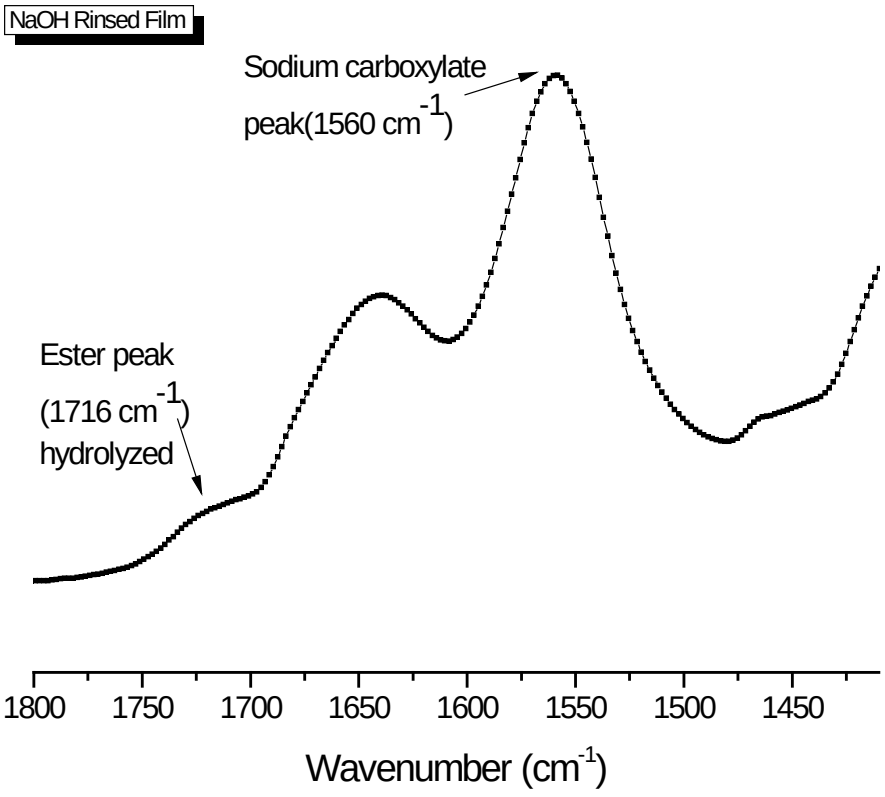

Fig. 11 ATR-FTIR spectrum of the MSS-BTCA-NaP crosslinked film after treating with 0.1 M NaOH

4.2.2 Degree of Substitution

Degree of substitution (DS) is the number of substituent groups attached per monomeric unit. The monomeric unit of starch consists of the D-glucopyranosyl ring with three hydroxyl groups. Thus the DS of starch may range from zero (pure starch, no substitution) to three (fully substituted). However, it is known that only the primary hydroxyl (C6) is readily available for reaction as compared to the other two hydroxyl groups (C2 and C3).[41] The DS of MSS-BTCA-NaP and MSS-BTCA-SHP films were calculated as per the method described earlier.[41] Figure 12

shows the DS of MSS-BTCA-SHP and MSS-BTCA-NaP crosslinked films with 40% BTCA as a function of curing temperature. It was observed that the DS increases significantly with the curing temperature. This is expected because most crosslinking occurs during hot pressing and the esterification reaction requires high temperature. The DS increased from 0.20 to 0.65 as the reaction temperature was increased from 120 $^{\circ}$C to 140 $^{\circ}$C for the MSS-BTCA-NaP crosslinked films while it increased from 0.18 to 0.53 for MSS-BTCA-SHP crosslinked films. Overall, the DS of MSS-BTCA-NaP crosslinked film was found to be significantly higher than that for MSS-BTCA-SHP films at 130 $^{\circ}$C and 140 $^{\circ}$C while no significant difference was observed at 120 $^{\circ}$C. The DS for MSS-BTCA-NaP crosslinked film was higher than MSS-BTCA-SHP crosslinked film at higher temperature because NaP dehydrates BTCA faster as compared to SHP. As a result, the rate of cyclic anhydride formation with NaP increases as compared to that using SHP. These anhydrides react when they come in the vicinity of the exposed hydroxyl groups from the MSS molecules and crosslink it. This results in higher crosslink density forming a tighter network. While NaP resulted in higher DS, the DS numbers of this non-edible starch are close to those found by other researchers. For example, the DS of pure corn starch and pure potato starch crosslinked with 37.5% malonic acid has been reported to be 0.10 and 0.19 respectively.[41] Zhang et al.[117] used a strong dicarboxylic acid (oxalic acid) and obtained DS between 0.08 to 0.87 depending on the starch variety and the acid molar ratio used. They also reported that, in general, it is difficult to obtain high DS by just using organic acids. For higher DS fatty anhydrides are more desirable.[117]

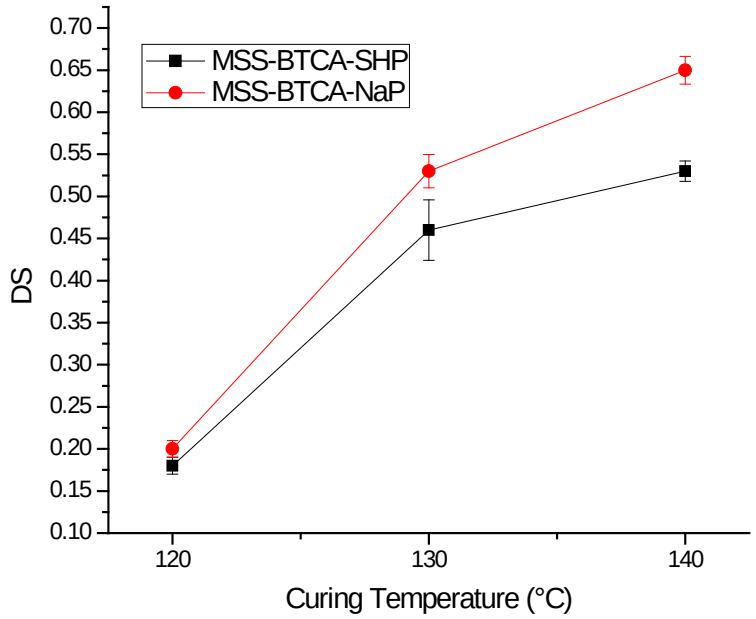

Fig. 12 DS of MSS-BTCA-SHP and MSS-BTCA-NaP crosslinked films with 40% BTCA as a function of curing temperature

4.2.3 Degree of Swelling

Degree of swelling was determined for MSS-BTCA-NaP, MSS-BTCA-SHP crosslinked films as well as the non-crosslinked (MSS-BTCA-No catalyst) films. Figure 13 shows the photographs of the crosslinked and the non-crosslinked films immersed in water at room temperature for 3 days. At the end of 3 days, it was observed that the crosslinked films did swell in water but remained intact (Figure 13a) while the non-crosslinked films disintegrated and the water became brownish as the MSS broke into pieces and the powdery part mixed with the water (Figure 13b). Prior to breaking the non-crosslinked film was observed to be highly swollen compared to the crosslinked one as water got readily absorbed by the film. As discussed earlier, starch contains hydroxyl groups which attract and retain water causing the films to swell. Crosslinking of starch converts the hydroxyl groups to ester groups by covalently bonding two molecules and forms a

tight network structure which restricts the water from entering the structure. Also, the newly formed ester group is hydrophobic compared to the hydrophilic hydroxyl group which it replaces. Both these changes; tighter network and ester groups, result in reduced moisture absorption and lower degree of swelling. Figure 14 shows the degree of swelling of MSS-BTCA-SHP and MSS-BTCA-NaP crosslinked films. As seen in Figure13b, the film without catalyst disintegrates and very tiny pieces that leach out. As a result, it was not possible to weigh the films after 3 days. The weight of these 2 pieces together was found to be less than the crosslinked piece that was put in because some MSS was lost in the water. While both NaP and SHP act as catalyst, as seen earlier results of the DS, NaP results in higher DS. This is clearly reflected in the swelling behavior of the crosslinked starch. As can be seen in Figure 14, the degree of swelling is higher when the starch is crosslinked using SHP as a catalyst as compared to NaP. When the crosslinked films were immersed in water, the MSS-BTCA-NaP films reached equilibrium in 24 h and no significant additional swelling was noticed. Whereas the MSS-BTCA-SHP films took almost 72 h to reach equilibrium and the degree of swelling was significantly higher.

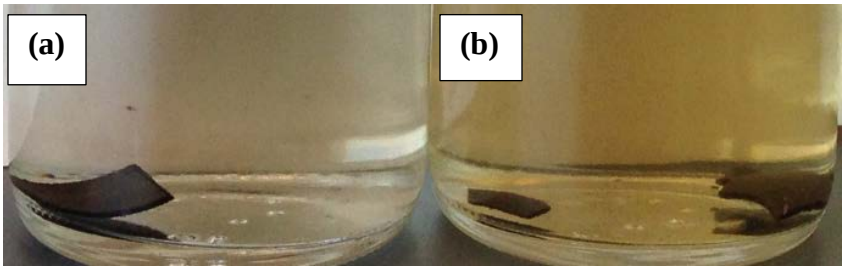

Fig. 13 Photographs of (a) MSS-BTCA-NaP crosslinked film and (b) non-crosslinked (MSS-BTCA-No catalyst) film immersed in water for 3 days at room temperature

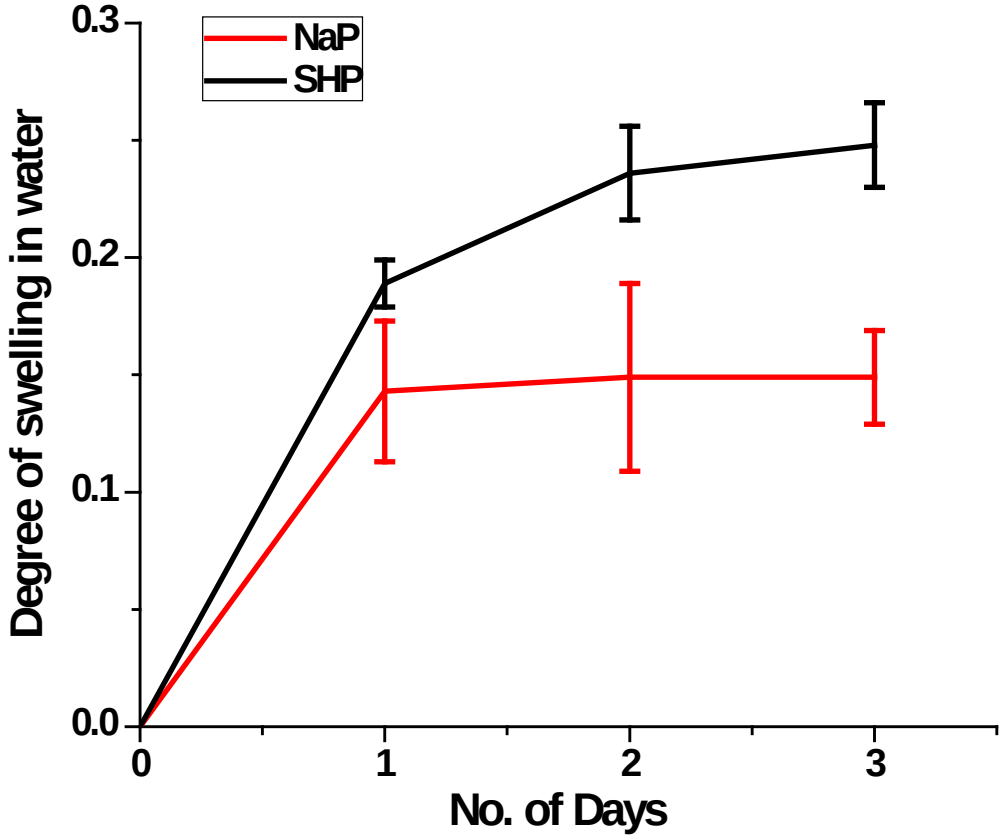

Fig. 14 Degree of swelling of MSS-BTCA-SHP and MSS-BTCA-NaP crosslinked films

4.2.4 Tensile Properties

Figure 15 shows typical stress vs strain plots of MSS-BTCA-NaP, MSS-BTCA-SHP, as well as control (non-crosslinked i.e. MSS-BTCA-No catalyst) films. The plots clearly indicate the differences due to the differing catalyzing efficiencies of SHP and NaP. The mechanical properties like tensile stress (strength), tensile strain, and Young's modulus of the films obtained are summarized in Table 2. Without any catalyst, esterification reaction can take place but at an extremely slow rate and requires high temperature and much longer time for reaching

equilibrium.[118] This is clearly reflected in tensile properties of the films. When MSS was reacted with BTCA without any catalyst for 1 h at 90 °C, strength was found to be very low (3.5 MPa) while the strength values of the crosslinked films formed using SHP or NaP at the same temperature and time were much higher, 8.8 MPa and 12.38 MPa, respectively. The tensile strain was found to be similar for both crosslinked films. As reported by Harifi and Montazer,[114] without any catalyst, BTCA requires much higher temperature of around 190 °C to form cyclic anhydrides which can in turn crosslink MSS by reacting with the hydroxyl groups. Since the reaction was carried out using water as a solvent in this study, it was not possible to reach 190 °C. Further, using catalyst results in higher crosslinking which, in turn, improves the mechanical properties. The Young's modulus values were also found to increase, as expected, when a catalyst was used along with the crosslinker. As discussed earlier, strong covalent ester bond formation through crosslinking was confirmed by ATR-FTIR spectra. This rigid crosslinked 3-D network structure also restricts moisture absorption which further enhances the tensile properties.[41,51] While both SHP and NaP improve the mechanical properties, NaP results in higher tensile properties confirming that NaP is a better catalyst. The strength and Young's modulus of the MSS-BTCA-NaP films were found to be 40% and 37% higher, respectively, compared to the values obtained for MSS-BTCA-SHP films. The tensile properties of these crosslinked biobased MSS resins were found to be comparable to other edible starch like waxy maize starch. Ghosh Dastidar and Netravali[51] reported the strength of crosslinked waxy maize starch film to be around 17 MPa and modulus of 1.7 GPa. The strength and modulus of MSS-BTCA-NaP was found to be higher than other biobased resins derived from agricultural waste such as protein derived from neem or karanja seed cake.[28,29] The fracture strain values were not significantly changed after crosslinking. The stress vs strain plots of all specimens showed no

yielding and the films were brittle with the highest fracture strain of only 1.64%. It should be noted that no plasticizer was used in preparing these sheets. Most of the earlier researchers used plasticizers to improve the fracture strains and the toughness of the starch based films, crosslinked or not.[28,29,51]

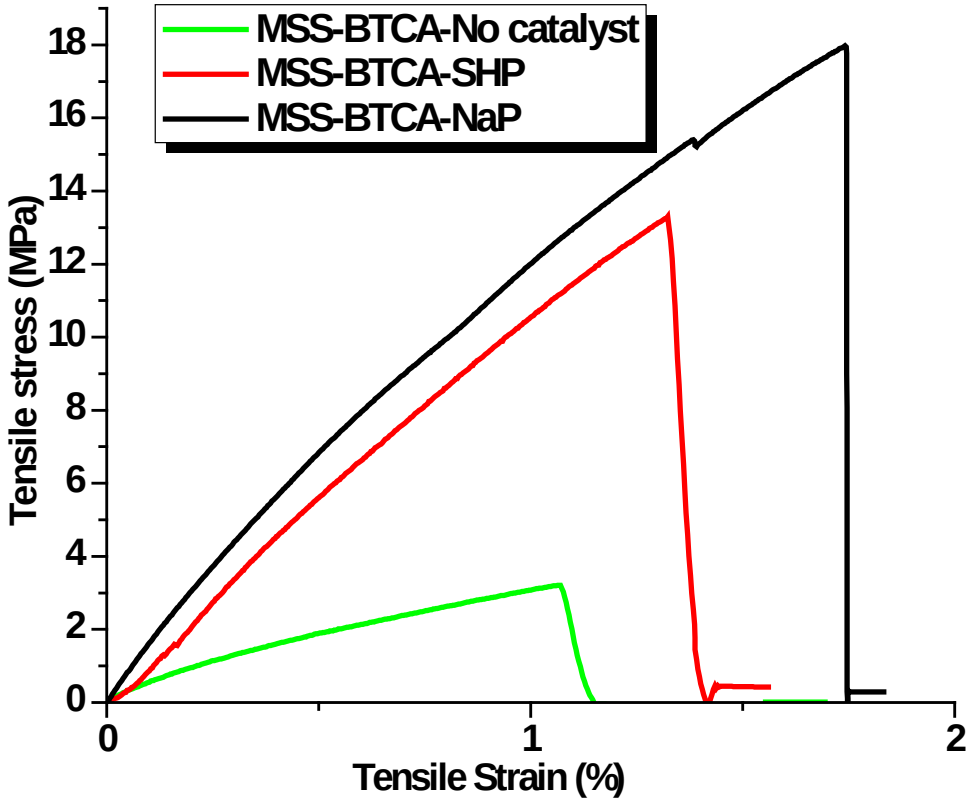

Fig. 15 Typical stress vs strain plots of MSS-BTCA-NaP, MSS-BTCA-SHP and MSS-BTCA-No catalyst films

Table 2. Tensile properties of the MSS-BTCA-No catalyst, MSS-BTCA-SHP, MSS-BTCA-NaP crosslinked films

MSS-BTCA-(Catalyst)	**Fracture stress (MPa)**	**Fracture strain (%)**	**Young's modulus (MPa)**
No catalyst	3.52 (0.06)*	1.34 (0.05)*	298 (6.35)*
SHP	8.82 (3.33)	1.41 (0.30)	897 (281)
NaP	12.38 (3.92)	1.64 (0.36)	1232 (402)

* The numbers in parentheses are standard deviations

4.2.5 Differential Scanning Calorimetry

Figure 16 (a) and 16 (b) show typical DSC thermograms of washed and unwashed MSS-BTCA-NaP and MSS-BTCA-SHP crosslinked films, respectively. The DSC thermograms of unwashed crosslinked films show a sharp peak at 300 °C corresponding to the melting point of the catalyst (NaP). This peak disappears after washing. This suggests that almost all of the catalyst has been removed by washing in water. This is most likely to occur since NaP is highly water soluble. The DSC thermograms of unwashed films show an endothermic peak at 190 °C corresponding to the melting temperature of BTCA. This means that excess unreacted BTCA was present, in crystalline form, even after carrying out the reaction. This peak corresponding to BTCA also disappeared after washing the films indicating that unreacted BTCA can also get washed out (Figure 16a). In the case of DSC thermograms obtained for MSS-BTCA-SHP films similar peak was observed (Figure 16b). Figure 17 shows the DSC thermograms of the washed MSS-BTCA-NaP and washed MSS-BTCA-SHP films from 25 °C to 220 °C. As seen in Figure 17, the DSC thermograms look similar for both films with no peak seen until about 220 °C which is the degradation temperature of the crosslinked starch. This confirms the TGA results that are discussed later. The absence of any peaks before degradation indicates the absence of

any crystals (e.g. starch or BTCA melting) in the starch films after washing, perhaps because of the gelatinization of starch prior to crosslinking and absence of BTCA.

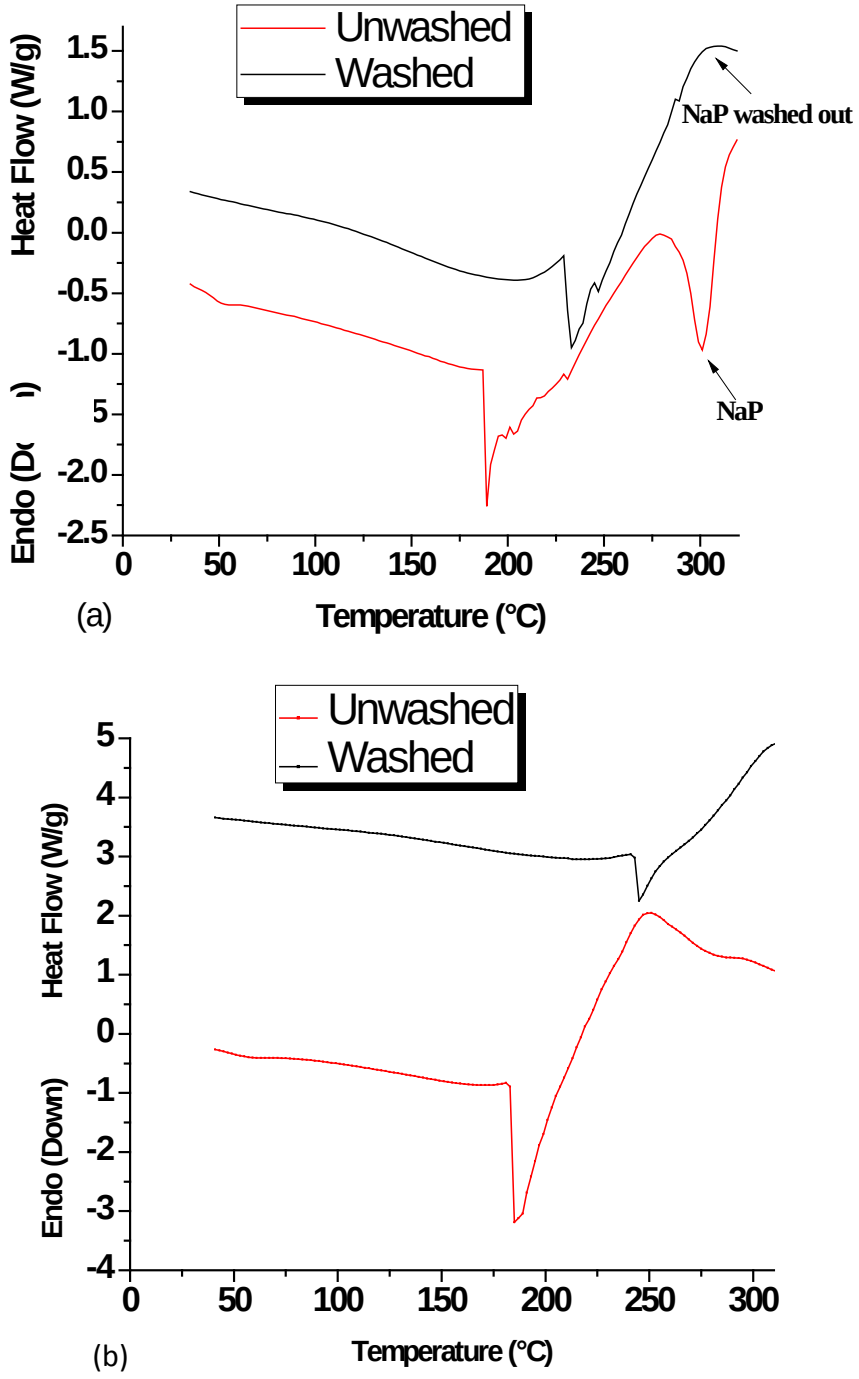

Fig. 16 DSC thermograms of washed and unwashed crosslinked films (a) MSS-BTCA-NaP (b) MSS-BTCA-SHP

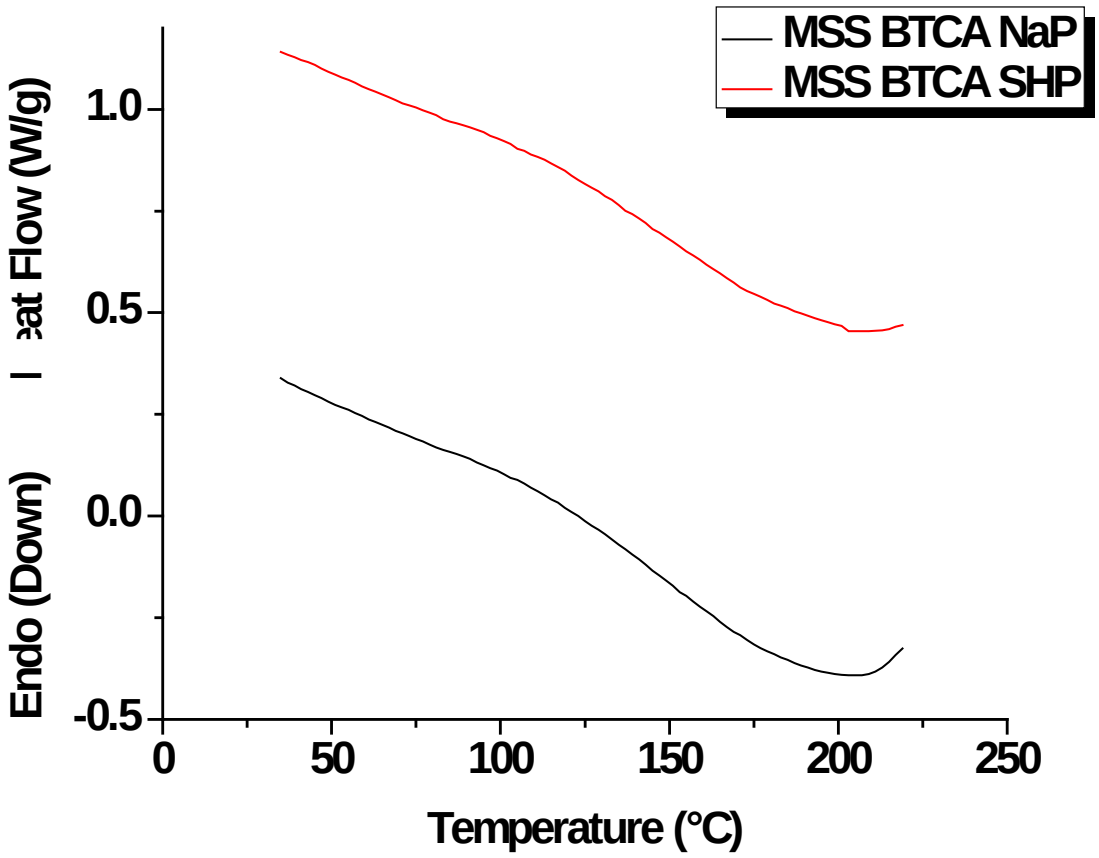

Fig. 17 DSC thermogram of washed and unwashed MSS-BTCA-SHP crosslinked films.

4.2.6 Thermal Degradation

Thermogravimetric analysis (TGA) was performed to characterize the thermal stability and weight loss of MSS and crosslinked (MSS-BTCA-NaP and MSS-BTCA-SHP) films. The TGA thermograms of MSS and the two crosslinked films are shown in Figure 18(a). Differential TGA (DTGA) plots were constructed from the TGA thermograms and are shown in Figure 18(b). As seen in Figure 18(a), MSS starts to degrade (onset degradation temperature, T_d) at 250 °C and the maximum degradation temperature defined as the temperature at which the rate of weight loss reduces significantly, after the specimen has degraded, (the peak in the DTGA plot, shown in Figure 18b) was found to be around 315 °C. This behavior is similar to the commerically

available waxy maize starch.[51] It was observed that the T_d (220 °C) was same for both the crosslinked films (Figure 18a) indicating that the thermal degradation characteristics of the films formed by using the two catalysts, SHP and NaP, were identical. This is perhaps because after the completion of the crosslinking reaction, unreacted BTCA and the catalyst were removed by the washing process. Thus both crosslinked films, consisted of similar network structure. The T_d of the crosslinked MSS was around 220 °C which was lower than that observed for MSS (250 °C). This might be due to the presence of few partially reacted carboxylic groups of BTCA which decompose at lower temperature. Similar behavior was observed by Zhang et al.[117] who esterified corn starch using oxalic acid. In their work gelatanized corn starch showed a T_d of 278 °C while after esterification with oxalic acid (DS of 0.87), the T_d reduced to 204 °C.[117] They also claimed that the reduction in T_d was due to the low thermal stability of unreacted carboxylic groups.[38] The T_d values of both MSS-BTCA-NaP and MSS-BTCA-SHP crosslinked films in this study were higher than that of corn starch crosslinked with oxalic acid. Also, crosslinking significantly reduced the percentage of degradation or the weight loss. As can be seen in Figure 18(a), MSS lost 67% of its weight at 350 °C, whereas after crosslinking, only 41% weight loss was observed. The maximum degradation temperature (defined as the temperature at which the degradation rate decreases) of MSS was 315 °C which reduced to 295 °C after crosslinking (Figure 18b). In this study the films crosslinked using SHP and NaP catalysts showed same T_d and maximum decomposition temperatures. This is because both of them alter the chemical structure of starch by forming ester bonds and also result in similar network.

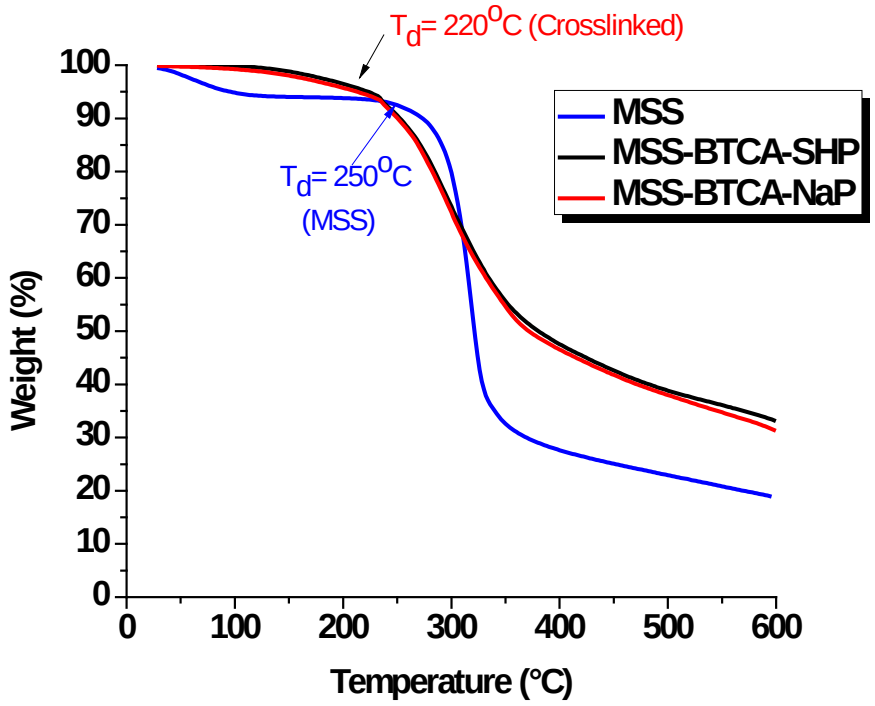

Fig. 18(a) TGA of MSS, MSS-BTCA-SHP and MSS-BTCA-NaP crosslinked films

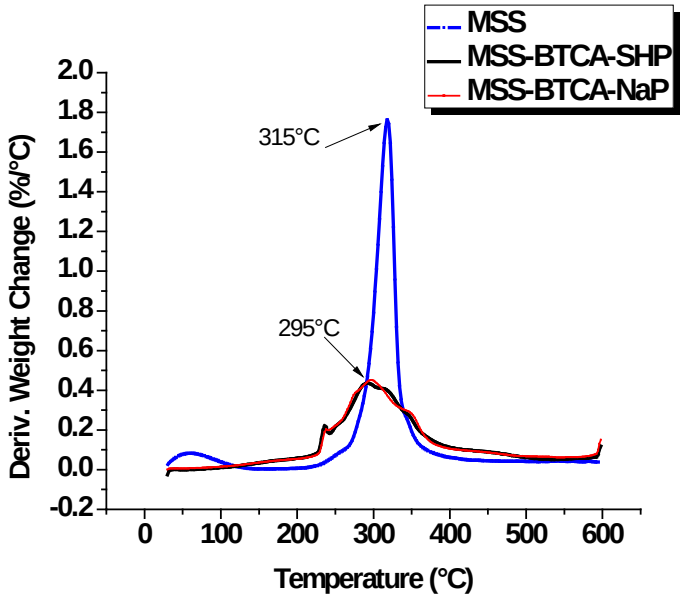

Fig. 18(b) DTGA of MSS, MSS-BTCA-SHP and MSS-BTCA-NaP films

4.3 Characterization of Biocomposites

4.3.1 Attenuated Total Reflectance-Fourier Transform Infrared (ATR-FTIR) Analysis

ATR-FTIR analysis was carried out to confirm the crosslinking reaction of BTCA with starch and cellulose (MFC). Figure 19 shows ATR-FTIR spectra of BTCA, MSS, MSS-BTCA-NaP, MFC-BTCA-NaP, 30:70 MFC:MSS biocomposite crosslinked using BTCA-NaP. As seen in Figure 18, the sharp peak at 1689 cm^{-1} observed in BTCA was completely shifted to a small peak at 1716 cm^{-1} for the MSS-BTCA-NaP crosslinked film. No such peak is observed in MSS. Thus, the peak at 1716 cm^{-1} indicated the formation of ester groups due to the crosslinking reaction between hydroxyl groups of the MSS and the carboxylic acid groups of BTCA. BTCA and NaP have been successfully used to crosslink cellulose earlier.[119] Thus, BTCA can be used to crosslink MFC as well which is pure cellulose. To confirm this pure MFC was reacted with BTCA and NaP in order to study the crosslinking of MFC. As seen in Figure 19, a peak at 1712 cm^{-1} was observed when MFC was reacted with BTCA and NaP and cured at 140 °C. No such peak at 1712 cm^{-1} was present in pure MFC due to the absence of any carbonyl groups. Crosslinking of cellulose using BTCA as crosslinker and NaP as catalyst requires high temperature as compared to starch. While BTCA can crosslink starch at 120 °C, minimum temperature of 140 °C was required to crosslink MFC. When the crosslinking or curing of the MFC-MSS nanocomposite was carried out at 140 °C in hydraulic hot-press carbonyl peak from ester at 1712 cm^{-1} was observed. No shift in the carbonyl peak from carboxylic acids observed at 1869 cm^{-1} was observed by Dastidar and Netravali[51] when curing was done at 120 °C for MFC crosslinked using BTCA as a crosslinker and Sodium hypophosphite (SHP) as a catalyst. However, when the curing temperature was increased to 140 °C using NaP as the catalyst instead of SHP with BTCA, in this study, a shift in peak from carbonyl acid region to ester region was

observed. Curing above 140 °C can be beneficial for crosslinking MFC using BTCA. However, since it's a composite of MFC and starch, it was cured at 140 °C to avoid degradation of MSS. The composite film made by crosslinking the dispersion of MFC in MSS using BTCA (crosslinker) and NaP (catalyst) and cured at 140 °C for 15 min showed a peak at 1716 cm^{-1} which was similar to the peak observed in crosslinked MSS. This confirms that when BTCA can crosslink MFC and MSS separately, it can be used to crosslink MFC and MSS together when mixed together. The proposed crosslinking or the esterification reaction between MSS and MFC using BTCA as a crosslinker and NaP as a catalyst is shown in Figure 20. The crosslinking reaction takes place in two steps. As seen in Figure 20, it forms a cyclic anhydride by dehydration of two adjacent carboxylic groups in step 1. This anhydride intermediate then reacts with the hydroxyl group from the starch and cellulose to crosslink them. (Step 2).

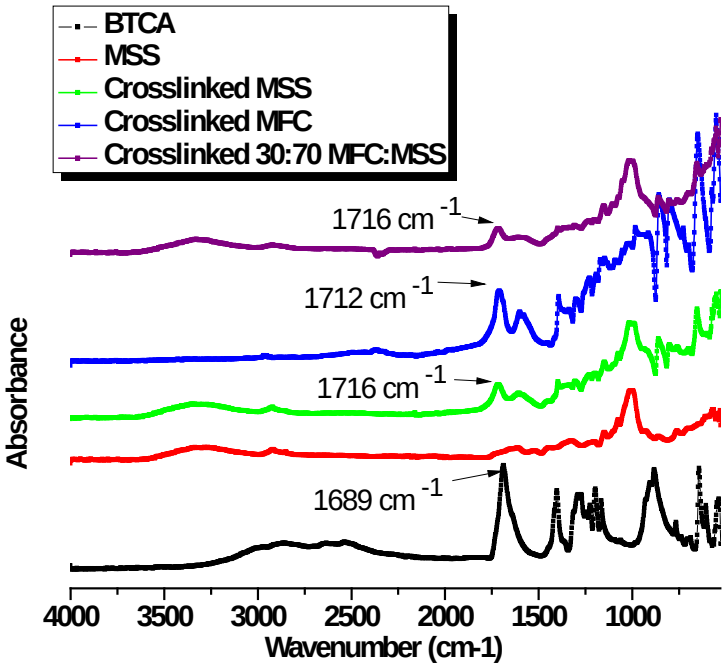

Fig. 19 ATR-FTIR spectra of BTCA, MSS, MSS-BTCA-NaP, MFC-BTCA-NaP, 30:70 MFC:MSS composite crosslinked using BTCA-NaP.

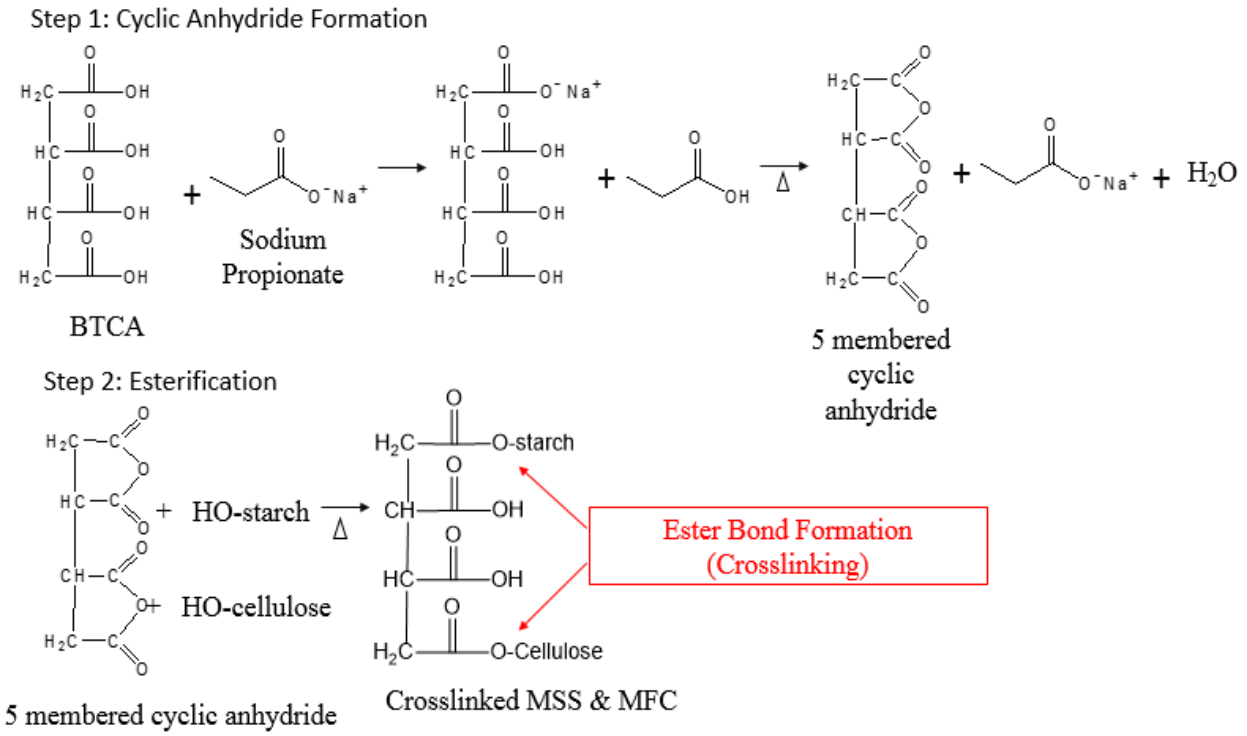

Fig. 20 Proposed crosslinking reaction between MSS and MFC using BTCA as a crosslinker and MFC as a catalyst.

4.3.2 Scanning Electron Microscopy of Fracture Surfaces

Figure 21 shows the fracture surfaces of MSS-MFC biocomposites with different MFC loadings that were fractured during the tensile tesing. Figure 21(a) shows the fracture surface of the MSS crosslinked resin without any MFC. The fracture surface of crosslinked resin is smooth as there are no fibers. The SEM images of the MSS-MFC biocomposites in Figures 21(b), 21(c) and 21(d) show that MFC has been embedded well into the MSS resin. This is due to the crosslinking of resin (MSS) and fibers (MFC) using BTCA and NaP. The crosslinking between MSS and MFC was confirmed using ATR-FTIR spectra and presented earlier in Figure 19. Also, the similar chemical structure of starch and cellulose leads to the strong hydrogen bonding. Ghosh Dastidar and Netravali[51] crosslinked MFC using BTCA and studied the cured film under

the SEM. They observed that the BTCA spreads on the MFC surface, but, no crosslinking absorption peak (ester peak) was detected in ATR-FTIR spectroscopy. This was because the curing was done at 120 °C, which is not sufficient to crosslink cellulose using BTCA. Curing the MFC-BTCA-NaP films at 140 °C in this study showed the ester absorbtion peak at 1712 cm^{-1} seen in Figure 18 in section 4.3.1. The fracture surface of the MSS-MFC biocomposites was rougher due to the presence of the fibers. The roughness of the surface increased with the increase in the fiber loading. Figures 21(b) and 21(c), which show fracture surfaces of 20:80 MFC:MSS and 30:70 MFC:MSS crosslinked composites, respectively, show partially smooth surface representing the crosslinked resin and partially rougher surface representing the MFC microfibrils used as a reinforcement phase in the resin. However, as seen in Figure 21(d) for 40:60 MFC:MSS composites, the surface is much rougher. This means that as the MFC loading increases to 40%, the porous MFC structure dominates the composite film properties and the crosslinked MSS occupies the voids within the porous MFC network.

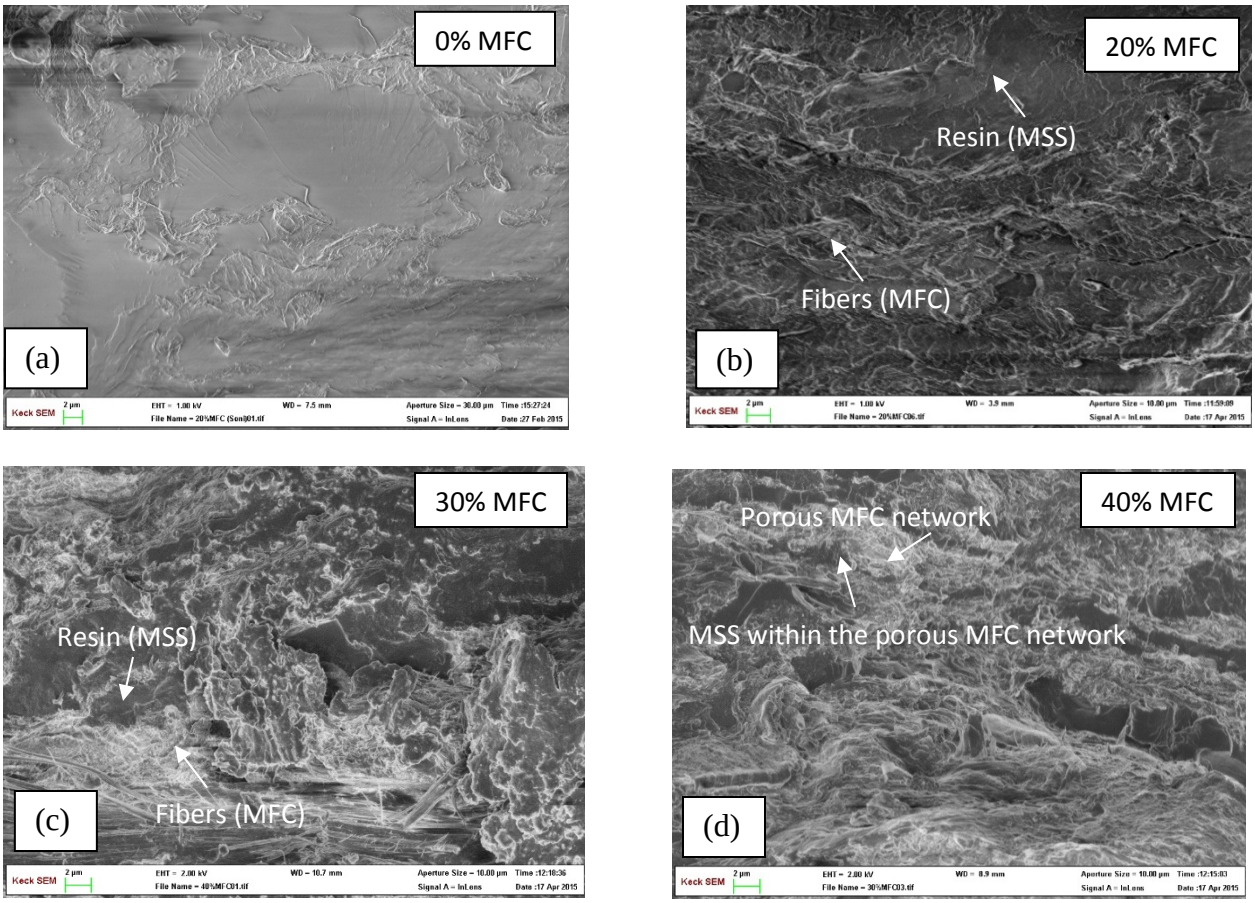

Fig. 21 Fracture surface of MSS-MFC biocomposites fractured during tensile tesing

4.3.3 Tensile Properties

Figure 22 shows the typical stress vs strain plots of crosslinked MSS resin and MFC:MSS biocomposites with different MFC contents (0%, 20%, 30%, and 40%). The plots show the effect of addition of MFC to MSS resin. A significant increase in the strength and Young's modulus values was observed with the addition of MFC to the MSS resin. The tensile properties such as fracture stress (strength), fracture strain and Young's modulus of crosslinked MSS resin and MFC:MSS biocomposites with different MFC contents (0%, 20%, 30%, and 40%) are summarized in Table 3. Higher tensile properties were observed with the addition of MFC which itself has excellent tensile properties. In addition, MFC has a very high surface area which leads

to increased interfacial area. Higher interfacial area along with the chemical similarity between cellulose and starch that provides ample hydrogen bonding between the two which leads to strong adhesion between MFC and the resin. A strong covalent bond can also be expected due to crosslinking between MSS and MFC through BTCA as explained earlier. The proposed crosslinking reaction has been shown earlier in Figure 20 and confirmed using ATR-FTIR spectra shown in Figure 18. Excellent fiber/resin bonding was also seen in the SEM images of fracture surfaces (Figure 21) which showed no protruding MFC fibrils. Excellent fiber/resin bonding contributes to an effective load transfer and results in higher strength and the Young's modulus of the composites.[120] When MFC content was increased from 0% (control) to 20 and 30%, the fracture strain of the composites increased from 1.65% (control) to about 3.9%. This is perhaps because of the crack bridging mechanism provided by the MFC. However, at 40% MFC, with slight clustering, the fracture strain decreased to 2.65%. Moisture content, however, decreased steadily with the MFC content. This is due to the fact that MFC is highly crystalline and does not provide space for the moisture. It, in fact, acts as a barrier for moisture. Uniform dispersion of MFC is the key to improve the strength and the modulus of the composites. Almost 35% increase in the modulus was obtained by adding 20% MFC to the MSS resin while it increased by 45% with 30% MFC addition. Significant improvement in the properties was obtained by adding 40% MFC which resulted in almost 95% increase in Young's modulus. Similar behavior was observed by Dastidar and Netravali[51] by adding MFC to waxy maize starch. They reported that MFC can act as crack-bridging mechanism and could be a potential substitute to commonly used plasticizers like glycerol or sorbitol for toughening, while also strengthening the resin. The properties of MFC reinforced crosslinked MSS resin composites were found comparable to the edible starch based resins such as potato, corn and waxy maize

starch[41,51] Thus, it is interesting to see the properties of crosslinked MSS and MFC because of the favorable fiber/resin interaction and excellent dispersion of MFC and MSS as both are hydrophilic polymers in nature. These results clearly show that crosslinking of MSS obtained from waste source and by adding MFC it can provide a resin with excellent mechanical properties. Such inexpensive resin can easily replace the resins prepared from edible starch sources for applications in packaging or as resins for fiber reinforced composites. The MSS resin, thus, can reduce the use of edible starches in non-edible applications.

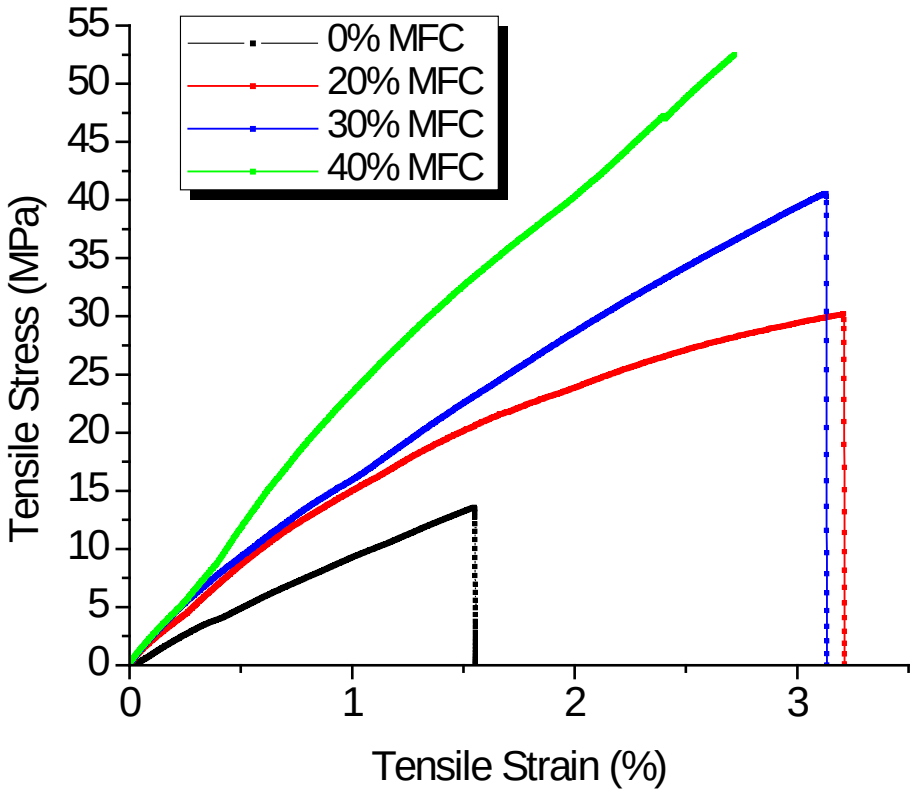

Fig. 22 Typical stress vs strain plots of crosslinked MSS resin and MFC:MSS biocomposites with different MFC contents (0%, 20 %, 30 %, and 40 %)

Table 3. Tensile properties of crosslinked MSS resin and MFC:MSS biocomposites with different MFC contents (0%, 20 %, 30 %, and 40 %)

MFC:MSS	Fracture stress (MPa)	Fracture strain (%)	Young's modulus (MPa)	Moisture content (%)
0:100	12.38 (3.92)*	1.64 (0.36)*	1232 (402)*	8.8
20:80	31.17 (7.01)	3.80 (0.72)	1667 (275)	7.3
30:70	38.69 (3.00)	3.95 (0.77)	1780 (221)	6.0
40:60	50.03 (1.97)	2.65 (0.13)	2407 (063)	5.8

* The numbers in parentheses are standard deviations

4.3.4 Thermal Degradation

The thermal stability of the MSS-MFC biocomposites was examined using thermogravimetric analysis (TGA). Figure 23(a) shows typical TGA thermograms of MSS, crosslinked MSS and the crosslinked MSS-MFC composites. DTGA thermograms, constructed from the TGA thermograms of MSS, crosslinked MSS and the crosslinked MSS-MFC biocomposites, are presented in Figure 23(b). As can be seen in Figure 23(a), the onset degradation temperature (T_d) was same for the crosslinked MSS resin as well as the crosslinked MSS-MFC biocomposite, both of which, however, were slightly less than the non-crosslinked MSS. This is due to the presence of some half reacted carboxylic groups from BTCA.[51] This has been discussed earlier, in depth, in section 4.2.6. The addition of MFC does not alter T_d of the composite because the thermal stability of MFC is not significantly different than that of starch.

It was observed that the weight loss reduced after crosslinking MSS and further on addition of MFC. At 500 °C, 80% weight loss was observed for pure MSS (control). But both, crosslinked MSS resin and crosslinked biocomposite showed weight loss of only 60% at 500 °C. As seen in Figure 23(b), the DTGA plot of pure MSS showed a maximum degradation peak at 315 °C while the crosslinked MSS showed the peak at 295 °C. This was discussed earlier in section 4.2.6. The DTGA of crosslinked MSS-MFC biocomposite showed a two stage degradation with the first degradation beginning at 295°C which was same as that observed for the crosslinked MSS. The second stage of degradation was observed at 340 °C which involves degradation of MFC. Identical peak was observed in TGA thermogram for waxy maize starch and MFC composites.[51] The TGA analysis indicates that the addition of MFC does not alter the thermal stability of the composite, particularly the resin. This is because MFC exists as a separate phase and does not affect the MSS and also that MFC is a cellulose polymer which is thermally not much different than starch. This is in contrast to other reinforcing agents such as nanoclay, which are inorganic and being thermally very stable lead to an increased thermal stability of the composites.[82]

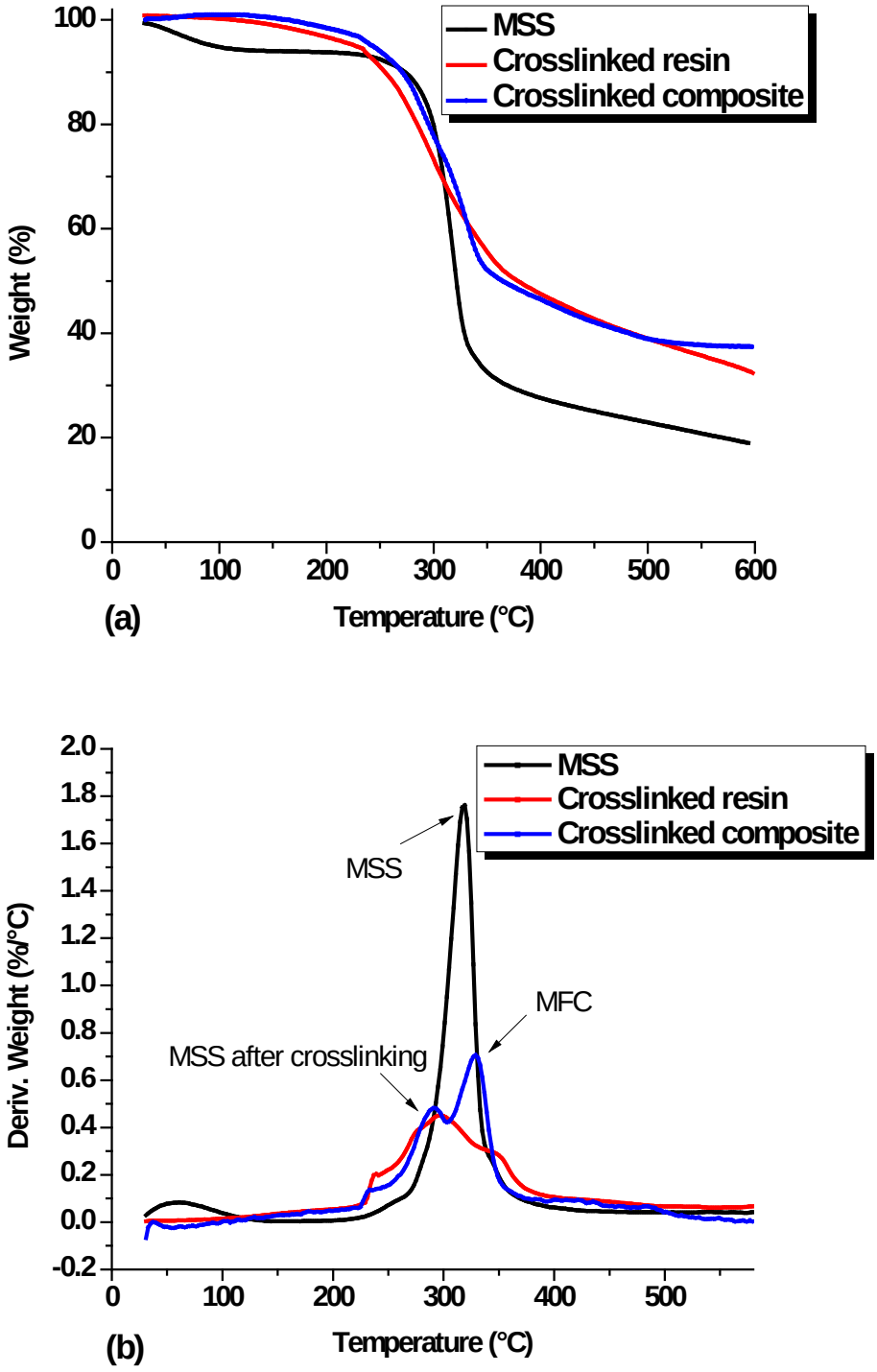

Fig. 23 (a) TGA thermograms of MSS, crosslinked MSS resin and crosslinked MFC-MSS biocomposites (b) DTGA thermograms of MSS, crosslinked MSS resin and crosslinked MFC-MSS biocomposites

4.4 Characterization of the Mercerized and Heat Treated Sisal Fiber

4.4.1 Attenuated Total Reflectance-Fourier Transform Infrared (ATR-FTIR) Analysis:

The mercerization and heat treatment process of the sisal fibers was expected to lead to changes in their chemical composition as well as morphology. ATR-FTIR spectra was used to study the changes at the fiber surface. Figure 24 shows the ATR-FTIR spectra of the control and the NaOH treated sisal fibers. As can be seen in Figure 24, the peaks at 1730 cm^{-1} and 1242 cm^{-1} change after the mercerization process. At the same time the peak at 1730 cm^{-1} disappears. This peak represents the absorbance assigned to the carbonyl unconjugated stretching carboxylic acids or esters present. A similar peak was observed in hemicellulose by Yang et al.[121] The absorbance peak at 1242 cm^{-1} which represents the C–O–C stretching vibration of aryl alkyl ether groups present in lignin was reduced. Yang et al.[121] also observed a peak at 1240 cm^{-1} for lignin which was absent in cellulose. Garside and Wyeth[122] showed typical ATR-FTIR spectra of all cellulosic fibers. Treatment of the fibers with NaOH has been shown to remove lignin present on the surface of the fibers.[36] Thus, the disappearance of these two peaks can be confirmed to be due to the removal of lignin and hemicellulose.[36]

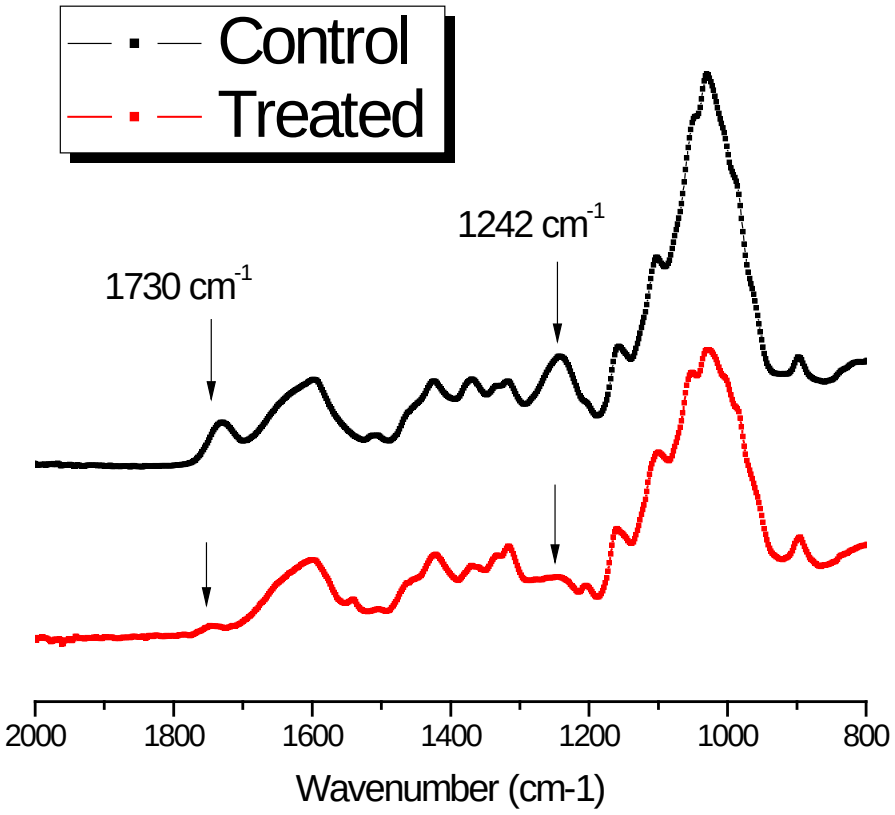

Fig. 24 ATR-FTIR spectra of control and NaOH treated sisal fibers

4.4.2 Surface Topography Characterization

Figure 25 shows SEM micrographs of surface of control (a, b) and mercerized and heat treated (c, d) sisal fibers. The surface of the control or untreated sisal fibers (Figures 25a and 25b) is relatively smooth as compared to that of the mercerized and heat treated ones (Figure 24c and 25d). As mentioned earlier, mercerization process helps in removing the natural as well as artificial impurities present in the sisal fibers. It also helps in partially removing the lignin and hemicellulose from the fibers (confirmed by ATR-FTIR shown in Figure 24). This causes the swelling of the fibers and the removal of lignin, which acts as a cementing material in sisal fibers, causing separation of the fibrils as seen in Figures 25 (c) and 25 (d). Coiled or spiraled

fibrils seen on the surface of the untreated fibers are exposed due to mercerization and straightened as the mercerization and the heat treatment is carried out under tension. A grid-like surface can be seen for the mercerized fibers. Rong et al.[92] also observed rougher surface after the alkali treatment of the fibers and reported that the mercerization causes the primary cell wall to dissolve exposing many fibrils seen in the treated fiber. These fibrils lead to higher surface area available for wetting by the resin. The roughness also provides excellent mechanical bonding by fibrils getting embedded in the resin. Both of which are beneficial to obtain higher fiber/resin interfacial shear strength. This can lead to higher strength and Young's modulus of the composites.

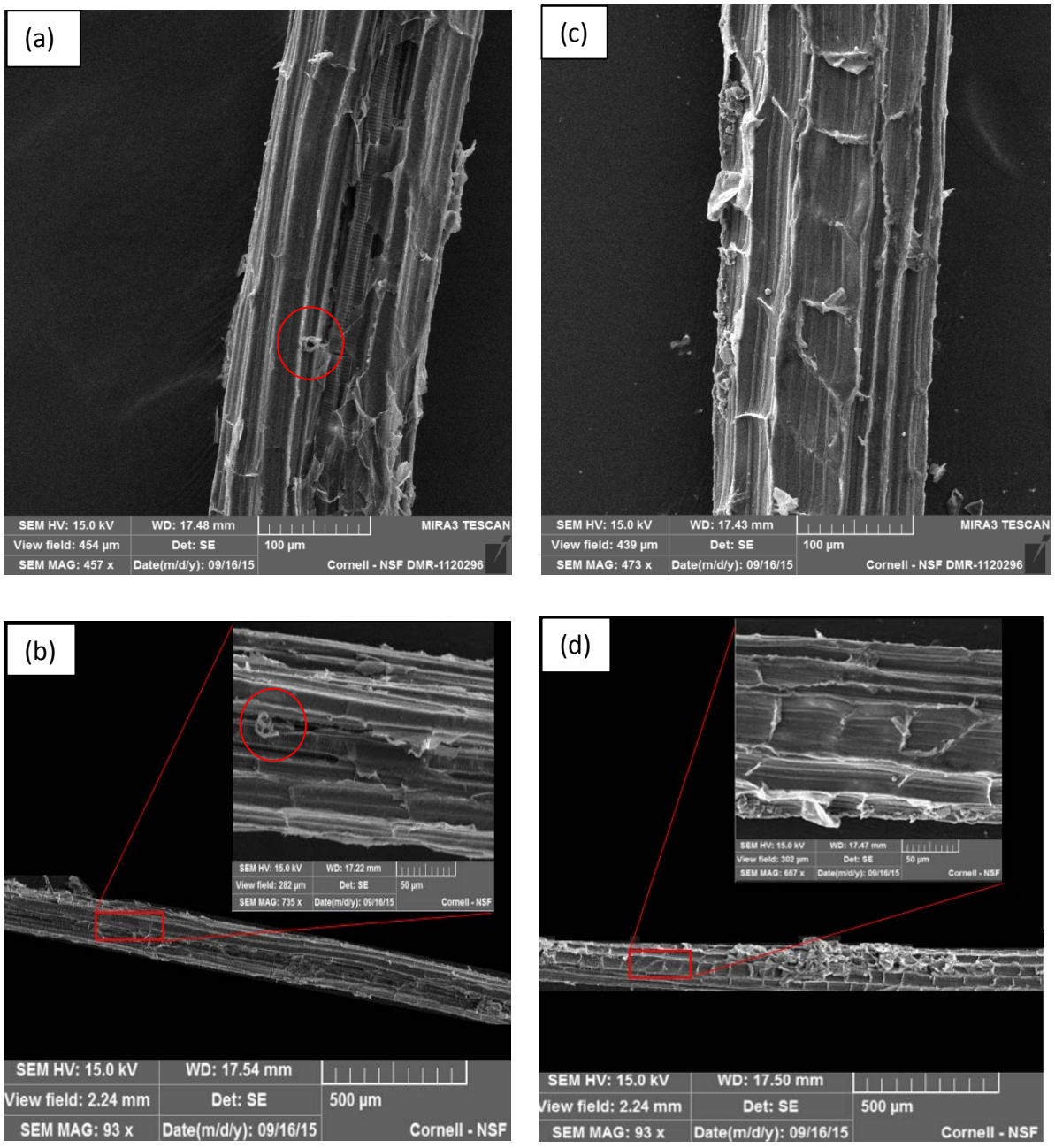

Fig. 25 SEM micrographs of surface of sisal fibers; control (a, b) and mercerized and heat treated (c, d)

4.4.3 Tensile Properties

The typical stress vs strain plots of control and alkali/heat treated sisal fibers are presented in Figure 26 and the tensile properties such as fracture stress (strength), fracture strain and Young's modulus values are summarized in Table 4. As can be seen in Figure 26, the mercerization process leads to a significant increase in the strength and the Young's modulus of the fibers but at the same time the strain is reduced. Mercerization process removes the hemicellulose and the lignin present in the fibers due to the NaOH treatment. Once, hemicellulose and lignin are removed, the cellulose content in the fibers increases. Amongst cellulose, hemicellulose and lignin, cellulose, a linear polymer, is the only one with crystallinity. Thus, mercerization improves the overall crystallinity of the fibers. The applied tension during mercerization is another factor which increases the molecular orientation as well as crystallinity. Both these factors lead to increased strength and modulus of the fibers. With increased crystallinity and molecular orientation the fibers show lower fracture strain, i. e., become brittle. Both stress vs strain plots and data in Table 4 confirm these observations. The tensile strain of the control fibers was found to be 6.5% which reduces to 3.32% after mercerization. In the present study the fibers were heat treated after mercerization. The purpose of the heat treatment of the fibers under tension was to further orient the molecules and the fibrils and thus enhance their tensile properties.[92] The applied tension during the mercerization as well as heat treatment indeed resulted in improved tensile properties. All these factors contribute to an increased strength and modulus of the fibers. The strength was found to increase significantly from 300 MPa (control fibers) to 465 MPa, a 55% increase, for the mercerized and heat treated fibers. The modulus of the fibers was also found to increase from 5 GPa to 15 GPa, a 200% increase. Kim and Netravali[36] carried out the mercerization of sisal fibers using 2 M NaOH solution under

tension (50 g per fiber) and found that the modulus of the fiber increased from 5 GPa to 11 GPa, a 120% increase. The strength increased from 280 MPa to over 380 MPa after mercerization, an increase of about 36%. The results of the present study indicate that the heat treatment of fibers carried out under tension leads to an additional increase in both the strength and Young's modulus of the sisal fibers.

Unpaired t-test was used to confirm that the alkali/heat treatment has a significant effect on the fibers. At significance level of $\alpha=0.05$, the P value equals 0.00002338, which is less than 0.0001. Thus it can be concluded that alkali/heat treatment shows significant increase on the tensile properties, both tensile strength and modulus of the treated fibers.

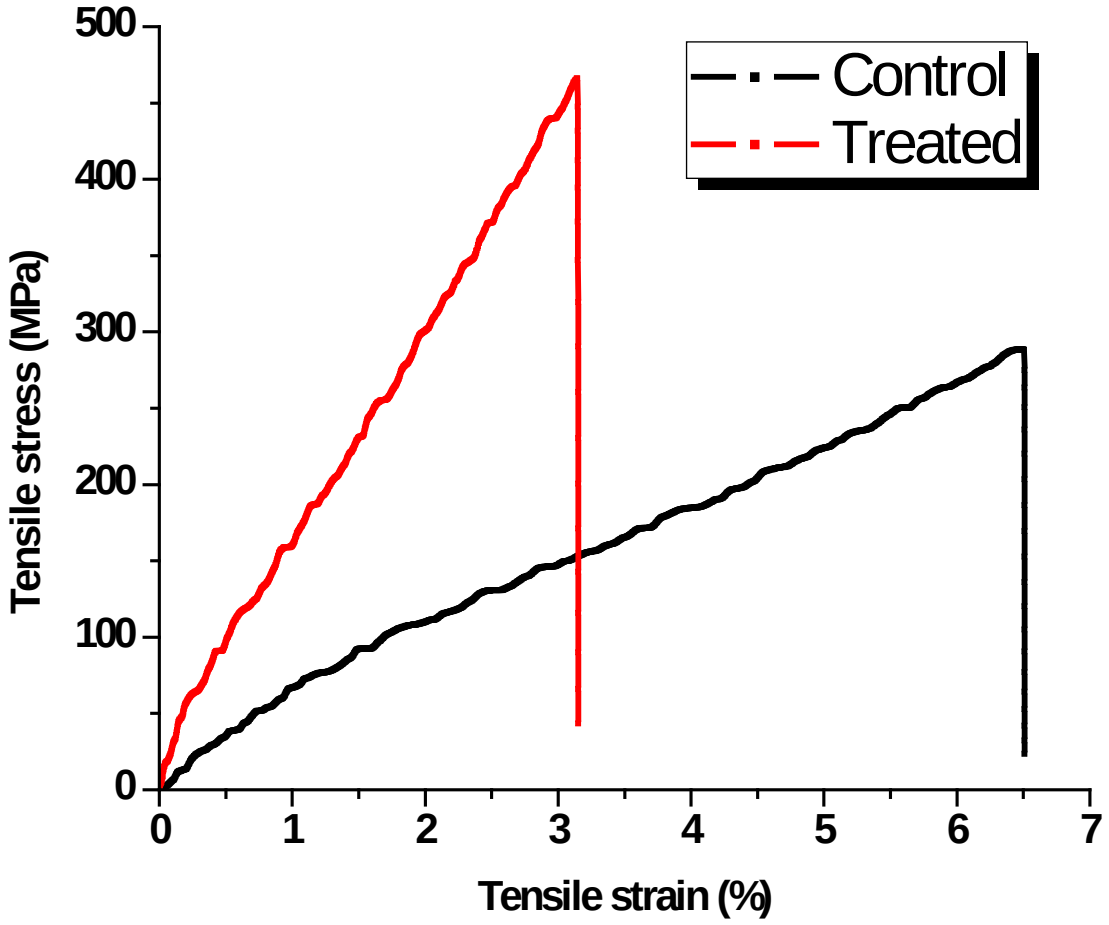

Fig. 26 Typical stress vs. strain plots of control and alkali/heat treated sisal fibers

Table 4 Tensile properties of control and alkali/heat treated sisal fibers

Fiber	**Fracture stress (MPa)**	**Fracture strain (%)**	**Young's modulus (GPa)**
Control	299.72 (74.22)*	6.75 (0.74)	6.24 (1.24)
Treated	464.42 (142.89)	3.32 (1.12)	15.02 (2.58)

***** The numbers in parentheses are standard deviation

4.5 Characterization of Hybrid-Green Composites

4.5.1 Tensile Properties of Hybrid Green Composites

Sisal fiber reinforced unidirectional hybrid green composites were fabricated using control sisal fibers (MSS-MFC-Sisal) as well as the alkali/heat treated sisal fibers (MSS-MFC-Treated sisal). Table 5 presents the experimental values for the tensile properties such as fracture stress (strength), fracture strain, Young's modulus and also the sisal fiber volume fraction for the composites. Tensile properties were obtained in the direction of the sisal fibers only. The sisal fiber volume fraction in the composites was calculated individually for different types of composites and was found to be 0.66 and 0.60 for MSS-MFC-Sisal composite and the MSS-MFC-Treated sisal composites, respectively. Compared to the crosslinked MSS resin or the MSS resin reinforced with MFC, a significant increase in the strength and the modulus of these unidirectional composites was observed. The Young's modulus of the crosslinked MSS resin was found to be 1.2 GPa which increased to 1.8 GPa after reinforcing it with 30% MFC, a 50% increase. Significant increase in the Young's modulus was observed when the MSS-MFC resin was reinforced with the unidirectional sisal fibers. The Young's modulus of the MSS-MFC-Sisal hybrid composite was found to be 4.28 GPa. Further increase in the modulus was observed when alkali/heat treated sisal fibers were used to make the hybrid composites. The Young's modulus of the MSS-MFC-Treated sisal hybrid composite was found to be 8.48 GPa, almost 100% increase over the MSS-MFC-Sisal hybrid composites. High Young's modulus of the composites on adding sisal fibers is purely because of the fact that the modulus of the composite material is controlled by the reinforcement which is sisal fibers in the present case. The strength of the MSS-MFC-Sisal hybrid composites was found to be 108 MPa which increased to 166 MPa for MSS-MFC-Treated sisal hybrid composites, a 54% increase. The improved Young's modulus

and the strength of the MSS-MFC-Treated sisal hybrid composites is because of the mercerization treatment which not only increases the strength and stiffness of the fibers but also improves the interfacial adhesion with the resin.[36] It increases the fiber's affinity for the hydrophilic resin as better wetting is achieved. Further, the increased surface roughness of the fibers contributes to mechanical adhesion. Both these factors lead to a strong fiber/resin bonding allowing efficient load transfer from the broken fibers to the intact fibers. This contributes to both stiffness and strength of the composites. The tensile strain of these composites was low, in the range of about 3%. This is because no external plasticizer was used in the resin. Various kinds of plasticizers can such as glycerol, sorbitol or maltitol that are compatible with starch, can be added to increase the tensile strain and reduce the brittleness of the composites if required.

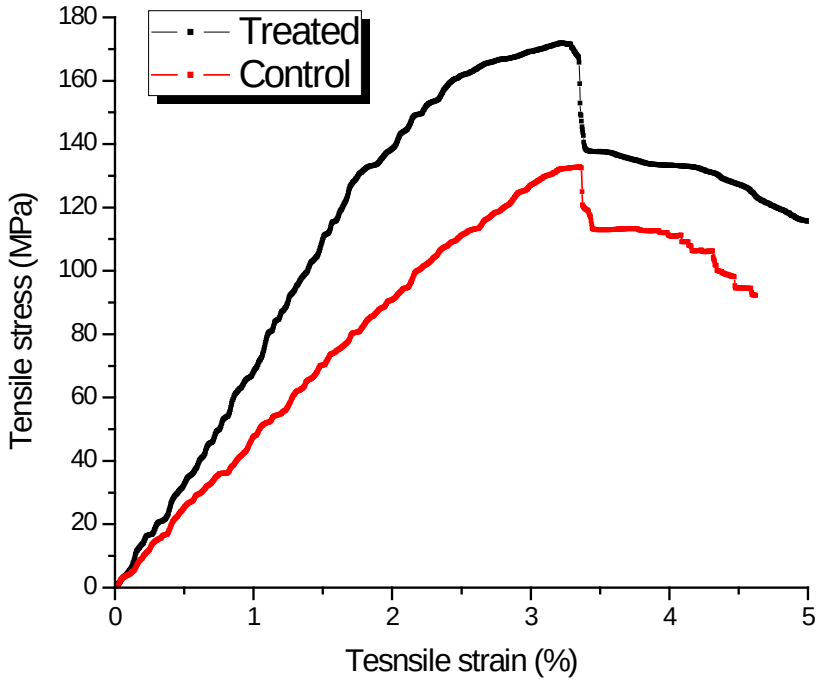

Fig. 27 Typical stress vs. strain plots of hybrid green composites with control and alkali/heat treated sisal fibers

Table 5 Tensile properties of hybrid green composites with control and alkali/heat treated sisal fibers

Composite	Fracture stress (MPa)	Fracture strain (%)	Young's modulus (GPa)	Fiber volume fraction
Control	108.53 (8.40)*	3.18 (0.56)	4.28 (1.71)	0.66
Treated	166.14 (15.12)	2.70 (0.56)	8.48 (0.88)	0.60

*The numbers in parentheses are standard deviations

4.5.2 Theoretical Analysis of the Hybrid Green Composites

Theoretical values for the Young's modulus for the composites based on the simple rule of mixture were calculated and compared to the experimental values. The theoretical density MSS-MFC hybrid biocomposite was calculated based on rule of mixtures.[123]

$$\rho_t = \left(\frac{M_{MFC}}{\rho_{MFC}} + \frac{M_{MSS}}{\rho_{MSS}} \right)^{-1}$$

where ρ_{MFC} and ρ_{MSS} are the densities of MFC and MSS, respectively, and M_{MFC} and M_{MSS} are the weight fractions of MFC and MSS, respectively, in the hybrid biocomposites. The density of MFC is assumed to be 1.5 and that of MSS to be 1.3. Thus the theoretical density of 30:70 MFC:MSS biocomposites was found to be 1.36 based on the above equation and was used for further calculations to calculate the theoretical modulus of the hybrid composites. The theoretical calculation for Young's modulus for the hybrid biocomposites based on MSS, MFC and sisal fibers were calculated using simple rule of mixture,

$E_c = E_f V_f + E_m V_m$

where E_c, E_f and E_m represent Young's modulus values of the composite, fiber and the matrix (resin), respectively. V_f and V_m represent the volume fraction of the fibers and the matrix

respectively. The density of sisal fibers was taken to be 1.45 from the literature.[124] The mass of the fiber and the resin in the composite was measured using gravimetric methods. Based on mass and the density values of the fiber, resin and the composites, the fiber volume fraction of the hybrid composite was calculated. The fiber volume fraction was found to be 0.66 and 0.60 for control and treated hybrid green composites, respectively. The Young's modulus for the sisal fibers, the MFC reinforced MSS resin and the composites was calculated experimentally using Instron, model 5566 at the strain rate of 0.06 min^{-1} (detailed procedure has been mentioned in sections 3.10.3, 3.9.2 and 3.11.1 respectively). The calculated Young's modulus for the MSS-MFC-Sisal fiber based hybrid green composite was found to be 4.91 GPa consisting of 66% fiber volume fraction. The experimentally obtained value for Young's modulus for this composite was 4.28 GPa, which is lower but close to the calculated value of 4.91 GPa. The calculated Young's modulus for the MSS-MFC-Treated sisal fiber based hybrid green composite was 9.88 GPa consisting of 60% sisal fiber volume fraction. The experimentally obtained value for Young's modulus for the same composite was 8.48 GPa, which is lower than the expected value based on the theoretical calculations. There can be several reasons for this discrepancy including the presence of voids in the composites and fibers being not well aligned as desired. Voids may be formed due to various reasons. Curing the composites under high temperature can cause the moisture or the water to be removed fast by boiling. The vapor generated can create voids if not allowed to escape. In the present case, the composites are pressed in between two metal platens which leave very little space around the 4 sides for the vapor to escape. The creation of voids as well as softening of the resin with high temperature can also facilitate the fiber movement within the composite and can change the fiber alignment in the composite.[36] Though the applied pressure during curing may help to fill the voids in the composites, there can be some voids

present which are not visible to the eyes. The applied pressure is also responsible for the movement of fibers during curing which changes the fiber orientation within the composite. Lower Young's modulus obtained in the experiments is thought to be due the presence of voids as well as the loss of alignment or the orientation of the fibers in the composites.

4.5.3 Fracture Surface of Hybrid Green Composites

Figure 28 shows the SEM images of typical fracture surfaces of MSS-MFC-Sisal hybrid green composites (a) side view (b) top view and MSS-MSS-Treated sisal hybrid green composites (c) side view (d) top view. It can be seen from Figures 28 (a) and (b) that the control sisal fibers were pulled out from the resin when fractured in tension as compared to the alkali/heat treated fibers shown in Figure 28 (c) and (d). Figure 28(c) shows that after the specimen fracture, the protruding length of the treated fibers is small and they are still held together with the resin. As opposed to this, Figure 28 (a) shows that longer fibers are pultruding out. In both cases, however, some resin still seems to be sticking to the protruding fibers. Kim and Netravali[36] reported that the fracture in the control fiber composites occurs partially due to debonding of the fibers from the resin first and then the fibers are broken. This is true because mercerization treatment increases cellulose content in the sisal fibers which have hydroxyl groups which can help in fiber wetting and bond well with the starch resin. The top view of the composites fractured in tensile also show that the control sisal fiber composites have long pull out length. Also, larger voids are seen due to the fracture because of the weaker fiber/resin interfacial bonding (Figure 28b). While, a very short fiber pull out length is observed for the composites containing treated fibers and also smaller voids are seen at the tensile fracture

surface. Stronger fiber/resin interfacial bonding is also confirmed as the resin is seen sticking to the fibers even after fracture (Figure 28d).

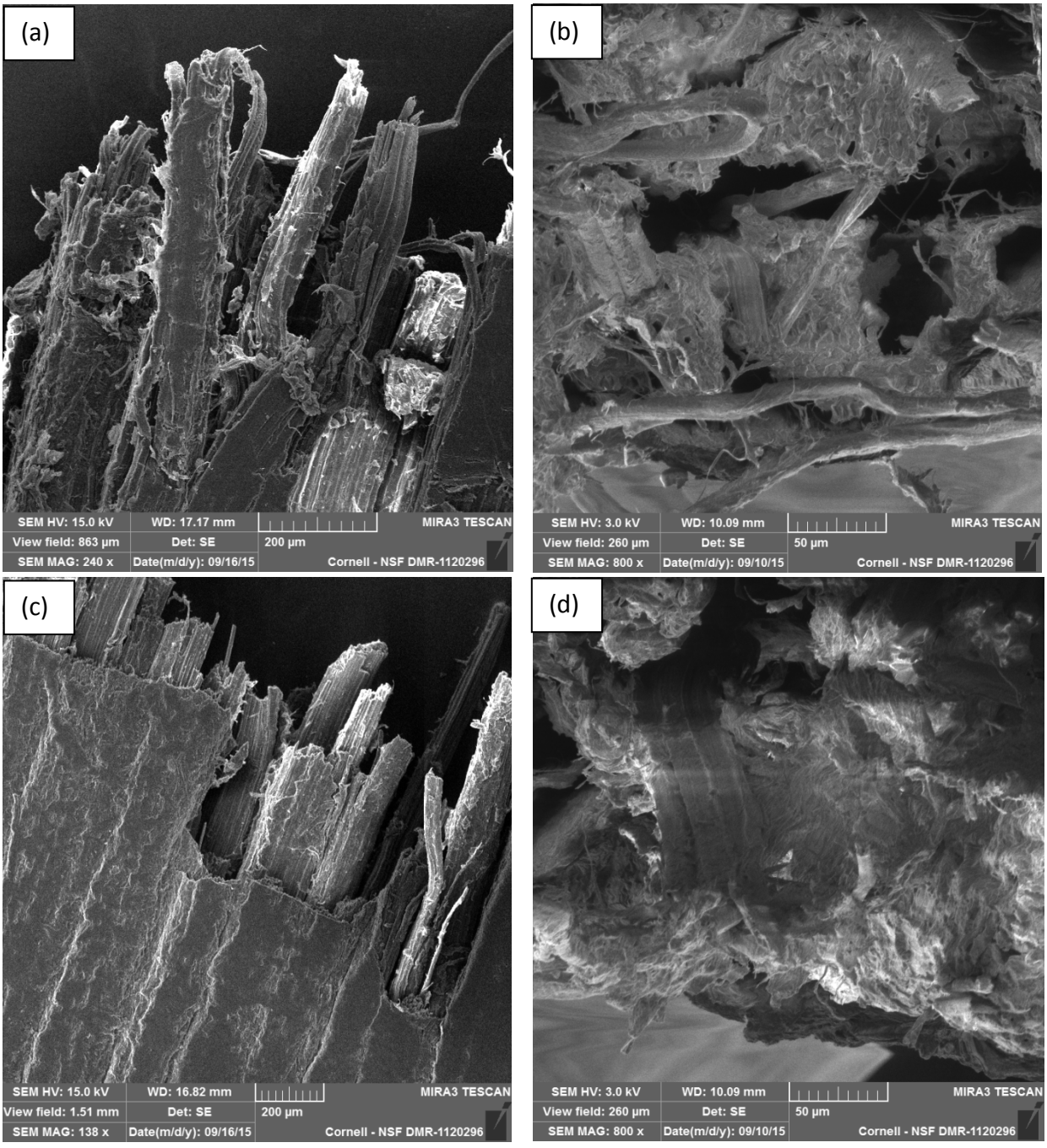

Figure 28. SEM pictures of the fractured surfaces of MSS-MFC-Sisal hybrid composite (a) side view (b) top view and MSS-MSS-Treated sisal hybrid composite (c) side view (d) top view

CHAPTER 5: CONCLUSIONS

Polysaccharide based hybrid green composites were fabricated using MSS, MFC and sisal fibers. Starch (MSS) was extracted from the residue obtained after extraction of oil from the mango seed kernels and crosslinked to improve its tensile properties and moisture resistance for use as a resin in composites. MFC was dispersed and crosslinked with MSS to form biocomposites. Sisal fibers were mercerized and heat treated under tension and incorporated in the crosslinked MSS and MFC and cured to form unidirectional hybrid green composites. Extracted starch, crosslinked resin, biocomposites, treated sisal fibers and the hybrid green composites were fully characterized at each stage of resin and composite preparation. Following conclusions can be drawn from the experimental analysis:

- The MSS extracted from defatted mango seed kernels, a waste source, showed rheological property and gelatinization behavior similar to the commercially available starches such as corn starch, potato starch. Thus, MSS can easily replace these edible starches currently used in non-edible applications.
- Crosslinking of starch was successfully carried out using water soluble butane tetracarboxylic acid (BTCA) and confirmed using the ATR-FTIR spectra, the degree of substitution (DS) values obtained by chemical titrations as well as their swelling behavior.
- A novel, inexpensive, ecofriendly catalyst, sodium propionate (NaP) was shown to be more effective than the currently used esterification catalyst, sodium hypophosphite (SHP). NaP is nontoxic and is approved as a food additive by EU, USA and Australia. Higher tensile properties of the crosslinked MSS resin using BTCA-NaP combination were obtained compared to the BTCA-SHP combination. This confirmed that NaP acted as a better catalyst for crosslinking starch.
- Crosslinking of MSS, as expected, reduced the moisture uptake by the films, the degree of swelling in water and increased the thermal stability.
- Good dispersion of MFC in MSS, up to 40% loading, was achieved using homogenizer and overnight stirring. This resulted in better tensile properties of the biocomposites.

- Crosslinking of MSS and MFC using BTCA-NaP combination was confirmed using ATR-FTIR. It was observed that crosslinking MFC requires a minimum temperature of 140 °C. No crosslinking of MFC was observed below 140 °C.

- The tensile strength and Young's modulus of the biocomposites increased significantly as the MFC loading increased from 20% to 40%.

- Addition of MFC to MSS did not cause any significant changes in the thermal properties of the biocomposites. MFC is a cellulosic material unlike other nanoparticles such as nanoclay which are high temperature inorganic materials which help in increasing the thermal properties of the composites.

- Mercerization and heat treatment of the sisal fibers under tension significantly increased the tensile properties of the fibers. Mercerization is known to remove hemicellulose and lignin from the fibers, which leads to an increase in the cellulose content (thus crystallinity) and the applied tension helps in better alignment of the fibrils along the fiber axis.

- Mercerization also increases sisal fibers to be wetted easily by MSS and facilitates fiber/resin bonding in the composite. Since both fibers and starch have similar chemistry with glucose as their monomeric unit, significant hydrogen bonding between the two can be expected. This further increases the fiber/resin interfacial bonding. This was evident from the SEM images of the fracture surfaces.

- Tensile properties of the biobased hybrid green composites were comparable to other composites made from edible protein and starch sources and thus, they can replace these edible sources.

CHAPTER 6: FUTURE SUGGESTIONS

In the present study MFC was randomly dispersed in the MSS resin. The MFC-MSS based biocomposites would have better properties if MFC could be aligned or oriented within the MSS resin.

The adhesion between sisal fibers and the starch resin was not measured. However, it can be measured and further increased to obtain better tensile properties of the composites. Treatments such as plasma can be used for this.

REFERENCES

1. Hull, D.; Clyne, T. *An introduction to composite materials;* Cambridge university press: 1996.

2. Miracle, D. B.; Donaldson, S. L. Introduction to composites. *ASM Hand book of composite materials* 2001, *21*.

3. Skakle, J.; Aspden, R. Neutron diffraction studies of collagen in human cancellous bone. *Journal of applied crystallography* **2002**, *35*, 506-508.

4. Chawla, K. K. Metal Matrix Composites. In *Materials Science and Technology*Wiley-VCH Verlag GmbH & Co. KGaA: **2006**.

5. Sugita, Y.; Winkelmann, C.; La Saponara, V. Environmental and chemical degradation of carbon/epoxy lap joints for aerospace applications, and effects on their mechanical performance. *Composites Sci. Technol.* **2010**, *70*, 829-839.

6. Stickel, J. M.; Nagarajan, M. Glass Fiber-Reinforced Composites: From Formulation to Application. *International Journal of Applied Glass Science* **2012**, *3*, 122-136.

7. Fujihara, K.; Teo, K.; Gopal, R.; Loh, P. L.; Ganesh, V. K.; Ramakrishna, S.; Foong, K. W. C.; Chew, C. L. Fibrous composite materials in dentistry and orthopaedics: review and applications. *Composites Sci. Technol.* **2004**, *64*, 775-788.

8. Garg, M.; Sharma, S.; Mehta, R. Pristine and amino functionalized carbon nanotubes reinforced glass fiber epoxy composites. *Composites Part A: Applied Science and Manufacturing* **2015**, *76*, 92-101.

9. Chawla, K. K. *Composite materials: science and engineering;* Springer Science & Business Media: 2012.

10. Ajayan, P. M.; Stephan, O.; Colliex, C.; Trauth, D. Aligned carbon nanotube arrays formed by cutting a polymer resin--nanotube composite. *Science* **1994**, *265*, 1212-1214.

11. Jia, X.; Li, G.; Liu, B.; Luo, Y.; Yang, G.; Yang, X. Multiscale reinforcement and interfacial strengthening on epoxy-based composites by silica nanoparticle-multiwalled carbon nanotube complex. *Composites Part A: Applied Science and Manufacturing* **2013**, *48*, 101-109.

12. Lu, J. P. Elastic properties of carbon nanotubes and nanoropes. *Phys. Rev. Lett.* **1997**, *79*, 1297.

13. Thostenson, E. T.; Ren, Z.; Chou, T.W. Advances in the science and technology of carbon nanotubes and their composites: a review. *Composites Sci. Technol.* **2001**, *61*, 1899-1912.

14. Al-Salem, S. M.; Lettieri, P.; Baeyens, J. Recycling and recovery routes of plastic solid waste (PSW): A review. *Waste Manage.* **2009**, *29*, 2625-2643.

15. Netravali, A. N.; Chabba, S. Composites get greener. *Materials Today* **2003**, *6*, 22-29.

16. Wang, R.; Schuman, T. I. Manufacturing of vegetable oils-based epoxy and composites for structural applications **2014**, *29*, 202.

17. Liu, F.; Zhu, J. Plant-oil-based Polymeric Materials and their Applications. *Green Materials from Plant Oils* 2014, *29*, 93.

18. Xiao, L.; Mai, Y.; He, F.; Yu, L.; Zhang, L.; Tang, H.; Yang, G. Bio-based green composites with high performance from poly (lactic acid) and surface-modified microcrystalline cellulose. *Journal of Materials Chemistry* **2012**, *22*, 15732-15739.

19. Mukherjee, T.; Kao, N. PLA based biopolymer reinforced with natural fibre: a review. *Journal of Polymers and the Environment* **2011**, *19*, 714-725.

20. Pietrini, M.; Roes, L.; Patel, M. K.; Chiellini, E. Comparative life cycle studies on poly (3-hydroxybutyrate)-based composites as potential replacement for conventional petrochemical plastics. *Biomacromolecules* **2007**, *8*, 2210-2218.

21. Luo, S.; Netravali, A.N. Interfacial and mechanical properties of environment-friendly "green" composites made from pineapple fibers and poly (hydroxybutyrate-co-valerate) resin. *J. Mater. Sci.* **1999**, *34*, 3709-3719.

22. Huang, X.; Netravali, A.N. Characterization of flax fiber reinforced soy protein resin based green composites modified with nano-clay particles. *Composites Sci. Technol.* **2007**, *67*, 2005-2014.

23. Huang, X.; Netravali, A.N. Biodegradable green composites made using bamboo micro/nano-fibrils and chemically modified soy protein resin. *Composites Sci. Technol.* **2009**, *69*, 1009-1015.

24. Lodha, P.; Netravali, A. N. Characterization of interfacial and mechanical properties of "green" composites with soy protein isolate and ramie fiber. *J. Mater. Sci.* **2002**, *37*, 3657-3665.

25. Lodha, P.; Netravali, A. N. Characterization of Phytagel® modified soy protein isolate resin and unidirectional flax yarn reinforced "green" composites. *Polymer composites* **2005**, *26*, 647-659.

26. Lodha, P.; Netravali, A. N. Characterization of stearic acid modified soy protein isolate resin and ramie fiber reinforced 'green'composites. *Composites Sci. Technol.* **2005**, *65*, 1211-1225.

27. Chabba, S.; Netravali, A. N. ‘Green’composites part 1: characterization of flax fabric and glutaraldehyde modified soy protein concentrate composites. *J. Mater. Sci.* **2005**, *40*, 6263-6273.

28. Rahman, M. M.; Ho, K.; Netravali, A. N. Bio-based polymeric resin from agricultural waste, neem (Azadirachta indica) seed cake, for green composites. *J Appl Polym Sci* **2015**, *132*, 1-11.

29. Rahman, M. M.; Netravali, A. N. Green Resin from Forestry Waste Residue “Karanja (Pongamia pinnata) Seed Cake” for Biobased Composite Structures. *ACS Sustainable Chemistry & Engineering (ACS Publications)* **2014**, *2*, 2318–2328.

30. Ghosh Dastidar, T.; Netravali, A.N. Improving Resin and Film Forming Properties of Native Starches by Chemical and Physical Modification. *Journal of Biobased Materials and Bioenergy* **2012**, *6*, *1-24*.

31. Milkowski, K.; Clark, J. H.; Doi, S. New materials based on renewable resources: chemically modified highly porous starches and their composites with synthetic monomers. *Green Chem.* **2004**, *6*, 189.

32. Takagi, H.; Ichihara, Y. Effect of fiber length on mechanical properties of" green" composites using a starch-based resin and short bamboo fibers. *JSME International Journal Series A* **2004**, *47*, 551-555.

33. Gurunathan, T.; Mohanty, S.; Nayak, S. K. A review of the recent developments in biocomposites based on natural fibres and their application perspectives. *Composites Part A: Applied Science and Manufacturing* **2015**, *77*, 1-25.

34. Kazmi, A.; Shuttleworth, P. *The Economic Utilisation of Food Co-products;* Royal Society of Chemistry: 2013.

35. Srivastava, A.; Maurya, M. Preparation and mechanical characterization of epoxy based composites developed by biowaste material. *International Journal of Research in Engineering and Technology* **2015**, 397-400.

36. Kim, J. T.; Netravali, A. N. Mercerization of sisal fibers: effect of tension on mechanical properties of sisal fiber and fiber-reinforced composites. *Composites Part A: Applied Science and Manufacturing* **2010**, *41*, 1245-1252.

37. Akil, H. M.; Omar, M. F.; Mazuki, A. A. M.; Safiee, S.; Ishak, Z. A. M.; Abu Bakar, A. Kenaf fiber reinforced composites: A review. *Mater Des* **2011**, *32*, 4107-4121.

38. Mohanty, A. K.; Misra, M.; Drzal, L. T. *Natural fibers, biopolymers, and biocomposites;* CRC Press: 2005.

39. Chen, L.; Qiu, X.; Deng, M.; Hong, Z.; Luo, R.; Chen, X.; Jing, X. The starch grafted poly(l-lactide) and the physical properties of its blending composites. *Polymer* **2005**, *46*, 5723-5729.

40. Thiré, R. Starch-based plastics. *Starches: characterization, properties, and applications;* CRC Press: 2010.

41. Ghosh Dastidar, T.; Netravali, A. N. 'Green' crosslinking of native starches with malonic acid and their properties. *Carbohydr. Polym.* **2012**, *90*, 1620-1628.

42. Dicker, M. P. M.; Duckworth, P. F.; Baker, A. B.; Francois, G.; Hazzard, M. K.; Weaver, P. M. Green composites: A review of material attributes and complementary applications. *Composites Part A: Applied Science and Manufacturing* **2014**, *56*, 280-289.

43. Kim, M.; Lee, S. Characteristics of crosslinked potato starch and starch-filled linear low-density polyethylene films. *Carbohydr. Polym.* **2002**, *50*, 331-337.

44. Carmona-Garcia, R.; Sanchez-Rivera, M. M.; Méndez-Montealvo, G.; Garza-Montoya, B.; Bello-Pérez, L. A. Effect of the cross-linked reagent type on some morphological, physicochemical and functional characteristics of banana starch (Musa paradisiaca). *Carbohydr. Polym.* **2009**, *76*, 117-122.

45. Kuniak, L.; Marchessault, R. Study of the crosslinking reaction between epichlorohydrin and starch. *Starch-Stärke* **1972**, *24*, 110-116.

46. Šimkovic, I.; Laszlo, J. A.; Thompson, A. R. Preparation of a weakly basic ion exchanger by crosslinking starch with epichlorohydrin in the presence of NH4OH1. *Carbohydr. Polym.* **1996**, *30*, 25-30.

47. Jyothi, A. N.; Moorthy, S. N.; Rajasekharan, K. N. Effect of Cross-linking with Epichlorohydrin on the Properties of Cassava (Manihot esculenta Crantz) Starch. *Starch - Stärke* **2006**, *58*, 292-299.

48. Koo, S. H.; Lee, K. Y.; Lee, H. G. Effect of cross-linking on the physicochemical and physiological properties of corn starch. *Food Hydrocoll.* **2010**, *24*, 619-625.

49. Majzoobi, M.; Radi, M.; Farahnaky, A.; Jamalian, J.; Tongdang, T. Physico-chemical properties of phosphoryl chloride cross-linked wheat starch. *Iran.Polym.J* **2009**, *18*, 491-499.

50. Reddy, N.; Yang, Y. Citric acid cross-linking of starch films. *Food Chem.* **2010**, *118*, 702-711.

51. Ghosh Dastidar, T.; Netravali, A.N. Cross-Linked Waxy Maize Starch-Based "Green" Composites. *ACS Sustainable Chemistry & Engineering* **2013**, *1*, 1537-1544.

52. Chang, P. R.; Jian, R.; Yu, J.; Ma, X. Starch-based composites reinforced with novel chitin nanoparticles. *Carbohydr. Polym.* **2010**, *80*, 420-425.

53. Wilhelm, H.; Sierakowski, M.; Souza, G.; Wypych, F. Starch films reinforced with mineral clay. *Carbohydr. Polym.* **2003**, *52*, 101-110.

54. Huang, M.; Yu, J.; Ma, X. Studies on the properties of montmorillonite-reinforced thermoplastic starch composites. *Polymer* **2004**, *45*, 7017-7023.

55. Lu, Y.; Weng, L.; Cao, X. Morphological, thermal and mechanical properties of ramie crystallites reinforced plasticized starch biocomposites. *Carbohydr. Polym.* **2006**, *63*, 198-204.

56. Kaur, M.; Singh, N.; Sandhu, K. S.; Guraya, H. S. Physicochemical, morphological, thermal and rheological properties of starches separated from kernels of some Indian mango cultivars (Mangifera indica L.). *Food Chem.* **2004**, *85*, 131-140.

57. Akubor, P. I. The suitability of African bush mango juice for wine production. *Plant Foods for Human Nutrition*. **1996**, 213-219.

58. Pino, J. A.; Queris, O. Analysis of volatile compounds of mango wine. *Food Chem.* **2011**, *125*, 1141-1146.

59. Reddy, L.; Reddy, O. Production and characterization of wine from mango fruit (Mangifera indica L). *World Journal of Microbiology and Biotechnology* **2005**, *21*, 1345-1350.

60. Reddy, L.; Reddy, O. Effect of fermentation conditions on yeast growth and volatile composition of wine produced from mango (Mangifera indica L.) fruit juice. *Food Bioprod. Process.* **2011**, *89*, 487-491.

61. Abdalla, A. E. M.; Darwish, S. M.; Ayad, E. H. E.; El-Hamahmy, R. M. Egyptian mango by-product 1. Compositional quality of mango seed kernel. *Food Chem.* **2007**, *103*, 1134-1140.

62. Solís-Fuentes, J. A.; Durán-de-Bazúa, M. C. Mango seed uses: thermal behaviour of mango seed almond fat and its mixtures with cocoa butter. *Bioresour. Technol.* **2004**, *92*, 71-78.

63. Schieber, A.; Stintzing, F. C.; Carle, R. By-products of plant food processing as a source of functional compounds — recent developments. *Trends Food Sci. Technol.* **2001**, *12*, 401-413.

64. Kittiphoom, S.; Sutasinee, S. Mango seed kernel oil and its physicochemical properties. *International Food Research Journal* **2013**, *20*, 1145-1149.

65. Nilani, P.; Raveesha, P.; Duraisamy, B.; Elango, K.; Dhamodaran, P. Formulation and Evaluation of Polysaccharide Based Biopolymer -- an Ecofriendly Alternative for Synthetic Polymer. *J. Pharm. Sci. & Res.* **2010**, *2*, 178-184.

66. Abdul Khalil, H. P. S.; Bhat, A. H.; Ireana Yusra, A. F. Green composites from sustainable cellulose nanofibrils: A review. *Carbohydr. Polym.* **2012**, *87*, 963-979.

67. Henriksson, M.; Henriksson, G.; Berglund, L.; Lindström, T. An environmentally friendly method for enzyme-assisted preparation of microfibrillated cellulose (MFC) nanofibers. *European Polymer Journal* **2007**, *43*, 3434-3441.

68. Nakagaito, A.; Yano, H. Novel high-strength biocomposites based on microfibrillated cellulose having nano-order-unit web-like network structure. *Applied Physics A* **2005**, *80*, 155-159.

69. Dufresne, A. Natural Polymers; Nanocellulose: Potential Reinforcement in Composites. **2012**, *2*, 1-32.

70. Iwatake, A.; Nogi, M.; Yano, H. Cellulose nanofiber-reinforced polylactic acid. *Composites Sci. Technol.* **2008**, *68*, 2103-2106.

71. Nakagaito, A. N.; Fujimura, A.; Sakai, T.; Hama, Y.; Yano, H. Production of microfibrillated cellulose (MFC)-reinforced polylactic acid (PLA) nanocomposites from sheets obtained by a papermaking-like process. *Composites Sci. Technol.* **2009**, *69*, 1293-1297.

72. Tingaut, P.; Zimmermann, T.; Lopez-Suevos, F. Synthesis and characterization of bionanocomposites with tunable properties from poly(lactic acid) and acetylated microfibrillated cellulose. *Biomacromolecules* **2010**, *11*, 454-464.

73. Lavoine, N.; Desloges, I.; Dufresne, A.; Bras, J. Microfibrillated cellulose – Its barrier properties and applications in cellulosic materials: A review. *Carbohydr. Polym.* **2012**, *90*, 735-764.

74. Tanpichai, S.; Quero, F.; Nogi, M.; Yano, H.; Young, R. J.; Lindström, T.; Sampson, W. W.; Eichhorn, S. J. Effective Young's modulus of bacterial and microfibrillated cellulose fibrils in fibrous networks. *Biomacromolecules* **2012**, *13*, 1340-1349.

75. Siró, I.; Plackett, D. Microfibrillated cellulose and new nanocomposite materials: a review. *Cellulose* **2010**, *17*, 459-494.

76. Lu, J.; Askeland, P.; Drzal, L. T. Surface modification of microfibrillated cellulose for epoxy composite applications. *Polymer* **2008**, *49*, 1285-1296.

77. Seydibeyoğlu, M. Ö; Oksman, K. Novel nanocomposites based on polyurethane and micro fibrillated cellulose. *Composites Sci. Technol.* **2008**, *68*, 908-914.

78. Qiu, K.; Netravali, A. N. Fabrication and characterization of biodegradable composites based on microfibrillated cellulose and polyvinyl alcohol. *Composites Sci. Technol.* **2012**, *72*, 1588-1594.

79. Lu, J.; Wang, T.; Drzal, L. T. Preparation and properties of microfibrillated cellulose polyvinyl alcohol composite materials. *Composites Part A: Applied Science and Manufacturing* **2008**, *39*, 738-746.

80. Suryanegara, L.; Nakagaito, A. N.; Yano, H. The effect of crystallization of PLA on the thermal and mechanical properties of microfibrillated cellulose-reinforced PLA composites. *Composites Sci. Technol.* **2009**, *69*, 1187-1192.

81. Wang, T.; Drzal, L. T. Cellulose-Nanofiber-Reinforced Poly(lactic acid) Composites Prepared by a Water-Based Approach. *ACS Appl. Mater. Interfaces* **2012**, *4*, 5079-5085.

82. Tingaut, P.; Eyholzer, C.; Zimmernn, T. Functional Polymer Nanocomposite Materials from Microfibrillated Cellulose. InTech: 2011.

83. Huang, X.; Netravali, A.N. Biodegradable green composites made using bamboo micro/nano-fibrils and chemically modified soy protein resin. *Composites Sci. Technol.* **2009**, *69*, 1009-1015.

84. Chiappone, A.; Nair, J. R.; Gerbaldi, C.; Jabbour, L.; Bongiovanni, R.; Zeno, E.; Beneventi, D.; Penazzi, N. Microfibrillated cellulose as reinforcement for Li-ion battery polymer electrolytes with excellent mechanical stability. *J. Power Sources* **2011**, *196*, 10280-10288.

85. Jabbour, L.; Gerbaldi, C.; Chaussy, D.; Zeno, E.; Bodoardo, S.; Beneventi, D. Microfibrillated cellulose–graphite nanocomposites for highly flexible paper-like Li-ion battery electrodes. *Journal of Materials Chemistry* **2010**, *20*, 7344-7347.

86. Li, Y.; Mai, Y.; Ye, L. Sisal fibre and its composites: a review of recent developments. *Composites Sci. Technol.* **2000**, *60*, 2037-2055.

87. Mishra, S.; Mohanty, A. K.; Drzal, L. T.; Misra, M.; Hinrichsen, G. A review on pineapple leaf fibers, sisal fibers and their biocomposites. *Macromolecular Materials and Engineering* **2004**, *289*, 955-974.

88. Chand, N.; Tiwary, R.; Rohatgi, P. Bibliography resource structure properties of natural cellulosic fibres—an annotated bibliography. *J. Mater. Sci.* **1988**, *23*, 381-387.

89. Mukherjee, P.; Satyanarayana, K. Structure and properties of some vegetable fibres. *J. Mater. Sci.* **1984**, *19*, 3925-3934.

90. Singh, B.; Gupta, M.; Verma, A. Influence of fiber surface treatment on the properties of sisal-polyester composites. *Polymer Composites* **1996**, *17*, 910-918.

91. Kumar, M. A.; Reddy, G. R.; Bharathi, Y. S.; Naidu, S. V.; Naidu, V. N. P. Frictional coefficient, hardness, impact strength, and chemical resistance of reinforced sisal-glass fiber epoxy hybrid composites. *J. Composite Mater.* **2010**.

92. Rong, M. Z.; Zhang, M. Q.; Liu, Y.; Yang, G. C.; Zeng, H. M. The effect of fiber treatment on the mechanical properties of unidirectional sisal-reinforced epoxy composites. *Composites Sci. Technol.* **2001**, *61*, 1437-1447.

93. Yang, G.; Zeng, H.; Jian, N.; Li, J. Properties of sisal fibre/glass fibre reinforced PVC hybrid composites. *Plastics Industry* **1996**, *1*, 79-81.

94. Mishra, S.; Mohanty, A.; Drzal, L.; Misra, M.; Parija, S.; Nayak, S.; Tripathy, S. Studies on mechanical performance of biofibre/glass reinforced polyester hybrid composites. *Composites Sci. Technol.* **2003**, *63*, 1377-1385.

95. Terzopoulou, Z. N.; Papageorgiou, G. Z.; Papadopoulou, E.; Athanassiadou, E.; Alexopoulou, E.; Bikiaris, D. N. Green composites prepared from aliphatic polyesters and bast fibers. *Industrial Crops and Products* **2015**, *68*, 60-79.

96. La Mantia, F. P.; Morreale, M. Green composites: A brief review. *Composites Part A: Applied Science and Manufacturing* **2011**, *42*, 579-588.

97. Oksman, K.; Skrifvars, M.; Selin, J. -. Natural fibres as reinforcement in polylactic acid (PLA) composites. *Composites Sci. Technol.* **2003**, *63*, 1317-1324.

98. Plackett, D.; Løgstrup Andersen, T.; Batsberg Pedersen, W.; Nielsen, L. Biodegradable composites based on l-polylactide and jute fibres. *Composites Sci. Technol.* **2003**, *63*, 1287-1296.

99. Paul, M.; Alexandre, M.; Degée, P.; Henrist, C.; Rulmont, A.; Dubois, P. New nanocomposite materials based on plasticized poly(l-lactide) and organo-modified montmorillonites: thermal and morphological study. *Polymer* **2003**, *44*, 443-450.

100. Wool, R.; Sun, X. S. *Bio-based polymers and composites;* Academic Press: 2011; .

101. O'Donnell, A.; Dweib, M. A.; Wool, R. P. Natural fiber composites with plant oil-based resin. *Composites Sci. Technol.* **2004**, *64*, 1135-1145.

102. Satyanarayana, K. G.; Arizaga, G. G. C.; Wypych, F. Biodegradable composites based on lignocellulosic fibers—An overview. *Progress in Polymer Science* **2009**, *34*, 982-1021.

103. Lodha, P.; Netravali, A. N. Characterization of interfacial and mechanical properties of "green" composites with soy protein isolate and ramie fiber. *J. Mater. Sci.* **2002**, *37*, 3657-3665.

104. Lodha, P.; Netravali, A. N. Characterization of stearic acid modified soy protein isolate resin and ramie fiber reinforced 'green' composites. *Composites Sci. Technol.* **2005**, *65*, 1211-1225.

105. Huang, X.; Netravali, A. Characterization of flax fiber reinforced soy protein resin based green composites modified with nano-clay particles. *Composites Sci. Technol.* **2007**, *67*, 2005-2014.

106. Rout, J.; Misra, M.; Tripathy, S. S.; Nayak, S. K.; Mohanty, A. K. The influence of fibre treatment on the performance of coir-polyester composites. *Composites Sci. Technol.* **2001**, *61*, 1303-1310.

107. Koronis, G.; Silva, A.; Fontul, M. Green composites: a review of adequate materials for automotive applications. *Composites Part B: Engineering* **2013**, *44*, 120-127.

108. Andresen, C.; Demuth, C.; Lange, A.; Stoick, P.; Pruszko, R.). Biobased automobile parts investigation. *A report developed for the USDA Office of energy policy and new uses* **2012**.

109. Niazi, M. B. K.; Broekhuis, A. A. Surface photo-crosslinking of plasticized thermoplastic starch films. *European Polymer Journal* **2015**, *64*, 229-243.

110. Ratnayake, W. S.; Jackson, D. S. Gelatinization and Solubility of Corn Starch during Heating in Excess Water: New Insights. *Journal of Agricultural and Food Chemistry (ACS Publications)* **2006**, *54*, 3712.

111. Krueger, B.; Knutson, C.; Inglett, G.; Walker, C. A differential scanning calorimetry study on the effect of annealing on gelatinization behavior of corn starch. *J. Food Sci.* **1987**, *52*, 715-718.

112. Singh, J.; Singh, N. Studies on the morphological, thermal and rheological properties of starch separated from some Indian potato cultivars. *Food Chem.* **2001**, *75*, 67-77.

113. Welch, C. M. Tetracarboxylic Acids as Formaldehyde-Free Durable Press Finishing Agents: Part I: Catalyst, Additive, and Durability Studies1. *Textile Research Journal* **1988**, *58*, 480-486.

114. Harifi, T.; Montazer, M. Past, present and future prospects of cotton cross-linking: New insight into nano particles. *Carbohydr. Polym.* **2012**, *88*, 1125-1140.

115. Trask-Morrell, B. J.; Andrews, B. A. K. Thermoanalytical characteristics of polycarboxylic acids investigated as durable press agents for cotton textiles. *J Appl Polym Sci* **1991**, *42*, 511-521.

116. Yang, C. Q. Infrared spectroscopy studies of the cyclic anhydride as the intermediate for the ester crosslinking of cotton cellulose by polycarboxylic acids. I. Identification of the cyclic anhydride intermediate. *Journal of Polymer Science Part A: Polymer Chemistry* **1993**, *31*, 1187-1193.

117. Zhang, S.; Zhang, Y.; Huang, H.; Yan, B.; Zhang, X.; Tang, Y. Preparation and properties of starch oxalate half-ester with different degrees of substitution. *Journal of polymer research* **2010**, *17*, 43-51.

118. Yang, C. Q.; Wang, X. Infrared spectroscopy studies of the cyclic anhydride as the intermediate for the ester crosslinking of cotton cellulose by polycarboxylic acids. II. Comparison of different polycarboxylic acids. *Journal of Polymer Science Part A: Polymer Chemistry* **1996**, *34*, 1573-1580.

119. Lee, E. S.; Kim, H. J. Durable press finish of cotton/polyester fabrics with 1,2,3,4-butanetetracarboxylic acid and sodium propionate. *J Appl Polym Sci* **2001**, *81*, 654-661.

120. Netravali, A.N.; Henstenburg, R.; Phoenix, S.; Schwartz, P. Interfacial shear strength studies using the single-filament-composite test. I: Experiments on graphite fibers in epoxy. *Polymer Composites* **1989**, *10*, 226-241.

121. Yang, H.; Yan, R.; Chen, H.; Lee, D. H.; Zheng, C. Characteristics of hemicellulose, cellulose and lignin pyrolysis. *Fuel* **2007**, *86*, 1781-1788.

122. Garside, P.; Wyeth, P. Identification of Cellulosic Fibres by FTIR Spectroscopy-Thread and Single Fibre Analysis by Attenuated Total Reflectance. *Studies in Conservation* **2003**, *48*, 269-275.

123. Rahman, M. M.; Hosur, M.; Zainuddin, S.; Jahan, N.; Miller-Smith, E. B.; Jeelani, S. Enhanced tensile performance of epoxy and E-glass/epoxy composites by randomly-oriented amino-functionalized MWCNTs at low contents. *J. Composite Mater.* **2015**, *49*, 759-770.

124. Paul, A.; Joseph, K.; Thomas, S. Effect of surface treatments on the electrical properties of low-density polyethylene composites reinforced with short sisal fibers. *Composites Sci. Technol.* **1997**, *57*, 67-79.